

5-2023

Evaluation of Hydrogeochemical Characteristics of San Joaquin, Tulare, and Mojave Aquifers, Southern California

Maedeh Hassanvand
University of Arkansas, Fayetteville

Follow this and additional works at: <https://scholarworks.uark.edu/etd>



Part of the [Environmental Indicators and Impact Assessment Commons](#), [Environmental Monitoring Commons](#), [Fresh Water Studies Commons](#), [Hydrology Commons](#), [Natural Resources and Conservation Commons](#), [Natural Resources Management and Policy Commons](#), and the [Water Resource Management Commons](#)

Citation

Hassanvand, M. (2023). Evaluation of Hydrogeochemical Characteristics of San Joaquin, Tulare, and Mojave Aquifers, Southern California. *Graduate Theses and Dissertations* Retrieved from <https://scholarworks.uark.edu/etd/5091>

This Thesis is brought to you for free and open access by ScholarWorks@UARK. It has been accepted for inclusion in Graduate Theses and Dissertations by an authorized administrator of ScholarWorks@UARK. For more information, please contact scholar@uark.edu.

Evaluation of Hydrogeochemical Characteristics of San Joaquin, Tulare, and Mojave Aquifers,
Southern California

A thesis submitted in partial fulfillment
of the requirements for the degree of
Master of Science in Environmental Dynamics

by

Maedeh Hassanvand
University of Shahid Chamran-Ahvaz,
Bachelor of Science in Geology, 2007
Shahrood University of Technology
Master of Science in Environmental Geology, 2011

May 2023
University of Arkansas

This thesis is approved for recommendation to the Graduate Council.

Phillip D. Hays, Ph.D.
Thesis Director

Matthew D. Covington, Ph.D.
Committee Member

Song Feng, Ph.D.
Committee Member

Abstract

Before making attempts to enhance and manage the quality of water, a thorough understanding of these processes is necessary since the chemical quality of groundwater is impacted by a number of linked processes. This would be more important in arid and semiarid regions like the southern part of California where more rely on groundwater for agriculture and drinking water uses than the other states. As a result, fundamental knowledge of the governing processes of groundwater chemistry is required for effective water resource management. Thus, this study is primarily concerned with three aspects in Mojave, Tulare, and San Joaquin aquifers: The first step is chemical properties of groundwater with respect to hydrogeochemical aspects and salinity. Without different managerial approaches, irrigation with poor-quality water can have a variety of adverse effects, such as increased soil salinity/sodicity, poor penetration, soil hardening, and/or plant-specific ion toxicity. Together, these variables inhibit crop growth and, eventually, a crop's economic output. Numerous indices have been proposed and are often employed in groundwater for this purpose, including Na%, SAR (sodium adsorption ratio), RSC (residual sodium carbonate), MH (magnesium hazard), PI (permeability index), and PS (potential salinity). In the second section, we go into more detail about the levels of heavy metals in groundwater and how pollution indices like HPI (heavy metal pollution index), HEI (heavy metal evaluation index), and CI (contamination index) can be used to evaluate the health risks of consuming groundwater that is overly contaminated with these heavy metals. The concentration of nitrate in the aquifers is the third factor. The multi-isotope systematics ($\delta^{15}\text{N}$ - and $\delta^{18}\text{O}$ - NO_3) method is highlighted in this study, along with typical $\delta^{15}\text{N}$ - and $\delta^{18}\text{O}$ - NO_3 ranges of known NO_3 sources, as well as many other parameters, including the effects of pH, EC, reduction-oxidation, and other elements/ions on nitrate concentration and $\delta^{15}\text{N}$ - and $\delta^{18}\text{O}$ - NO_3 determination. In addition, this paper covers how to

map water quality indicators in the Mojave, Tulare, and San Joaquin aquifers using a GIS (geographical information system) based on water quality information system and spatial analysis with IDW (inverse distance weighted) interpolation.

Table of Contents

Chapter 1: Introduction	1
Chapter 2: Mojave Aquifer	12
2.1 Water Quality Assessment for Irrigation	15
2.1.1 Salinity Index and Salinity Hazard	19
2.1.2 Sodium Percent (%Na) and Sodium Absorption Ratio (SAR)	22
2.1.3 Residual Sodium Carbonate and Residual Sodium Bicarbonate	26
2.1.4 Magnesium Ratio and Magnesium Hazard	28
2.1.5 Permeability Index	29
2.1.6 Potential Salinity	30
2.2 Nitrate Assessment in The Mojave Aquifer	32
2.2.1 The Correlation Between Nitrate and Various Factors in Mojave Aquifer	38
2.2.2 Evaluation of Nitrate Sources Using Stable Isotopes	42
2.3 Heavy Metals Evaluation in Groundwater	46
Chapter 3: Central Valley-San Joaquin Valley- Tulare Basin	56
3.1 Water Quality Assessment for Irrigation in Tulare Aquifer	60
3.1.1 Salinity Index and Salinity Hazard	62
3.1.2 Sodium Percent (%Na) and Sodium Absorption Ratio (SAR)	64
3.1.3 Residual Sodium Carbonate and Residual Sodium Bicarbonate	67
3.1.4 Magnesium Ratio and Magnesium Hazard	68
3.1.5 Permeability Index	69

3.1.6 Potential Salinity	70
3.2 Nitrate Assessment and its Stable Isotopes	71
3.3 Heavy Metals Evaluation in Groundwater	79
Chapter 4: San Joaquin Aquifer	86
4.1 Water Quality Assessment for Irrigation in San Joaquin Aquifer	88
4.1.1 Salinity Index and Salinity Hazard.....	89
4.1.2 Sodium Percent (%Na) and Sodium Absorption Ratio (SAR)	90
4.1.3 Residual Sodium Carbonate and Residual Sodium Bicarbonate	93
4.1.4 Magnesium Ratio and Magnesium Hazard.....	94
4.1.5 Permeability Index	95
4.1.6 Potential Salinity	96
4.2 Heavy Metals Evaluation in San Joaquin Aquifer	97
4.3 Nitrate Evaluation in San Joaquin Aquifer	104
4.3.1 The Correlation Between Nitrate and Major Ions.....	105
4.3.2 Evaluation of Nitrate Sources Using Stable Isotopes	107
Chapter 5: Discussion and Results	112
References	121

Chapter 1: Introduction

Having access to clean freshwater would be one of the most threatening issues in regard to global resources in a near future. As living standards increase and the human population continues to grow, the need for freshwater is growing. As a result, the preservation of groundwater as a natural resource is a critical environmental concern. Although surface waters supply a substantial volume of drinking water, groundwater is often desired, particularly in developing countries, since it requires less treatment and has a greater bacteriological purity, which helps to avoid the spread of water-borne diseases such as cholera (Appelo and Postma, 2005; Giordano, 2009). In addition, due to limited precipitation and surface water supplies and the effects of climate change, groundwater is getting more valuable for human existence, agricultural demands, industry and production development particularly in dry and semi-arid locations (Megdal, 2018). About 95% of the rural population receives their drinking water from groundwater, which is the primary source of water for 40 to 50% of the world's population (EPA, 1977). According to Dennehy et al. (2015), groundwater provides all or a portion of the water for around 75% of American towns, and the dependence on groundwater in California is much greater. Irrigation and industrial supply water also rely to a large extent on groundwater. Increasing agricultural activities and industrial demand due to an increase on human population and predicted dryness due to the climate change are just a few examples among all factors contributing to increase our reliance over groundwaters in the future.

California is the United States' greatest groundwater consumer and 10% of the nation's total groundwater pumping for agricultural and drinking water is distributed among eight counties in the San Joaquin Valley. The development of water resources in California has a lengthy and distinguished history. From the Gold Rush to the twenty-first century, the state's expanding

population and economy have always depended on water. Since the establishment of irrigation districts in the 1880s to the present with vast metropolitan zones, the state has battled to deliver appropriate fresh water for home usage, agriculture, and the environment. The legacy of infrastructure and legislation is changing as California cities get more and more involved with new urban water infrastructure. Cities in arid and semiarid regions all across the world are learning from this revolution how to satisfy future water demands more sustainably than in the past. (2015) (Lassiter).

The topography and population of California helped shape the state's existing water infrastructure. Two-thirds of the state's annual precipitation falls in the north, whereas much of southern California has desert terrain. The majority of the state's agricultural production is located in the parched Central Valley, where around 70% of the state's population lives in large coastal cities (Department of Water Resources, 2014). Both surface water and groundwater are used to supply water in California, although groundwater is more important for the state's environmental, social, and economic health. Groundwater provides around 38% of the state's total water supply in an average year, and up to 46% (or possibly more) during drought years (DWR, 2019). Groundwater is also essential to California's \$46 billion agriculture industry (Mehta et al., 2018). Many small towns and rural areas only get their water from the ground (DWR, 2019). While groundwater use varies by place and over time, it has consistently increased from over 11 km³ (9 million acre-feet) in 1947 to nearly 24 km³ (20 MAF) year between 2005 and 2009. (Mehta et al., 2018). When droughts hit California, groundwater plays a crucial role in mitigating their harshest impacts, making up as much as 46% (or maybe more) of the state's annual supply (Lund et al., 2018). The capacity to lessen these effects, however, has wide-ranging effects, including hurting groundwater-dependent ecosystems, severe overdraft, decreased long-term water supply

dependability, increases in groundwater pumping costs, and infrastructure damage (Mehta et al., 2018).

California's Central Valley, which has a land area of around 52,000 km² and a population of 6.5 million, grows more than 250 different kinds of crops and is in charge of more than 70% of the state's groundwater supply. Droughts increased the burden on the aquifer systems that supply the area as groundwater levels across the region declined significantly as a result of over-drafting and insufficient rates of natural recharge (Ojha et al., 2018). The aquifers system in the Central Valley is made up of "unconfined, semi-confined, and confined aquifers" that are mostly found in the top 300 meters of alluvial deposits deposited by streams draining the nearby "Sierra Nevada and Coast Ranges". Contrary to the Coast Ranges' shale-rich composition, which results in finer-grained sediments on the valley's western side, the Sierra Nevada's crystalline composition provides a greater source of coarse material to the Central Valley (Faunt et al., 2010). The Central Valley is one of the most lucrative agricultural regions in the world, with more than \$40 billion in earnings in 2013. Agriculture is the predominant land use in the region (Great Valley Center, 2014; USDA, 2012).

During normal climatological years, groundwater resources in the central valley are exploited to fulfill water demands, and withdrawals are increased during droughts to make up for decreases in surface water supplies (Thomas and Famiglietti, 2015). While surface water reservoirs and soil moisture storage can be swiftly replenished after a storm or by an increase in snowfall over the season, groundwater droughts often continue longer (Mishra and Singh, 2010). According to Thomas et al. (2017), groundwater drought frequently occurs after drought is indicated by soil moisture and precipitation indicators. The central valley has seen severe, ongoing drought

conditions in recent years, which have transformed the role of groundwater and made it the primary supply of water. The present drought in California has caused a 30% decrease in the amount of surface water that is available for agriculture (Medelln-Azuara et al., 2015). Pumping groundwater has been widely employed to make up for the lack of surface water needed for agricultural irrigation. But because of the unsustainable level of groundwater extraction (Scanlon et al., 2012), the Central Valley aquifer has been ranked as one of the most stressed aquifers in the world (Famiglietti, 2014). Groundwater-dependent surface ecosystems, infrastructure degradation from land subsidence, and poor groundwater quality are all indirect effects of excessive groundwater use (Howard and Merrifield, 2010).

Tens of thousands of synthetic chemicals are utilized today, raising the risk of contaminating water supplies. There are a number of various methods for these organic and inorganic contaminants to infiltrate the aquatic environment, including direct discharge through wastewater treatment facilities, landfills, and land application of human and animal waste to agriculture (Zabala et al., 2016; Kurwadkar, 2014). Since the industrial revolution, groundwater pollution has received a lot of attention as a well-known issue (Heyden and New, 2004). An aquifer may become useless for decades if it is contaminated with dangerous pollutants. The duration of the contaminants' residence in groundwater bodies can range from weeks to decades, depending on their physico-chemical properties and the surrounding environment (Freitas et al., 2015). In addition, the effects of groundwater contamination go beyond the loss of well water access. Contamination from dump or spill sites may move to nearby lakes and rivers as water moves through the hydrologic cycle (Conant et al., 2004).

In order to prevent salinization of soil and decreased agricultural production, it is crucial to evaluate the quality of any groundwater that may be utilized for irrigation (Arslan, 2012). Salinity is the most common issue with irrigation water, and groundwater is categorized as salinity when the amount of dissolved solids in terms of concentration exceeds a specified limit (Total Dissolved Solid (TDS) higher than 1,000 mg/L) (Brady, 2002). Since more than 2,000 years ago, salinity and waterlogging have reduced the agricultural output in dry regions, causing an annual loss of land of roughly 10 million hectares (Suresh and Nagesh, 2015). In California's San Joaquin Valley, salinity and drainage issues have also grown to be quite difficult (Wichelns and Qadir, 2015). In addition to California's geological structures, which results in high salinity in most of the groundwater and soil naturally, human activities have a substantial impact on groundwater salinity (USEPA, 2010). So that Agricultural operations, urban run-off, and imported water sources in Southern California alone produce almost 600,000 tons of salt each year (See, 2000). High saline levels are an issue throughout the southern coast of California, as well as in the Central Valley.); hence, that groundwater meet the minimal irrigation quality criteria before it can be utilized for irrigation. Otherwise, it might have detrimental effects on the soil and the plant. Therefore, assessing the quality of groundwater for irrigation is an essential duty (Brady, 2002).

Urbanization, agriculture, the use of fertilizers, the application of wastewater, and other human activities can all result in the production of a range of pollutants that have a detrimental effect on groundwater quality. Nitrate, heavy metals, and metalloids are the three most prevalent dangerous pollutants in groundwater, all of which are environmentally dangerous (Salman et al., 2019). Scientific research and water planning agencies throughout the world are heavily focused on the issue of nitrate pollution of groundwater. The main causes of nitrate pollution are wastewater discharges and extensive use of synthetic and organic fertilizers (Hernández-Del Amo

et al., 2018). Nitrate has been utilized as a substitute indicator to determine how susceptible groundwater resources are to contamination and is an important parameter for monitoring diffuse groundwater pollution (Fabro et al., 2015). High nitrate levels in water can result in a number of health issues, such as methemoglobinemia and blue baby syndrome, as well as increase the risk of cancers such as colorectal, stomach, and lymphoma (Huang et al., 2011). One of the greatest challenges to aquatic ecology is rising nitrate levels in groundwater, which also produce algal blooms and eutrophication in sources of surface water (Kumar et al., 2014). Many studies have found a connection between CV's (central valley) land use practices and nitrate pollution in groundwater. A high groundwater nitrate sensitive region in the nation has previously been discovered in parts of CV. According to data from 2007, 6.7 million acres of irrigated farmland in California received 740,000 tons of nitrogen fertilizer (Harter, 2009). Farmland's extra nitrogen is swiftly leached into the groundwater, contaminating it. Shallow wells are particularly susceptible because nitrate takes longer to seep into the deeper aquifer. The EPA's MCL has been found to be exceeded in a number of wells in the Central Valley's Sacramento Valley, San Joaquin Basin, and Tulare Basin (Shrestha and Luo, 2017). Along with land use, lithology, slope, recharge rate, precipitation, permeability, and groundwater geochemical conditions, there are other factors that can affect how much nitrate gets transferred into groundwater. Shrestha and Luo (2017) assert that no study has been done to quantify how these factors' interconnections affect transportation, despite the fact that they naturally interact to either increase or reduce mobility. There have also been few studies for the entire aquifer, despite the fact that there have been several local level research in the Central Valley (Harter et al., 2012; Lockhart et al., 2013). Central Valley include the most major aquifers in the united stated; hence, aquifer level assessments are essential to create regional-scale policies and preserve the aquifer's long-term health (Shrestha and Luo, 2017).

In comparison to household wells, typical public supply wells have longer screens and access to deeper aquifer systems, making them more resilient to supply failure during drought (Voss et al., 2019). Water quality degradation is a significant and potentially expensive issue for providers of drinking water in the Central Valley, where legacy agricultural recharge with elevated concentrations of nitrate, fumigants, salinity, and uranium has penetrated to depths commonly exploited for public drinking water supply (Hansen et al., 2018). In comparison to conditions before to development, intensive irrigation and pumpage from production wells have hastened the movement of agricultural recharge to depth over the Central Valley, leading to a sixfold increase in downward vertical seepage rates (Faunt, 2009). Public supply wells (PSWs) may temporarily be invaded by nitrate-rich groundwater from shallower depth zones due to seasonal pumpage fluctuations, but the long-term effects of overdraft on groundwater quality have not been thoroughly researched (Bexfield and Jurgens, 2014).

Evaluation of aquifers' groundwater quality is a critical part in groundwater management and preservation (Shand et al., 2007). Because groundwater pollution detection, monitoring and treatment are relatively expensive, groundwater quality management has focused on resource protection. On the other hand, protection strategies must be concentrated so that resources like manpower, money, and technology may be directed toward the areas that are most susceptible (Merchant, 1994). Targeting must be based on precise predictions of the threat of groundwater contamination based on a variety of future climatic, socioeconomic, and land-use scenarios, it is commonly recognised today (Twarakavi and Kaluarachchi, 2006). California has been manipulating the natural water resources in order to meet its rising population demands and to maintain the world's fifth biggest economy. However, the past approaches—groundwater

overdraft, stream depletion, and increasing imports—to fulfill California's urban water needs won't be sufficient to meet 21st-century expectations (Luthy et al., 2020).

Hydrogeological and geochemical research are essential for assessing groundwater quality and managing groundwater resources. Polluted groundwater treatment is a time-consuming and often difficult task. As a result, the best and most successful method is to prevent pollution from entering this vital resource. One of the most significant hydrogeological investigations is determining the amount of groundwater pollution, and in this case, identifying vulnerable regions and assessing aquifer vulnerability is critical. A good quality indication for healthy drinking water should be present (such as physical and chemical properties). One of these signs is the amount of main ions in the water (Norouzi and Asghari Moghaddam, 2020). Indicators of water quality have been created to collect data on water quality in a manner that is both efficiently comprehensible and justifiable (Saeedi et al., 2010). Nature's water quality is impacted by five different risk categories: salinity, permeation or porousness risk, specific harmful ions, trace element pollution of a water source, and various affects on crops that are sensitive and in a risky category. This method of classifying irrigation waters into three suitability levels yields the IWQ index by linearly adding these danger categories. It should be stressed that numerous risks or negative effects might manifest simultaneously, making it more challenging to conduct water analyses (Simsek and Gunduz, 2007). As a result, in order to properly evaluate the quality of irrigation water, each of these factors must be taken into account (Simsek and Gunduz, 2007).

Heavy metal contamination in the environment has recently increased dramatically, causing disaster effects, particularly in farming lands, by accumulating in the soil and absorbing by plants in (Toth et al., 2016). Many heavy metals are required in small amounts for the healthy

development of biological cycles, but they become hazardous in excessive doses. Heavy metals are released into the environment as a result of both natural events and human activities such as waste disposal, transportation, and agriculture (Samudring et al., 2009). Heavy metals are very persistent and hazardous contaminants in the environment. Using polluted water with heavy metals has increased mortality and morbidity rates in the world and has long-term and short-term impacts, including decreased immunity, oxidative stress, gastrointestinal ulcers, as well as cancer (Kim et al., 2017). Therefore, the heavy-metals pollution index (HPI), heavy-metal evaluation index (HEI), and contamination index (CD) also gauge the general heavy metal quality of water (Singh and Kamal, 2017). In terms of heavy metals, both HEI and HPI provide an overall assessment of water quality (WHO 2011). The HPI is created in two parts, the first of which is creating a rating scale for each parameter (heavy metal) chosen, and the second of which is choosing the parameter for the pollutant on which the index will be based. The HPI is based on "the weighted arithmetic quality means" technique. The rating scale is a numeric value between 0 and 1, and the choice of that value is based on the relative relevance of each quality concern. Alternatively, the rating scale may be evaluated by producing inverse values in accordance with the recommended standard for the pertinent parameter (Horton, 1965). The combined effects of a variety of quality parameters that are regarded to be dangerous for drinking water are summed up by the contamination index (CD). It considers both number of parameters exceeding the upper allowable limit and the concentration of these parameters that exceed these limit values (Kwaya et al., 2019).

Anthropogenic high nitrate sources in aquatic settings are likely to include the overuse of chemical fertilizers, discharge of home and industrial wastewaters, leakage of human and animal waste, and modification of nitrogen-fixing plants (Chen et al., 2021). Although the use of fertilizers has increased agricultural yields, excessive fertilizer applications that are not fully absorbed by the

crop and irrigation return flow have led to rising NO_3^- levels in surface water and groundwater (Torres-Martnez et al., 2020). As a result, the biogeochemical cycle system's nitrogen allocation ratios change, with detrimental effects on the environment and human health. The dual isotopes technique ($\delta^{15}\text{N}-\text{NO}_3^-$ and $\delta^{18}\text{O}-\text{NO}_3^-$) has been utilized extensively for the analysis of NO_3^- pollution sources due to the overlapping ranges of isotope characteristic values in different pollution sources.

The aim of this research is to measure groundwater quality with the application of weighted arithmetic WQI method, heavy metals evaluation indices, and salinity assessment based on chemical parameters. The main focus of these indices is the classification of groundwater quality for drinking water and irrigation uses and identify hydro-geochemical characteristics of groundwater in terms of these parameters. The other aspect of this study is to examine nitrate contamination in groundwater and stable isotopes application to identify its potential sources, and the effects of several chemical parameters on nitrate concentration, nitrification and denitrification. Also, the application of ArcGIS maps and their connection with hydro-chemical parameters of groundwater has been discussed.

The overall research goal is groundwater evaluation of San Joaquin, Tulare, and Mojave aquifers located in the southern part of California in the last two decades. The identified information of these aquifers will help us to answer: What is the quality of aquifers for agriculture and drinking purposes in terms of the anions, cations, heavy metals, and nitrate concentration, and the accumulated impacts of these parameters in the aquifers, special in arid and semiarid regions? What are the potential sources and mechanisms impacting NO_3^- concentration in aquifers based on stable isotopes ($\delta^{15}\text{N}$, $\delta^{18}\text{O}$)? What is the spatial distribution of pollutants and their variations

in polluted areas? This information will be extremely useful to individuals who rely on the aquifers for drinking water, as well as many others who utilize the studied aquifers for other purposes such as agriculture and industrial purposes.

"The National Water Information System (NWIS) of the U.S. Geological Survey (USGS)" (<https://waterdata.usgs.gov/nwis/qw>) is a complete distributed program that allows the collection, processing, and long-term archiving of water data. The publicly accessible NWIS portal contains data from 1899 to the present that comes from all 50 states, as well as border and territory sites. The majority of the more than 1.5 million sites providing NWIS data are for wells, but there are also numerous sites with atmospheric data, such as precipitation, and 10,900 of the sites provide data on present conditions. Although the types of information in NWIS vary, in general, this website offers both recent and old data. Data are obtained by geographic area and classified into surface water, groundwater, or water quality. This information is accessible to the general public, State and local governments, public and private utilities, and other Federal organizations involved in water resources assessment.

In the tutorial part of this website (<https://help.waterdata.usgs.gov/tutorials/water-quality-data/how-do-i-access-real-time-water-quality-data>) the steps to access water quality data have been explained. These steps " start at <http://waterdata.usgs.gov>" 1. select the bottom of " field/lab samples" 2. Choice of the state (California) 3. Click the " Show sites on a map" to see the exact location of sampled wells in the study areas, then export the water quality data of each studied well. As a result, to the evaluation of the Mojave, Tulare, and San Joaquin aquifers, data were compiled from "The U.S. Geological Survey's (USGS) National Water Information System (NWIS)" taken from 154 domestic and public supply wells in San Joaquin aquifer, 48 domestic wells and 11 monitoring wells screened in Mojave aquifers, and 95 domestic wells in Tulare and Kings Counties.

Chapter 2: Mojave Aquifer

The Mojave Desert may be found in southeastern and central California, southern Nevada, south-western Utah, and northwest Arizona in the United States. A growing demand for freshwater resources has been created by the Mojave Desert's rapidly increasing population, low humidity, high summer temperatures, and lack of precipitation (100-140 mm/year). Surface water is limited to ephemeral flow during the winter and spring rain seasons. The two main groundwater basins in the southern Mojave Desert (MGB) have been recognized as the Mojave River Groundwater Basin (MRGB) and the Morongo Groundwater Basin (fig 1). While runoff and groundwater flow from the San Bernardino Mountains, which are nearby, melt snowpack in the southern portions of the MRGB and MGB, the northern and central portions of the basin are primarily refilled by groundwater and surface flow from neighboring mountain ranges like the Cougar Buttes and Granite Mountains, as well as infiltration through the Mojave River floodplain aquifer (Stamos et al., 2001). Different effects have been seen throughout the basin as a result of increased groundwater extraction from the MRGB and MRB. Water levels in the MRGB's central sections decreased steadily over time (20 m from 1950 to 1986), but just little or not at all in the areas close to the mountains.

The Mojave River groundwater basin contains the Mojave River floodplain aquifer. The less productive regional aquifer lies underneath and surrounds it. The Mojave River drainage basin include both. The Mojave Desert has an arid climate with minimal precipitation (150 mm or less per year), low humidity, and hot summer temperatures. The majority of precipitation falls between November and March, with higher amounts (over 1,000 mm in some years) sometimes falling close to the Cajon Pass, which separates the two mountain ranges, and in the Mojave River's headwaters at higher elevations of the San Bernardino and San Gabriel Mountains (Izbicki et al.,

2007).

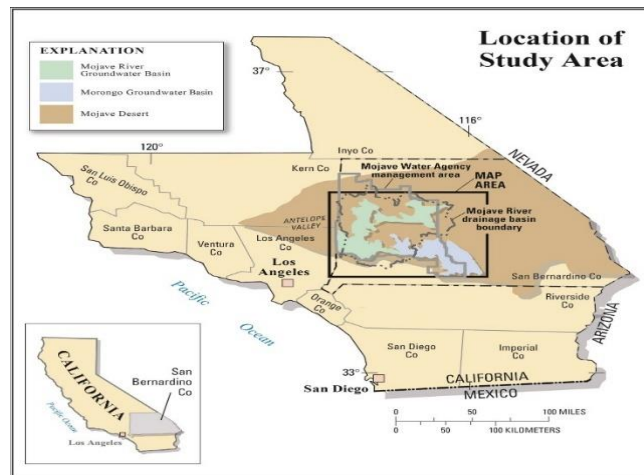
The deposition of salt in groundwater basins is another possible water quality concern for MWA. It is uncommon to remove salt from imported reclaimed wastewater and State Water Project (SWP) supplies since the Mojave River Basin and the Morongo Basin/Johnson Valley are closed basins. About 8,400 acre-feet of State Water Project water is imported each year, while about 5,400 acre-feet of recovered wastewater from outside the MWA is discharged into it (Regional Water management Plan, 2004).

The groundwater basin of the Mojave River covers 3,626 km² and can hold around 5 million acre-feet of water in total. The Mojave Basin is essentially closed, with little any groundwater entering or leaving. However, there is groundwater movement inside the basin, as well as exchanges between subareas, surface water, and the atmosphere. The major methods for releasing groundwater from the basin include well pumping, evaporation via the soil, transpiration by plants, seepage into dry lakes where stored water evaporates, and seepage into the Mojave River. Sedimentary alluvial basins bordered by igneous and metamorphic mountain ranges and uplands define the geology of the Mojave Basin Area. The main water-bearing elements are gravel, sand, silt, and clay produced by the nearby mountains (Dawson and Belitz, 2012).

The Mojave River, which provides the majority of the region's surface water because of the dry local climate, is an inconsistent source of water. As a result, the primary supply of water for drinking, agriculture, and municipal needs in this area is groundwater (USGS, 2018). In this location, the household drinking water wells are shallower than the public supply wells. In the examined wells, the average depth to the completed zone's top (measured in feet below LSD) is 186 feet, and the average depth to the completed zone's bottom (measured in feet below LSD) is roughly 283 feet. They are more vulnerable to pollution since they are at lower depths (Groover et

al., 2019).

Groundwater is the only guaranteed supply of water for the rapidly growing population in the Mojave Basin, yet when compared to the amount of water extracted, ground-water recharge is negligible (John et al., 2004). A growing requirement to comprehend groundwater quality exists as a result of the fact that water levels are dropping as a result of an increasing population and water demand (Mendez and Christensen, 1997).



https://ca.water.usgs.gov/mojave/gen_location.html

Fig.1. Mojave shallow aquifer location in south California

At southern California, one-third of the wells' water supplies had at least one chemical parameter in excessive concentration compared to health guidelines. The most prevalent contaminants in this area are total dissolved solids (TDS), nitrate (NO_3), and volatile organic compounds (VOC) (Williams et al., 1998). Nitrate is the most pervasive of these contaminants in California's drinking water systems (Harter et al., 2017; Burow et al., 2008). Because it can cause methemoglobinemia in newborns and has been linked to cancer in some instances, nitrate is classified as a contaminant in drinking water (Spalding and Exner 1993; Ward et al., 2005).

As a result, there are rising worries in California about groundwater quality and the effect of contamination on the availability of this resource. Due to the identification of some pollutants

like nitrate, and some heavy metals, over 8,000 public groundwater drinking water sources have been shut down since the 1980s (GAMA, 2016; Dennehy et al., 2015).

2.1 Water Quality Assessment for Irrigation

Elevated chemical element concentrations in groundwater have an impact on both soils and plants as a result of water loss from evaporation and falling groundwater levels, particularly in the summer. This is a significant problem in many semi-arid rock-dominated regions all over the world. High salt and sodium content in the water, which results in salinity in the soil and the formation of alkaline soil, are the main issues. When it comes to using groundwater for irrigation, the most crucial characteristics to consider are salinity and sodium risks (FAO, 2011).

One of the most important direct effects on groundwater quality is an increase in "irrigation return flow (IRF)" salinity. To fulfill crop water needs and remove salts from the soil, more irrigation water is regularly given (FAO, 2011). The fraction of water eventually reaching the water table (recharge) will typically show an increase in salinity relative to the applied irrigation water "because of concentration by crops transpiration and evaporation or mobilization of salts accumulated in soil and the unsaturated zone," according to research (Scanlon et al., 2010). This can cause return flows to have salt levels that are one to 10 times higher than they would be with only applied water.

The salt content of IRFs is affected by a number of factors, including the quality, quantity, and rate of applied water, the climate, the soils, the depth of the water table, the type of aquifer, and particular agricultural, drainage, and irrigation management techniques (Merchan et al., 2015). The degree of groundwater salinization will be significantly influenced by the quality of irrigation water, which might vary greatly depending on the source from fresh to salty. Because groundwater (particularly deep or ancient groundwater) has a higher salinity than surface water, irrigation

effects on groundwater quality will differ depending on whether groundwater or surface water is used for irrigation (Bohlke, 2002). Solute recycling from irrigation in groundwater-fed irrigation systems can also cause aquifer salinization (Milnes and Renard, 2004). Due to less salt leaching, lower irrigation rates (such as drip irrigation) lessen IRF's detrimental effects on aquifer salinity, but they also tend to speed up the salinization of soil and shallow groundwater (Scanlon et al., 2010). The primary salt concentration factor in the crop root zone will thus be determined by irrigation application rates in relation to crop evapotranspiration. IRFs are particularly problematic in dry and semi-arid areas since there is little precipitation there and there is frequently considerable evapotranspiration and salt content in the soil. Large stocks of soluble salts naturally exist in soils and the unsaturated zone throughout vast parts of the planet with dry and semi-arid climates.

Soil characteristics can also affect how much salt accumulates. Clayey to loamy sandy soils have higher salt levels than coarser textures due to longer residence times and more time for evapotranspiration (Scanlon et al., 2010). The salinization process is typically more intensive in irrigated areas with shallow groundwater, particularly those with high rates of evaporation. Shallow groundwater evaporation can increase as groundwater moves deeper into the soil's non-saturated region as a result of capillary rise (up to about 1.5 m; Van Weert et al., 2009). The primary cause of soil and groundwater salinization in irrigated desert regions with shallow groundwater levels has been identified as upward capillary water flow (Northey et al., 2006). The main human-made action causing soil salinization is the persistent dry spells have resulted in water with low quality being used for agricultural irrigation, and excessive poisons (Pena et al., 2020). Isidoro and Grattan (2011) used a model to anticipate the salinity of rootzone under various irrigation techniques and various soil types, with equal rainfall but differing monthly distributions.

Eight scenarios were used to calculate a rootzone daily water and salt balance: two different soil types (coarse vs. fine grained) in two different multi-year series with two different irrigation techniques. During the growth season, all elements impacted the rootzone's mean electrical conductivity (EC): Surface irrigation resulted in lower EC than spray irrigation; winter-concentrated rainfall resulted in lower EC than rainfall dispersed evenly throughout the year; and coarser-textured soil resulted in lower EC than finer-textured soil (fig. 2). The method of irrigation, the pattern of rainfall, and the water-retentiveness of the soil are all factors that affect the electric conductivity. In determining the required amount of leaching and the permitted salinity of irrigation water for crop protection, taking these site-specific factors into account may be helpful.

The qualities of irrigation water are impacted by temperature, pH, salinity, and alkalinity. Since the temperature and pH of groundwater significantly impact irrigation water requirements, the water quality for irrigation water is often assessed using salt and alkali damage. "Increased salinity of groundwater increases kinematic viscosity, leading to an increase in friction resistance". As a result, Lower agricultural yields occur from a reduction in seepage speed and permeability coefficient that prevents water from reaching plant branches and leaves. Salt builds up in soils during irrigation with highly salinized water, which leads to secondary salinization and changes in the chemical make-up of soil solutions. This impacts the growth of plant roots and the movement of water through the soil, diminishing the stability of the overall soil structure and causing the physical characteristics of the soil to deteriorate. When groundwater is very alkaline, soil organic matter content decreases, soil nutrient conditions worsen, and plant growth is hampered (Syed et al., 2021).

Table 3 displays the determined water quality parameters for irrigation. The following chemically significant indices are used to assess irrigation water quality:

All water samples are alkaline with a pH range from 7 to 9.4, and a mean of 8. With a mean of 907 $\mu\text{s}/\text{cm}$, the electrical conductivity values were in the range between 193 and 3,990 $\mu\text{s}/\text{cm}$. This wide range of EC, ranging from a more natural level (680 $\mu\text{s}/\text{cm}$) to an increased one (3,990 $\mu\text{s}/\text{cm}$, likely anthropogenic), is proof that both geogenic and human processes are influencing the hydrogeochemistry of the studied region.

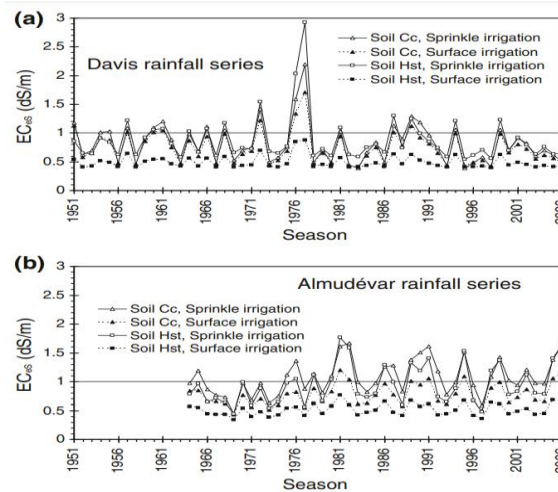


Fig. 2. Average EC of the saturated paste extract for the simulated years in the 8 scenarios throughout the growth season (Isidoro and Grattan, 2011)

"Piper trilinear diagram (Piper 1953)" is using to classify samples and to determine the chemical type of water. The proportion of ions indicated on the side triangles and the matching points on the side of the triangles will display on the middle lozenge. The total number of anions and cations is taken to be 100. Finally, a Piper diagram is utilized to evaluate the type of water's quality in relation to the region that is being focused on. According to this categorization, water is divided into three phases: bicarbonate, calcium bicarbonate, and sodium bicarbonate, as well as bicarbonate, sulfate, and chloride types.

The Piper diagram plotting of the water data reveals that the dominating anions are HCO_3^- + SO_4^{2-} and the primary cations are Na^+ or Ca^{2+} . Indeed, water type in 20 samples (N=41) is Na+K- SO_4^{2-} , in 14 samples is Na+K- HCO_3 , and in 6 samples is Ca- HCO_3 type. The groundwater pumped

from the Mojave aquifer, known locally as the floodplain aquifer are from alluvial deposits of recent Quaternary and Pleistocene nonmarine sediments. The water type of this regions mostly is alkaline with the dominance of Na-HCO₃²⁻. However, almost all of the groundwater is pumped from alluvial aquifers made of weathered granitic and metamorphic rock from the San Bernardino Mountains, which are in the southern part of the study area, and weathered granitic, metamorphic, and volcanic rock from smaller mountains farther to the east of the Mojave River. The water types range from alkaline to weak acids, with Na and SO₄²⁻ as the dominant elements (fig. 3).

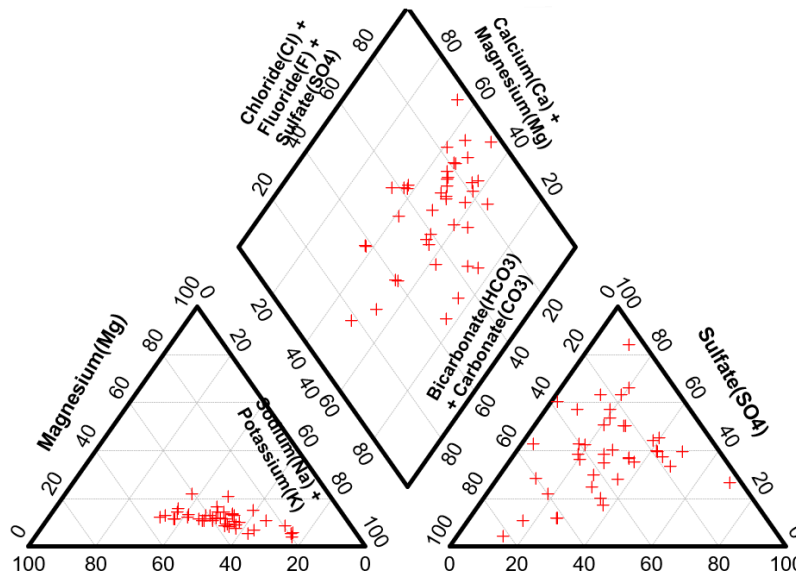


Fig. 3. Water types in the research region depicted in a Piper diagram.

2.1.1 Salinity Index and Salinity Hazard

According to Ravikumar et al. 2011, one of the most used quality metrics, the EC value, exhibits a strong association with the concentrations of soluble salts in water.

The water quality of the examined wells varied from medium to extremely high salinity based on the EC values, with the exception of two samples (Table 1). 90% of samples are classified as having medium to high water salinity.

Table 1) EC-based classification of water salinity (Handa1969)

EC ($\mu\text{S}/\text{cm}$)	Water salinity	EC range (no. of sample)	Percent
0-250	Low (excellent quality)	230 (1 sample)	2
251-750	Medium (good quality)	192-751 (27 samples)	54
751-2,250	High (permissible quality)	774-1,420 (18 samples)	36
2,251-6,000	Very high	2,690-3,990 (4 samples)	8
6,001-10,000	Extensively high	-	-
10,001-20,000	Brine weak concentration	-	-
20,001-50,000	Brine moderate concentration	-	-
50,001-100,000	Brine high concentration	-	-
>100,000	Brine extremely high concentration	-	-

The overall concentration of soluble salts in irrigation water, or salinity danger, is categorized into four groups based on electrical conductivity (EC) measurements calculated in this area (Table 2). Groundwaters of the C1 class may be used to irrigate the majority of crops and soils (low-salinity hazard). If just a little amount of leaching occurs, groundwater of the C2 class (medium-salinity danger) can be utilized for irrigation. Although plants with a high resistance to salt may benefit from water with a moderately high salinity (C3 class), it should not be used for normal irrigation, especially in soils with poor drainage. High salinity water (C4) cannot be utilized with soils with poor drainage (Ravikumar et al. 2011). Two samples are classified as being of outstanding quality class C1, 26 samples as being of good quality class C2, 18 samples as being of uncertain class C3, and the other 8 samples are classified as being of C4 and unsuitable for irrigation (Table 2).

Table 2) Water categorization for the research region based on salinity risk

Salinity hazard class	EC ($\mu\text{S/cm}$)	Quality	range (no. of sample)	Percent
C1	100-250	Excellent	192-230 (2 sample)	4
C2	250-750	Good	275-715 (26 samples)	52
C3	750-2,250	Medium	774-1,420 (18 samples)	36
C4	>2,250	Unsuitable	2,690-3,990 (4 samples)	8

Table 3) Groundwater samples from the Mojave River Basin aquifer and irrigation water quality characteristics

Na%	PS	MH	SAR	PI	RSC
56.89	3.86	44.74	2.78	86.89	-0.17
63.56	0.70	19.02	2.44	127.56	1.66
76.50	1.07	15.78	3.76	57.98	-1.83
42.44	3.33	22.61	2.02	62.27	-2.23
39.73	1.86	32.31	2.02	79.26	-0.20
26.74	3.80	18.09	1.14	57.36	-2.27
46.11	3.54	24.03	2.27	68.29	-1.43
54.03	2.22	18.09	2.72	98.78	0.49
37.53	3.62	17.96	1.90	80.08	-0.29
48.81	2.72	22.51	2.32	57.29	-1.66
53.82	0.52	29.18	1.83	36.17	-28.98
55.58	2.12	18.55	2.88	64.29	-1.98
32.84	2.63	18.27	1.40	56.54	-6.86
34.12	21.66	19.79	3.97	65.04	-1.14
47.45	3.34	24.59	2.31	82.38	-0.05
55.04	1.85	19.27	2.67	68.69	-1.43
41.52	3.75	27.46	2.26	58.46	-3.51
66.56	17.71	40.76	8.87	99.23	0.36
48.53	9.64	21.22	3.47	58.98	-3.87
95.00	0.18	6.66	8.43	76.97	-1.66
37.23	21.69	25.51	4.49	69.49	-2.29
37.09	0.74	22.67	1.32	89.81	0.32
37.73	0.88	18.67	1.11	60.95	-1.42
49.00	2.70	21.86	2.24	53.59	-4.84
45.99	6.19	20.64	2.74	96.28	0.78
75.30	1.69	20.31	4.59	63.96	-5.25
46.85	7.44	20.28	3.01	77.26	-0.99
56.96	2.93	26.91	2.98	69.86	-1.50
68.71	6.20	34.14	5.97	70.97	-2.15
57.02	5.26	20.85	3.49	94.38	1.38
53.57	0.85	29.87	2.05	67.40	-1.58
37.57	1.57	34.73	1.44	90.38	-0.30
44.77	7.64	20.50	2.77	59.01	-2.14
48.86	0.44	40.52	1.62	84.89	0.37
55.65	8.84	23.74	4.84	79.15	-0.87
57.91	2.38	17.93	2.85	60.25	-3.76
57.09	0.57	32.93	2.09	68.99	-1.33
49.37	6.15	21.91	3.12	74.15	-0.93
57.84	4.93	23.23	3.64	87.59	0.56
75.82	3.08	24.17	6.79	55.90	-11.29
50.80	3.34	28.64	2.63	72.02	-0.75
71.86	2.00	30.47	4.72		
40.77	4.73	22.46	1.76		
62.20	3.11	14.21	3.87		
63.87	5.81	18.22	4.85		
47.81	5.70	31.45	3.29		
49.60	3.80	24.04	2.82		
54.47	2.34	28.58	3.05		
54.21	1.32	20.56	2.42		
52.93	21.12	24.05	5.48		
40.86	1.51	20.80	1.45		

2.1.2 Sodium Absorption Ratio (SAR) and Sodium Percent (%Na)

Another crucial factor for water quality is sodium percent, which relates to Na^+ interacting with the soil and restricting its permeability (Ravikumar et al., 2011). Because minerals are soluble in water and additional elements are present, the Na% is computed as follows:

$$\text{Na\%} = (\text{Na}^+ + \text{K}^+) * 100 / (\text{Ca}^{2+} + \text{Mg}^{2+} + \text{Na}^+ + \text{K}^+)$$

where all values in meq/L.

High Na^+ concentrations in irrigation fluids have a tendency to absorb clay particles, dislodging Mg^{2+} and Ca^{2+} ions in the process. Soil loses permeability when soluble Na^+ is exchanged for Ca^{2+} and Mg^{2+} , which finally results in inadequate internal drainage. When air and water flow are impeded under wet conditions, soil becomes firmer after drying (Xu et al., 2020). The categorization of water samples according to salt percent is shown in Table 4. Accordingly, the results show that 16% of the samples fall into the "Good" group, 64% are legal, and 20% are in the "relatively Unsuitable" category.

The spatial map made using GIS and "inverse distance weighted (IDW) interpolation" techniques demonstrated the progressive behavior of physico-chemical pollutants that had already been identified and evaluated in the characterization analysis as well as the decreasing and increasing pollutants values from the various selected sites. The harmful zone was shown in red and the safe area in green in the interpolation technique for the geographical distribution of the different pollutants. The quality of the water in the Mojave aquifer steadily altered each hue. Figures 4 and 6 show the geographical distribution of SAR and Na% in the Mojave aquifer. According to the map, the north is where the majority of the aquifer's wells with Na% and SAR are located. In the map, wells with Na% and SAR are mostly located on north part of the aquifer. These contaminants wells are drilled in alluvium Pleistocene nonmarine sediment. Also, wells located on the cities of Barstow, Helendal, and Victorville have the most concentration showing

the effect of anthropogenic sources on salinity beside the geological formation of Mojave aquifer.

Table 4) Classification of water depending on "salt percent" (Wilcox,1955)

"Sodium (%)"	"Water class"	"Range (no. of sample)"	Percent
<20	Excellent	-	-
20-40	Good	26-39 (8 samples)	16
40-60	Permissible	40.8-57(32 samples)	64
60-80	Doubtful	62-76 (9 samples)	18
>80	Unsuitable	95(one sample)	2

A soil's permeability is reduced by an excessive sodium content as compared to calcium and magnesium, which consequently prevents the crops from getting the water they need to grow.

SAR evaluates the surplus sodium and computes it as follows (Davraz and Ozdemir, 2014):

$$SAR = \frac{Na^+}{\frac{\sqrt{Ca^{2+} + Mg^{2+}}}{2}}$$

where all values in meq/L.

Table 5 presents the SAR classification of the groundwater samples from the Mojave aquifer. All samples fall into the S1 (good) class of sodium hazard rating for irrigation since their salt absorption ratios are less than 10.

Table 5) water danger classes based on "USSL classification" and sodium hazard classes based on SAR values (Ravikumar et al., 2011)

"SAR values"	"Sodium hazard class"	Quality	Range	Percent
<10	S1	Excellent	1.1-8.8	100
10-18	S2	Good	-	-
19-26	S3	Doubtful	-	-
>26	S4 and S5	Unsuitable	-	-

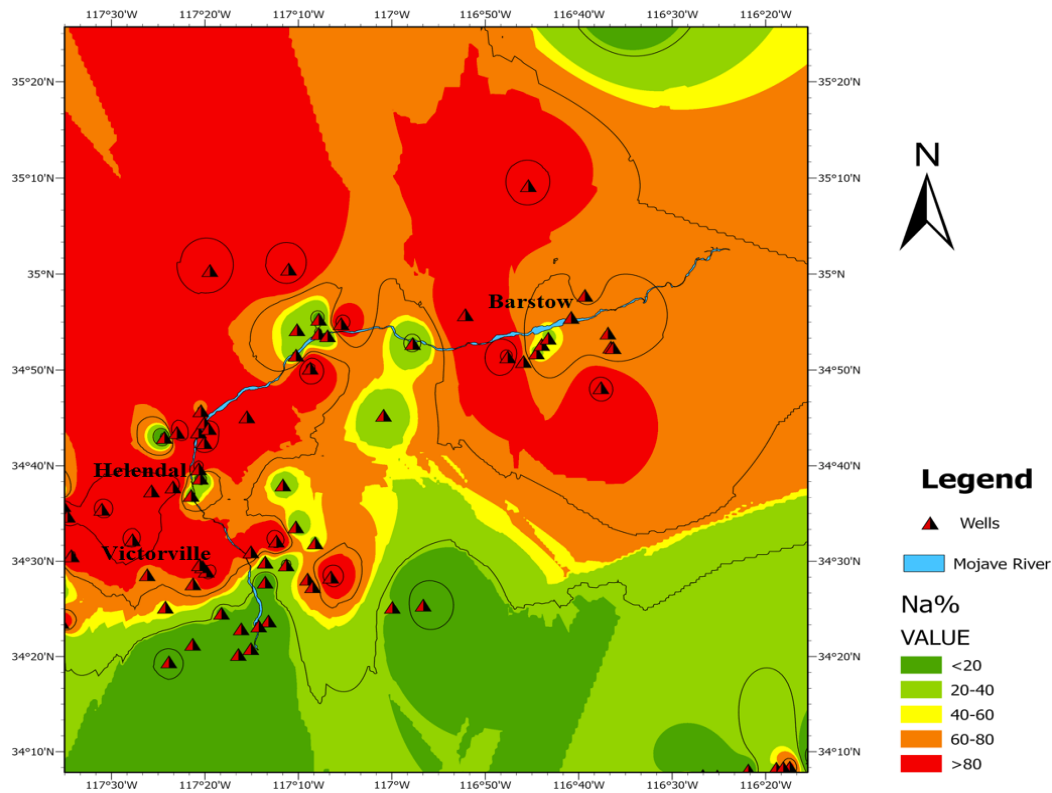
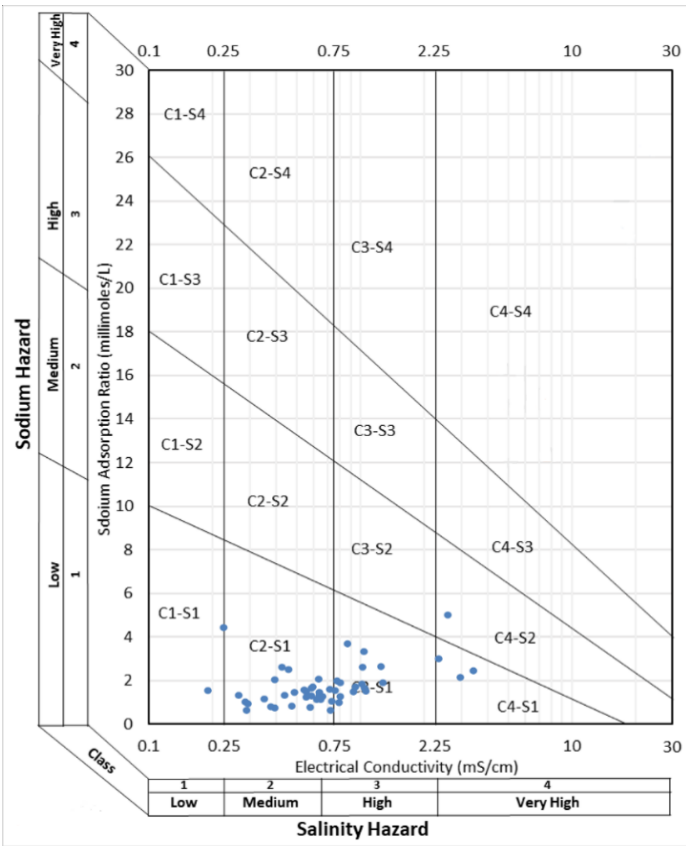


Fig. 4. spatial distribution of Na% in Mojave aquifer

Plotting the electrical conductivity and sodium absorption ratio (Fig. 5) data on the "U.S. Salinity Laboratory (USSL) diagram" allows for a more thorough investigation of the suitability of the water for irrigation. The two factors taken into account in this classification are the EC and the salt absorption ratio. The C1S1 category of waters has the best irrigation qualities, while the C4S4 category has the poorest. As a result, waters are categorized into 16 categories.

According to the "Wilcox diagram", 35.3% of samples fall in C3S1 with saline water, 51% in C2S1 with slightly saline, and 9.8% of the samples are very saline. Furthermore, the graph indicates that while sodium threat is quite low, groundwater is enriched in salinity and deteriorate in poorly drained soils.



Water quality for agriculture	Type	Row
"Suitable for agriculture"	C1S1	1
"Slightly saline-almost suitable for agriculture"	C1S1, C2S2, C2S1	2
"Saline-by some preparations is usable for agriculture"	C1S3, C2S3, C3S1, C3S2, C3S3	3
"Very saline-unsuitable for agriculture"	C1S4, C2S4, C3S4, C4S4, C4S3, C4S2, C4S1	4

Fig. 5. Groundwater in the Mojave Aquifer is categorized using a diagram of sodium adsorption ratio and salinity for irrigation usage

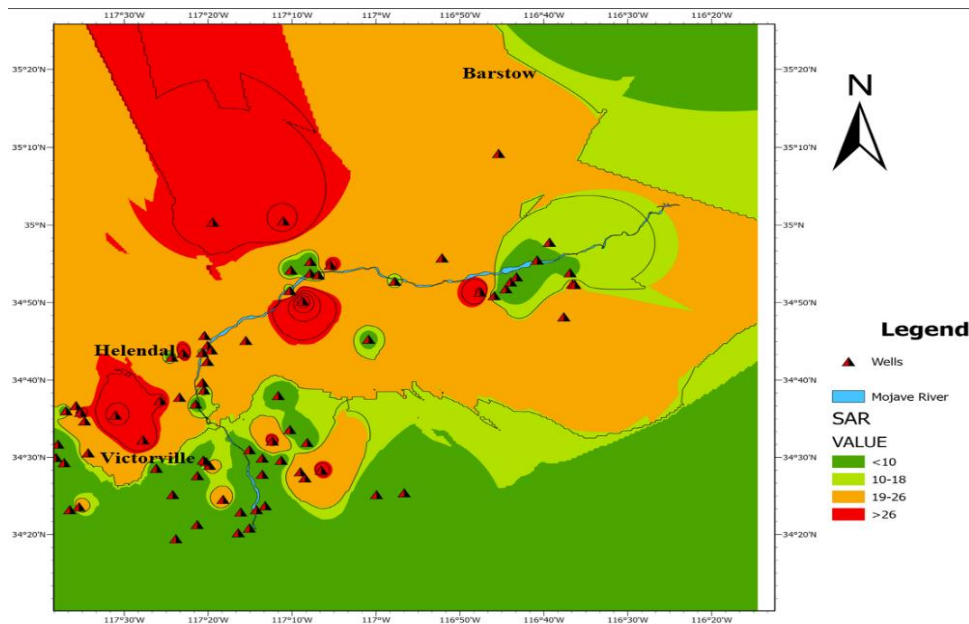


Fig. 6. spatial distribution of sodium adsorption ration (SAR) in Mojave aquifer

2.1.3 Residual Sodium Carbonate

In addition to SAR and Na%, the amount of carbonate and bicarbonate in groundwater that is more than the amount of calcium and magnesium has an influence on the quality of groundwater for irrigation (Xiao et al., 2014).

Because sodium bicarbonate and carbonate encourage the dissolution of organic matter in the soil, which results in a black stain on the soil surface as it dries, their high concentrations are believed to be detrimental to the physical properties of soil (Kumar et al., 2007).

The RSC is determined by deducting the alkaline earths concentration from the carbonate's concentration, as demonstrated below, with all concentrations represented in milliequivalents per liter:

$$\text{RSC} = (\text{CO}_3^{2-} + \text{HCO}_3^-) - (\text{Ca}^{2+} + \text{Mg}^{2+})$$

Positive RSC readings indicate that the sodium content in the soil is high and that the bulk of the calcium and magnesium in the soil have precipitated out. It also shows the high concentration of bicarbonate which causes a higher pH. As a result of the higher pH levels, organic matter precipitates (Hopkins et al., 2007). Based on the RSC measurements, the water can be classified as acceptable, slightly appropriate, and unsuitable if the RSC is less than 1.25 meq/L, between 1.25 and 2.5 meq/L, and greater than 2.5 meq/L respectively (Rao et al., 2012).

Long-term use of high RSC water leads salt to accumulate in the soil, altering its physical and chemical properties. The electrical conductivity is a good indicator of salinity, but the sodium adsorption ratio (SAR) is an excellent indicator of irrigation water's sodicity risk. It has been discovered that waters with high RSC values are more dangerous than waters with low RSC but the same SAR (Murtaza et al., 2021). If some CO_3^{2-} and HCO_3^- precipitates as CaCO_3 (or) MgCO_3 , the RSC in irrigation waters is high. By removing Ca^{2+} and Mg^{2+} from irrigation water, solubility of Na^+ is increased. Depending on the soil texture, crops, soil organic matter, and farmer

management skills, high Na^+ concentrations coupled with low Ca^{2+} concentrations in irrigation fluids, including river waters, often generate variable degrees of soil permeability challenges (Ghafoor et al., 2004). In other words, this situation raises the SAR of soil solution by increasing the amount of Na^+ in the solution and stimulating the precipitation of CaCO_3 in soils. "Long-term irrigation water usage affects soil permeability, which is influenced by the soil's Na^+ , Ca^{2+} , Mg^{2+} , and HCO_3^- concentrations". High RSC also hinders the growth of plants by upsetting their nutritional balance and/or damaging the physical condition of the soil (Murtaza et al., 2021). Six rice and wheat crops were irrigated in rotation with high RSC waters, and Ghafoor et al. (2011) examined the growth response of these crops. High RSC irrigation fluids (14.9 mmol/L) had a negative impact on the first rice crop's grain filling at site 1, whereas site 2's development was successful with relatively low RSC (8.98 mmol/L) water (fig. 7). According to the RSC values, the examined groundwaters were divided into categories (Table 6). Approximately 95.12% of the water samples tested had RSC values under 1.25, making them safe for irrigation.

Table 6) Based on RSC, the quality of groundwater

"RSC"	Quality	Range	Percent
<1.25	Good	-28.9-0.78 (39samples)	95.12
1.25-2.5	Doubtful	1.38-1.66 (2 samples)	4.87
>2.5	Unsuitable	-	-

The regional distribution of residual sodium carbonate (RSC) in the Mojave aquifer is shown in Fig. 7. It reveals that while the best water quality values were discovered in the study area's eastern region, where wells are situated on Miocene volcanic and Mesozoic granitic rocks, the lowest WQI values were found there.

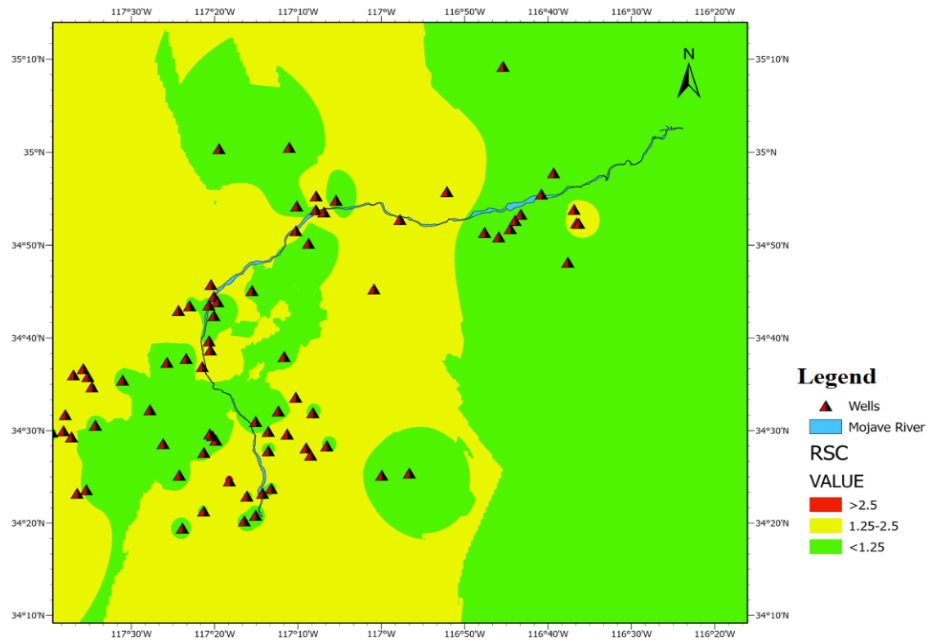


Fig. 7. "spatial distribution of residual sodium carbonate (RSC)" in Mojave aquifer

2.1.4 Magnesium Hazard

Water is divided into three categories: Safe, Intermediate, and Dangerous based on the Mg^{2+}/Ca^{2+} ratio (Ravikumar et al. 2011). Ca^{2+} and Mg^{2+} typically maintain an equilibrium state in most fluids, however they behave differently in soil systems. Magnesium degrades soil structure, particularly in waters that are highly salinized and Na^{+} -predominant. Because of the availability of exchangeable Na^{+} in irrigated soils, there is a high Mg^{2+} concentration. Increased Mg^{2+} levels in water will, in equilibrium, have a detrimental effect on soil quality and lead it to become alkaline, which will negatively affect crop production (Ravikumar et al., 2011).

In order to assess if water quality is appropriate for agricultural usage, Szaboles and Darab (1964) established the magnesium hazard (MH). If the MH value is greater than 50, groundwater cannot be used for irrigation.

$$MR = [Mg^{2+}/(Mg^{2+} + Ca^{2+})] * 100$$

where all values in meq/L.

As the soils grow more alkaline, magnesium hazard (MH) levels more than 50% would have a negative impact on crop output. MH values ranged from 14.2 to 44.8 in the study region. All examined samples had MH values below 50 and may be used for irrigation (fig. 8).

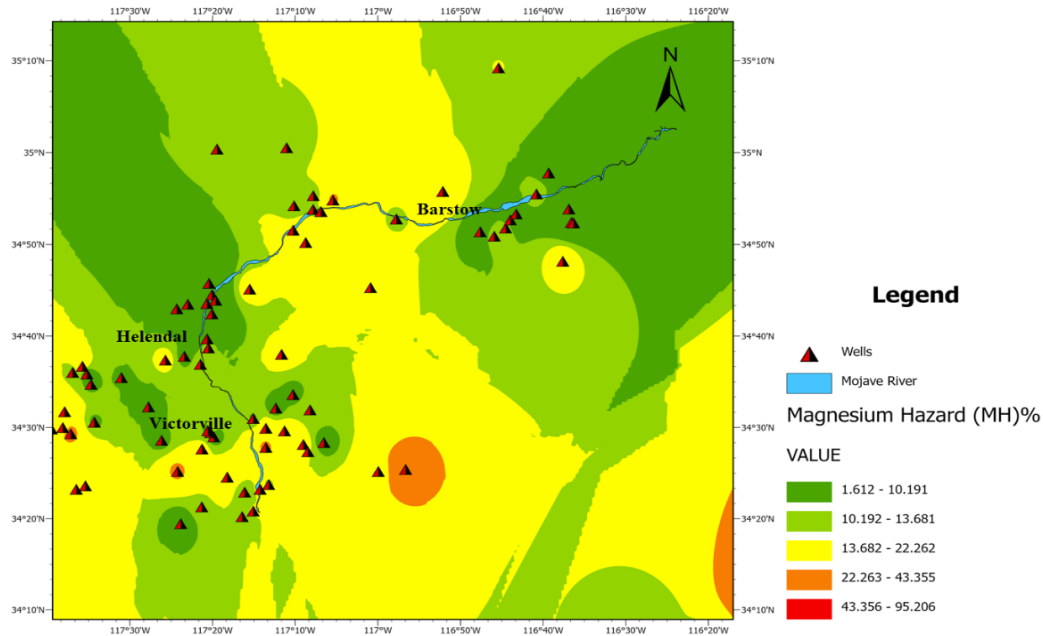


Fig. 8. Spatial distribution of Magnesium hazard (MH) in Mojave aquifer

2.1.5 Permeability Index

The permeability of the soil is significantly impacted by prolonged irrigation with water that is mineral-rich (Ca^{2+} , Mg^{2+} , Na^+ , HCO_3^-). The permeability index controls the degradation of agricultural soil. Utilizing irrigation water that is mineral-rich over an extended period of time reduces soil aeration, making it difficult to plow and delaying seedling emergence. Doneen (1964) created standards for classifying water based on the Permeability Index value. Three categories— I, II, and III—were used to group these requirements. Class I and II soils that have permeability indices of 75 or above are thought to be acceptable for irrigation. Water classified as Class III and having a permeability index of 25 or less is not recommended for irrigation (Rao et al., 2012). As a result, Doneen (1964) developed a standard based on the Permeability Index (PI) calculation for assessing the suitability of groundwater for irrigation:

$$PI = (Na^+ + \sqrt{HCO_3^-}) \times 100 / (Ca^{2+} + Mg^{2+} + Na^+)$$

In the Mojave Aquifer, 39% of the samples are classified as Class I (PI > 75%) and 61% as Class II (PI = 25-75%), indicating that the influence of the examined groundwater is a limit on soil permeability (fig. 9). According to the aforementioned calculation, the high permeability index values might be attributed to the water samples' high Na⁺ and HCO₃⁻ contents.

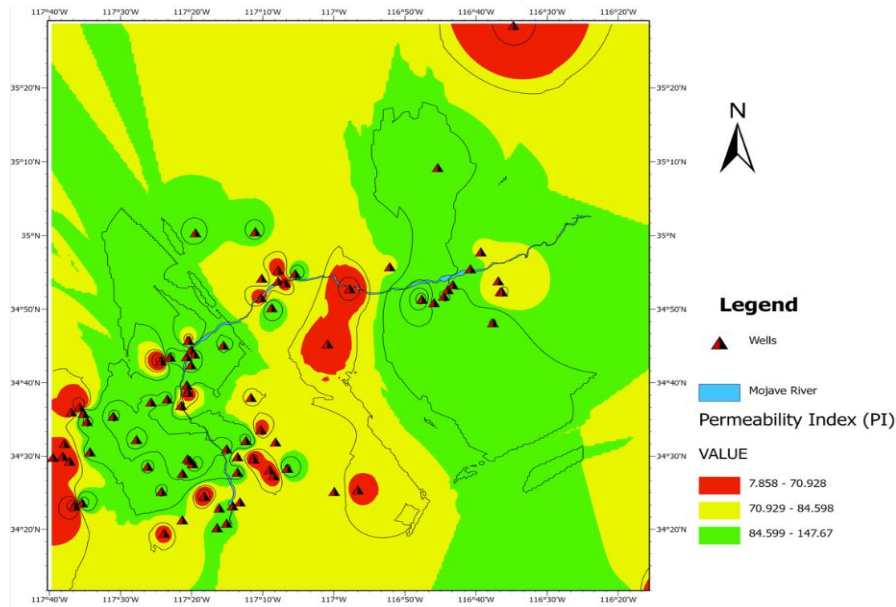


Fig. 9. "Spatial distribution of permeability index (PI)" in Mojave aquifer

2.1.6 Potential Salinity

Another indicator of the quality of the water is potential salinity (PS). The following equation, which assesses the risk of excessive salt concentration caused by Cl⁻ and SO₄²⁻, is used to represent it (Khanoranga and Khalid, 2019). Compared to Cl salts, SO₄²⁻ salts are substantially less hazardous. So, half of the SO₄²⁻ salt is taken into account when estimating potential salinity (Sutradhar and Mondal, 2021). Three categories of water are determined by this parameter: appropriate (PS3 meq/L), medium (3–15 meq/L), and unsuitable (>15 meq/L) (Delgado et al., 2010).

$$PS = Cl^- + SO_4^{2-}/2$$

Table 7) "The groundwater classification based on potential salinity"

Potential Salinity	Water class	Range	Percent
<3.0	Excellent to Good	0.18-2.93(24samples)	47
3.0-5.0	Good to Injurious	3.1-4.93 (13samples)	25.5
>5.0	Injurious to Unsatisfactory	5.26-21.69(14samples)	27.46

The range of possible salinity in the examined water samples is 0.18 to 21.7 meq/L. About 47% of the water samples are in the "excellent to good class", 25.5% of samples are in the class of "good to injurious", whereas 27.5% of the samples fall into "injurious to unsatisfactory" category (Table 7). Wells located in the cities of Victorville, Helendale, and Barstow are based on the geographical distribution map of potential salinity. Sulphate and chloride are utilized economically, primarily in the various chemical industries, and are naturally present in a variety of minerals (fig.10). Although they are released into the environment by air deposition and industrial waste, the greatest concentrations in groundwater are often caused by natural sources. Ammonium sulphate may also be present in groundwater that has been contaminated by fertilizer and industrial waste.

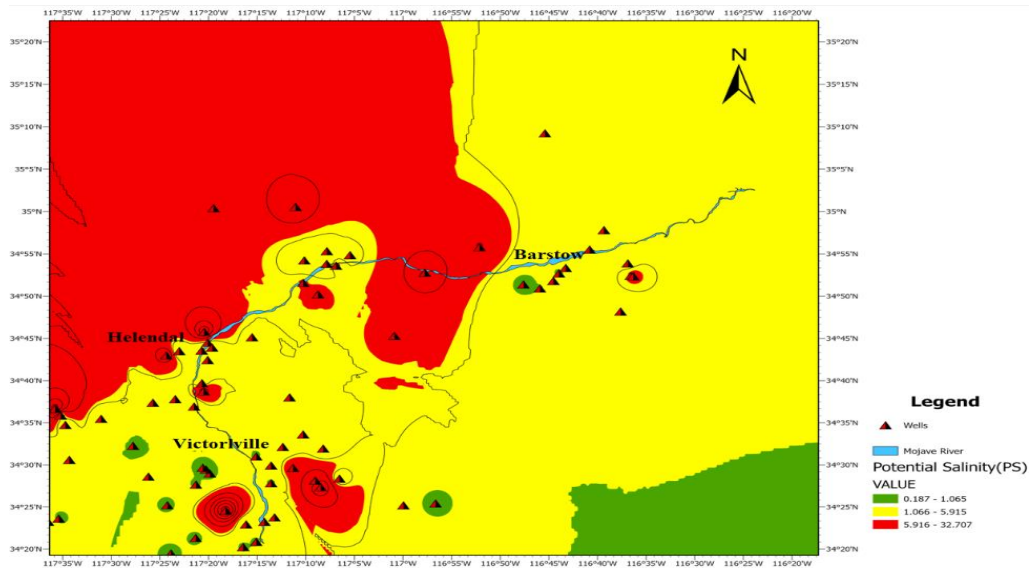


Fig. 10. "Spatial distribution of potential salinity (PS)" in Mojave aquifer

2.2 Nitrate Assessment in the Mojave Aquifer

Although it can originate from natural sources, nitrate is one of the most prevalent contaminants in California's groundwater and is mostly over the MCL (maximum concentration limit) as a result of human activities (Brown et al., 2020).

A thorough scientific knowledge of N species transit and change in the subsurface is needed to address the concerns of nitrogen species contamination in groundwater. This is a challenging task, though, as various aquifers may be impacted by many sources of pollution at once and be identified by the presence of "diverse N-cycle activities" along groundwater flow paths. Investigation of subsurface N fluxes in agricultural regions may appear even more difficult due to the predominance of diffusive N pollution, which makes estimating the entire pollutant intake into aquifers difficult. It may be very difficult to comprehend pollutant transmission across various aquifer regions and between various environmental compartments within a given catchment, such as sediment, soil, the atmosphere, groundwater, surface water, and biota, in such a situation (Nikolenko et al., 2018). Stable isotope analysis is used by many environmental researchers to learn more about the source, movement, and alteration of nitrogen in groundwater. Understanding N migration and mixing from various sources, identifying various chemical and biological processes involving N species, and investigating the dynamics and effects of reactions that take place are all made easier with the help of this strategy (Kaushal et al., 2011).

" $\delta^{14}\text{N}$ and $\delta^{15}\text{N}$ are two naturally occurring stable isotopes of nitrogen, with natural abundances of 99.633 percent and 0.366 percent, respectively". $\delta^{16}\text{O}$ (99.757%), $\delta^{17}\text{O}$ (0.038%), and $\delta^{18}\text{O}$ (0.205%) are also the three stable isotopes of oxygen. Nitrogen and oxygen are involved in a variety of physical and chemical reactions in the natural world. The stable isotope composition is often expressed in terms of the appropriate international standards using per mil notation and

delta units:

$$\delta (\text{‰}) = [(R_{\text{sample}} - R_{\text{standard}}) / R_{\text{standard}} - 1] * 1000$$

where " $(^{15}\text{N}/^{14}\text{N}$ or $^{18}\text{O}/^{16}\text{O})$ R" is the ratio of heavy to light isotopes. The positive and negative results represent, respectively, an enrichment and a depletion of heavy isotopes in the test sample as compared to the reference sample. In contrast to N_2 (air) and "Vienna Standard Mean Ocean Water (V-SMOW)", the nitrogen and oxygen isotope ratios (R) are represented as a percentage deviation from the $^{15}\text{N}/^{14}\text{N}$ or $^{18}\text{O}/^{16}\text{O}$ ratios, respectively (Zhang et al., 2019). The microbial denitrifier method, which uses denitrifying microorganisms to produce nitrous oxide (N_2O) from nitrate, is used to evaluate the isotopes of nitrate (snow et al., 2018).

N isotope measurements in groundwater have been used for decades in denitrification investigations to identify the source of N pollution and calculate its attenuation. The method of N stable isotope analysis is currently being utilized more often in studies of N_2O transport and production/consumption in the subsurface due to the growing interest in climate change. Applications of this approach in this field are anticipated to improve quantification of N_2O fluxes, identify areas vulnerable to such emissions, and aid in the understanding of mechanisms governing indirect N_2O emissions via groundwater pathways. These outcomes will all help to improve the constraint and more realistic delineation of N budget and GHG emission on a regional and global scale (Nikolenko et al., 2018). Interpreting the experimental data can be challenging even though changes in stable N isotope ratios ($^{15}\text{N}/^{14}\text{N}$) may possibly reveal important information about N fluxes in agro-ecosystems. The observed patterns of isotopic enrichment factor of N species are significantly influenced by shifting dynamics of various microbiological (denitrification) processes, in addition to the continuous simultaneous mixing of N species derived from various N pools, such as atmospheric precipitation, soil organic matter, synthetic fertilizers, and manure

characterized by different isotope compositions (Kendall, 1998). Therefore, it is crucial for proper interpretation of isotope signature variability to comprehend the factors and processes that may contribute to such variability, take into account the likely magnitude of potential alterations, confirm the findings of observations across a variety of ecosystems with various environmental settings, and support the interpretation of observed ^{15}N values with findings from other experimental methods (Hosono et al., 2013).

The reported intake of nitrogen into groundwater in agricultural areas comes from a variety of sources, including inorganic and organic fertilizers, soil organic N, manure, sewage, and atmospheric precipitation. Each source of nitrogen has distinct periods of $\delta^{15}\text{N}\text{-NO}_3$ enrichment values that may be used to identify the source of the NO_3 and calculate how much of the groundwater's content each source of NO_3 contributes. Organic and inorganic fertilizers have been shown to have different isotopic signatures, which may be accounted for by how they were made. However, due to N isotope fractionation during various physicochemical or biochemical processes (such as NH_3 volatilization, nitrification, or denitrification), the typical isotopic composition of inorganic fertilizers in groundwater periodically fluctuates (Xue et al., 2016). On the other hand, compared to inorganic fertilizers, organic fertilizers, such as plant compost and liquid and solid animal manure, have higher starting $\delta^{15}\text{N}$ values and a wider range of isotopic composition (+6 ‰ to +30 ‰). This is explained by mechanisms occurring in animal wastes, such as isotopically light N excretion in urine, the accumulation of heavy $\delta^{15}\text{N}$ isotope in leftover waste, and the volatilization of $\delta^{15}\text{N}$ -deficient ammonia with subsequent oxidation of leftover waste (Sharp, 2007). Due to the significant enrichment of $\delta^{15}\text{N}$ caused by the volatilization of NH_3 during storage, treatment, and application, and the majority of this NH_4^+ being subsequently oxidized to $\delta^{15}\text{N}$ -enriched NO_3 , NO_3 produced by nitrification of manure-N has a higher $\delta^{15}\text{N}\text{-NO}_3$ than both

organic and inorganic fertilizers (Widory et al., 2004).

Bacterial decomposition of organic materials derived from the degradation of plant and animal manure results in soil organic-generated NO_3 . The " $\delta^{15}\text{N}-\text{NO}_3$ " of soil NO_3 can range from +3‰ to +8‰. The likely mixing of nitrogen (N) from fertilizer inputs and N mineralized from soil organic matter, which might not be taken up by crops if their needs are already satisfied, must also be taken into consideration in fertilizer-polluted groundwater (Li et al., 2007). For instance, Danielescu and MacQuarrie (2013) discovered that 72% of the surface and groundwater samples from the Trout catchment were within the overlapped range of +3‰ to +5‰. This suggests that the reported levels may be related to the use of NH_4^+ fertilizers or the presence of NO_3 generated from organic materials in the soil. Contact with soil N frequently has less of an effect on the isotopic signature of NO_3 coming from animal or sewage waste since the distribution of waste is typically restricted at point sources with high concentrations.

The amount of nitrogen in atmospheric precipitation is influenced by a number of processes, including NH_3 volatilization, nitrification and denitrification in soils, and the effects of several anthropogenic sources. According to Bedard-Haughn et al. (2003), rain generally contains more $\delta^{15}\text{N}-\text{NO}_3$ than the co-existing $\delta^{15}\text{N}-\text{NH}_4^+$. The sources of NO_3 pollution are distinguished by somewhat diverse $\delta^{15}\text{N}-\text{NO}_3$ isotope ranges, as seen in this overview: "Rainwater – 12 to +11 ‰, inorganic fertilizers – 8 to +7 ‰, organic fertilizers + 6 to +30 ‰, soil organic matter + 3 to +8 ‰, manure +5 to +35 ‰, and household sewage + 3 to +25 ‰". The lowest values are for inorganic fertilizers, followed by the highest values, which may overlap, for NO_3 produced from soil organic matter and manure. However, the isotopic composition of NO_3 from various sources may be susceptible to considerable variations because of fractionation processes occurring during certain biochemical or physicochemical events during migration to or within the aquifer (Clark,

2015).

The ambient characteristics of hydrogeological systems where nitrification and denitrification occur, such as the availability of electron donors, dissolved oxygen content, temperature, pH, residence duration, and other factors, have an impact on the amplitude of the reactions (Böttcher et al., 1990). When discussing the impacts of fractionation caused by denitrification, the availability of electron donors is typically taken into account. In general, it is suggested that when there are few electron donors, denitrification may not have a substantial impact on increasing the $\delta^{15}\text{N}$ of NO_3 (Choi et al., 2003). The microbial oxidation of organic C or reduced S that may be present in the water might provide the denitrification process with the electrons needed. The amounts of dissolved oxygen (DO) in hydrogeological systems can also have a sizable impact on the NO_3 isotope signatures. It could affect the kinds of N biochemical processes that take place, which might lead to changes in the $\delta^{15}\text{N}$ of NO_3 that are either positive or negative. Low oxygen levels and denitrification processes, which raise $\delta^{15}\text{N}\text{-NO}_3$, are typically linked. On the other hand, nitrification reactions usually include higher oxygen levels, which leads to low $\delta^{15}\text{N}\text{-NO}_3$ ratios. Any seasonal changes could affect the $\delta^{15}\text{N}\text{-NO}_3$, resulting in higher isotopic enrichment in aquifers where denitrification occurs in the summer or lower values in groundwater influenced by nitrification activity in the winter. This is because water temperature influences microbial activity and, as a result, DO content in groundwater. Evidence of the impact of water temperature is still not obvious, yet, since other articles contend that seasonal fluctuations in $\delta^{15}\text{N}\text{-NO}_3$ levels are not present (Danielescu and MacQuarrie, 2013). To better understand NO_3 production/consumption mechanisms and the impact of temperature on their dynamics, it is essential to look at microbial communities and the distribution of possible denitrifying species (Hernández-del Amo et al., 2018). The pH range is another important factor that controls the

intensity of microbiological activities and the degree of fractionation impact. It has been discovered that the optimal pH range for nitrification is between 6.5 and 8, with reaction rates anticipated to be significantly decreased below pH 6.0 and above pH 8.5. The ideal pH is site-specific, however denitrification processes often take place in a range of 5.5 to 8 due to the effects of adaptation on microbial populations (Tomaszewski et al., 2017). The extent of confined and unconfined zones in the subsurface system, their connection, and the location of recharge areas along the aquifer are a few examples of the hydrogeological characteristics that should be thoroughly examined in conjunction with a thorough examination of the distribution of $\delta^{15}\text{N-NO}_3$ in groundwater (Nikolenko et al., 2018).

Different human sources and atmospheric and terrestrial NO_3 sources may be distinguished using both the $\delta^{18}\text{O}$ and $\delta^{15}\text{N}$ of NO_3 (Xue et al., 2016). Additionally, the difference between N_2O produced by nitrification and N_2O produced by denitrification may be determined using oxygen isotope ratios (Jin et al., 2015). It may be possible to discriminate between NO_3 inflows coming from fertilizer application and other sources, such as nitrification of NH_4^+ or organic N, using the isotopic signature $\delta^{18}\text{O-NO}_3$ in particular. The $\delta^{18}\text{O}$ value of synthetic NO_3 fertilizers, which are produced from atmospheric N_2 , is around +23.5‰ in the atmosphere (Moore et al., 2006). Because NO_3 from nitrification processes only includes one $\delta^{18}\text{O}$ atom from dissolved air O_2 and the remaining two atoms from water, NO_3 from other sources has a lower $\delta^{18}\text{O}$ value (Kendall and Aravena, 2000). The isotopic signature of nitrified $\delta^{18}\text{O-NO}_3$ may be calculated using the following equation:

$$" \delta^{18}\text{O}_{\text{NO}_3} = 1/3 * \delta^{18}\text{O}_{\text{O}_2} + 2/3 * \delta^{18}\text{O}_{\text{H}_2\text{O}} "$$

Nitrification has been associated with $\delta^{18}\text{O-NO}_3$ levels that are near to zero (Böhlke et al., 2006) or between -2‰ and +6‰ (Liu et al., 2006). However, a number of mechanisms that might

alter those numbers affect the isotopic composition of NO_3 produced during nitrification: 1) Evaporation may enrich H_2O in $\delta^{18}\text{O}$ isotopes (Hoefs and Hoefs, 2015), 2) In contrast to air O_2 , O isotope fractionation during respiration can increase the soil's ^{18}O value, 3) "the ratio of O incorporation from H_2O and O_2 is not exactly 2:1 (e.g. more O_2 may be derived from atmospheric O_2 when NH_4^+ is limiting)" (Kool et al., 2011), 4) Nitrification may be suppressed by low pH conditions that promote the growth of another microbial activity that consumes more ambient O_2 than nitrification (Xue et al., 2016) , and 5) "oxygen isotope exchange of intermediates (particularly NO_2) with natural water" (Granger and Wankel, 2016).

Furthermore, atmospheric precipitation may have an impact on "the isotopic expression of $\delta^{18}\text{O}\text{-NO}_3$ " in groundwater. Its $\delta^{18}\text{O}$ range is from +30 to +70‰ (Barnes et al., 2010). A seasonal variation was identified in atmospheric NO_3 deposition of $\delta^{18}\text{O}\text{-NO}_3$ by Williard et al (2001). They connected atmospheric NO_3 with $\delta^{18}\text{O}$ in the range of 52.5‰ to 73.4‰. However, such high $\delta^{18}\text{O}$ concentrations are uncommon in agricultural regions like the southern portion of California and are frequently found in groundwater beneath forest ecosystems that have not had significant anthropogenic impact. The typical $\delta^{18}\text{O}$ values of NO_3 derived from nitrification are significantly lower than those of NO_3 derived from precipitation and NO_3 derived from fertilizer application (including $\delta^{18}\text{O}$ values of NO_3 derived from NH_4^+ in fertilizers and precipitation, NO_3 derived from soil N, and NO_3 derived from manure and sewage). Constant ratios can be used to identify the simultaneous enrichment of residual NO_3 with $\delta^{18}\text{O}$ and $\delta^{15}\text{N}$ isotopes caused by denitrification. Therefore, combining N and O isotope measurements with O isotope analysis can aid in the understanding of the nature of the $\delta^{15}\text{N}$ variation in groundwater (Zhang, et al., 2019).

2.2.1 The Correlation Between Nitrate and Various Factors in Mojave Aquifer

The concentration of nitrate in the Mojave aquifer varied from 1.36 to 21.8 mg/L, with a

mean value of 4.5 mg/L. (fig.11). All water samples, with the exception of one well in the southwest corner of the Mojave basin aquifer, had nitrate concentrations below the Maximum Contaminant Level (MCL) established by the Environmental Protection Agency (fig.12). The mean level of nitrate in the aquifer is around 4.2 mg/L, however 30% of the examined wells have nitrate concentrations greater than 3 mg/L. The so-called "human influenced value" is the nitrate concentration in groundwater that exceeds the 3 mg/L NO_3^- -N threshold and is deemed contaminated as a result of human activity (Babiker et al., 2004). According to the graph (fig. 12), the years from 2007 to 2009 had the highest concentration of nitrate. The California Department of Water Resources (2010) has estimated that this period (2007-2009) has been " the 12th driest period in recorded climatic history" in southern part of California.

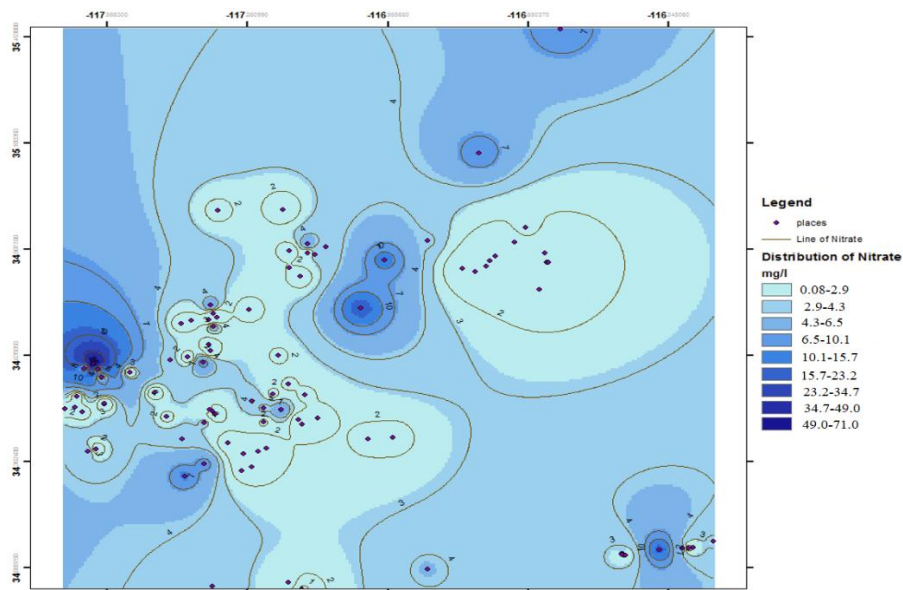


Fig.11. Spatial distribution of nitrate in Mojave aquifer

According to Jutglar et al (2021), Increasing the intensity and durations of wet-dry cycles, which may result in higher groundwater nitrate concentrations due to nitrate flushes after drought termination, are one primary factor in high nitrate values.

The amount of nitrate that is available for leaching from soil is the key factor affecting the

nitrate content of groundwater in shallow groundwater where oxygen is typically present. In the top 30 m of an aquifer in the Mojave, nitrate levels dropped with depth. In many circumstances, it is challenging to forecast the time needed for nitrate to flow through the soil into ground water because of various factors such as application rate, the soil type and the depth to the water table (Mike Nugent et al., 1993). (Mike Nugent et al., 1993). The relation between nitrate content and well depth is inverse, as seen in Fig. 13. In the research location, the top 50 m of groundwater typically has high nitrate values. Nitrate content reduces with depth below 50 m. No definitive conclusions can be drawn regarding the vertical nitrate profile in groundwater, despite the possibility that land cover, soil type, and groundwater recharge all have a significant influence on nitrate concentrations. The typical statistical characteristics of nitrate levels relative to well depth are provided in Fig. 14 and table 8 in order to more clearly illustrate how nitrate content varies with depth.

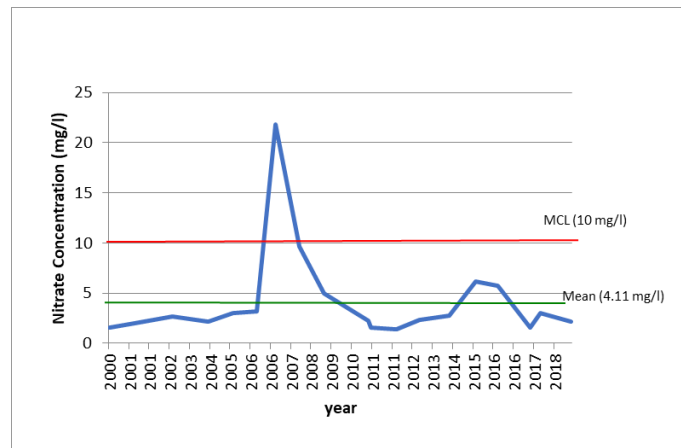


Fig. 12. nitrate concentration of Mojave aquifer in the range date of 2000-2018 (the average value of all sampled well in each year)

The result demonstrates that nitrate concentration reaches its peak between 0 and 30 meters below the surface. The denitrification process, which occurs when nitrate is reduced chemically or biologically in the presence of organic carbon and denitrifying bacteria, is likely the cause of

certain wells' nitrate concentrations in the 30–50 m range being lower than those in the >50 m range (Majumder et al., 2008). The characteristics of nitrate's horizontal and vertical distribution in groundwater point to a surface source of nitrate contamination.

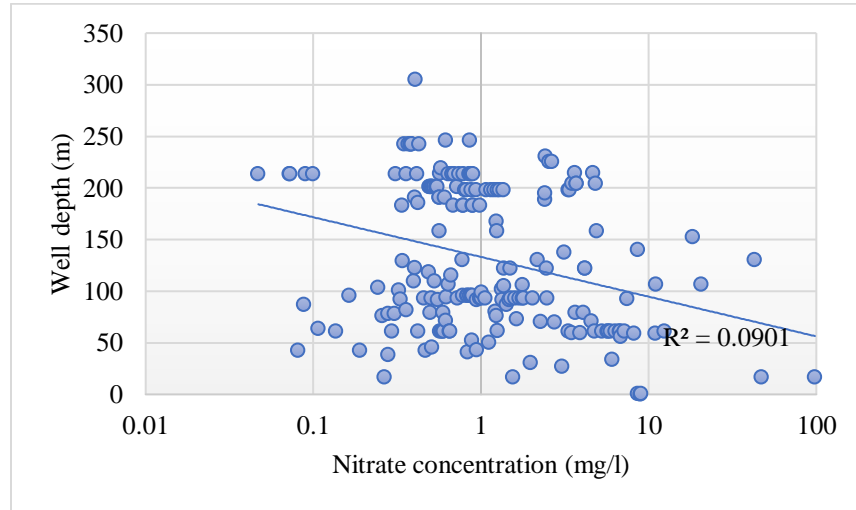


Fig. 13. Vertical distribution of nitrate contents in Mojave aquifer

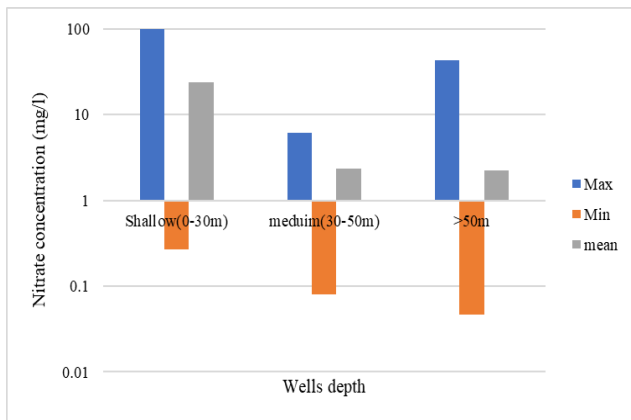


Fig. 14. The max, min, and mean value of nitrate in different depths

Table.8) Nitrate concentration in different depths

value	Depth		
	Shallow(0-30m)	medium(30-50m)	>50m
Max	98.1	6	42.8
Min	0.3	0.08	0.05
mean	23.8	2.4	2.2

Additionally, in this study the spearman correlation between main factors such as well depth, EC, SO₄, Ca, Mg and K may affect the nitrate concentration in the groundwater is evaluated using bivariate plots against NO₃ (fig.15). A rise in NO₃ with an increase in the ionic strength of the groundwater in the Mojave aquifer was shown by a positive relation between EC and nitrate

(Fig 6). This demonstrates that nitrate and major ions might be generated from the same source(s).

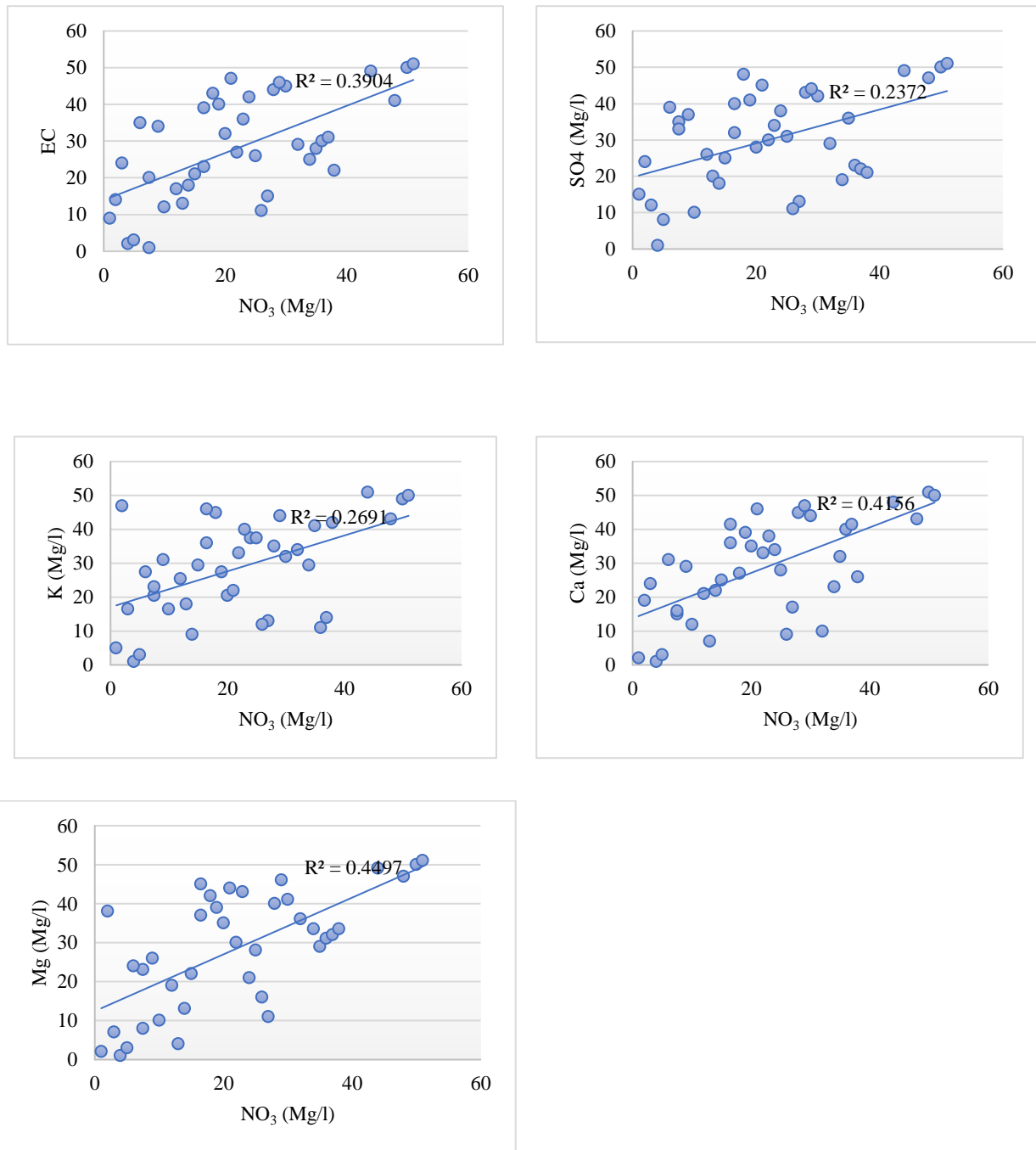


Fig. 15. The graphs showing correlation between nitrate and major ions in the Mojave aquifer

2.2.2 Evaluation of Nitrate Sources Using Stable Isotopes

In the Mojave aquifer the $\delta^{15}\text{N-NO}_3$ ranged from +1.0 to +11.5‰, while $\delta^{18}\text{O-NO}_3$ ranged from -1.7 to 7.8‰ respectively from 2005 to 2019 (Fig. 16), (table 9). However, the $\delta^{15}\text{N-NO}_3$ and $\delta^{18}\text{O-NO}_3$ in one well located on Fort Irwin (the north part of Mojave Desert) is +18.5 and +11.1‰ respectively. This well is located in urban area with a shallow depth of 3.2 feet showing the effect of manure and septic wastewater on nitrate concentration in the groundwater. Hence, according to the typical end-members ranges of nitrate isotopes (Kendall, 1998) in the studied wells, the most samples fall the overlapped ranges between soil organic matter (from +3‰ to +8‰), manure (from +5‰ to +25‰), and of chemical fertilizers (from -6‰ to +6‰) and Mixing of different sources could also provide the general trend observed in the data (fig. 16). Therefore, the ratios of $\delta^{15}\text{N-NO}_3^-$ and $\delta^{18}\text{O-NO}_3^-$ were mostly spread among the chemical fertilizer, soil and organic matter, and manure whereas the ratios of $\delta^{15}\text{N-NO}_3^-$ and $\delta^{18}\text{O-NO}_3^-$ were moderately scattered, suggesting that the nitrate contamination was brought on by the three sources together. It is challenging to determine which of the sources is prominent due to the overlap.

Manure is the most likely source of NO_3^- in the polluted wells because active agricultural regions, urban areas, and a small number of dairy farms are all present. The NO_3^- pollution may result from manure being used as fertilizer to agricultural lands or from direct contamination of urban wastewater.

The enrichment ratios of $\delta^{15}\text{N}$ and $\delta^{18}\text{O}$ are positively associated by a factor ranging from 1.3:1 to 2.1:1, and the nitrification raises the values of $\delta^{15}\text{N}$ and $\delta^{18}\text{O}$ nitrate. This demonstrates that even if isotope fractionation via denitrification occurs, the initial isotope composition may still be inferred by knowing the enrichment factor. However, it seems that denitrification doesn't the only factor affecting nitrate concentration in the Mojave aquifer. if denitrification was responsible for the increasing δ values, the wells with heavier values would have a lower nitrate concentration.

This does not appear to be the case as the wells with heavier δ values also have a higher nitrate concentration (Fig. 16).

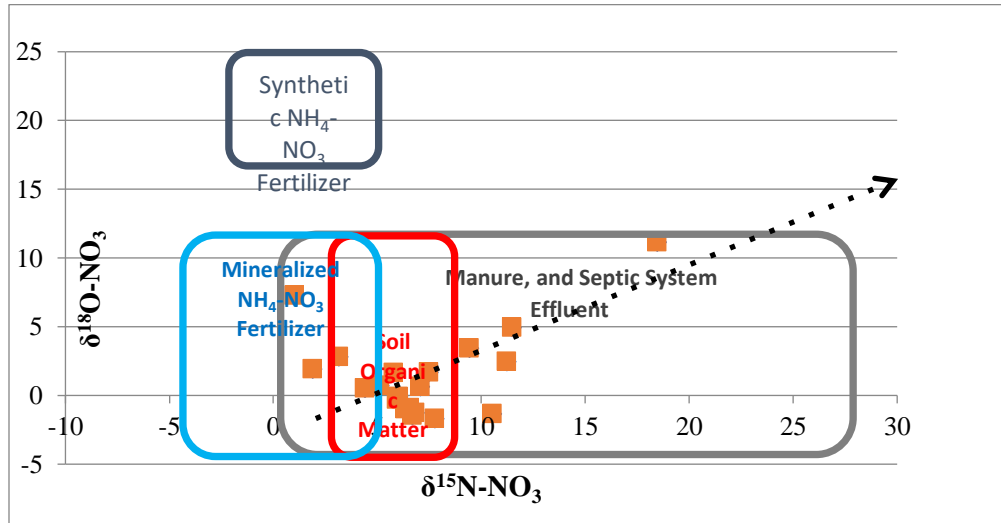


Fig. 16 "Expected $\delta^{15}\text{N-NO}_3$ versus $\delta^{18}\text{O-NO}_3$ ranges for natural and anthropogenic nitrate sources. (The ranges of isotopic composition of various sources including atmosphere deposition, Chemical NO_3^- fertilizer, chemical nitrogen fertilizer, soil organic nitrogen and manure & sewage in the diagram were based on Kendall (1998))"

The correlation between the well depths and nitrate concentration indicated that NO_3^- contamination is most prevalent in about 70% ($n=110$) of shallower wells of the Mojave aquifer demonstrating how NO_3^- travels from the surface to the aquifer system. or through advection and dispersion, flows through the aquifer system. On the other hand, 30% of the studied wells with depth more than 100 m have nitrate concentration more than 3 mg/L and the mean value of 15.7 mg/L. Most likely, the pollution was brought on by irrigation water that had come into contact with manure over a period of time that may have spanned many years. Isotopic data can be used to assess the infiltration of irrigation water polluted with NO_3^- . The enriched δH and $\delta^{18}\text{O}$ values in wells with high NO_3^- concentrations (Fig. 17) (table 9) suggest that either groundwater is pumped from the enriched water of all the examined wells or that groundwater is refilled by

irrigation canals.

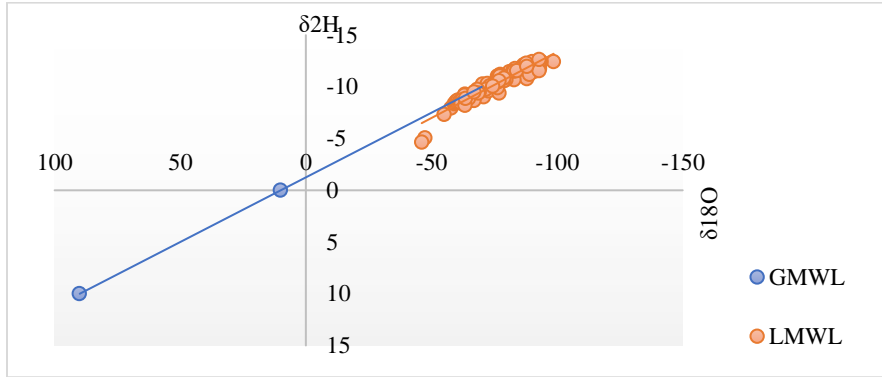


Fig. 17. "The global meteoric water line (GMWL) compared to the local meteoric water line" in the study area

Table 9) the nitrate and stable isotopes values in the studied wells-Mojave aquifer

well-no	NO ₃ (mg/L)	$\delta^{15}N$ (air) %	$\delta^{18}O$ (V-SMOW) %	Ln (NO ₃)	1/NO ₃
USGS 340821116185801	4.5	5.9	-0.3	1.50	0.2
USGS 340718116263701	2.0	6.4	-1	0.7	0.5
USGS 340734116264301	3.3	1.0	7.2	1.2	0.3
USGS 345551116520801	4.2	9.5	3.4	1.4	0.2
USGS 342316117362501	4.0	7.8	-1.7	1.4	0.2
USGS 340729116264702	2.4	3.1	2.8	0.9	0.4
USGS 340809116215201	18.4	5.9	-0.1	2.9	0.05
USGS 340738116244301	5.0	6.8	-1.2	1.6	0.2
USGS 340831116172201	2.6	5.1	0.7	0.9	0.3
USGS 340824116180701	21.8	7.5	1.7	3.0	0.05
USGS 352829116344501	8.6	5.8	1.6	2.1	0.1
USGS 350918116452401	8.9	18.5	11.1	2.2	0.1
USGS 340824116180701	2.1	7.0	0.6	0.8	0.4
USGS 341932117235101	11.1	1.9	1.9	2.4	0.09
USGS344522117005301	20.7	10.5	-1.3	3.0	0.05
USGS345523117074901	1.2	6.0	-0.09	0.2	0.8
USGS345356116365301	1.6	4.4	0.5	0.5	0.6
USGS345251116574203	12.4	11.5	4.9	2.5	0.08
USGS343646117354501	98.1	11.2	2.5	4.6	0.01
USGS345136117101201	2.0	6.7	-1.5	0.7	0.5
USGS 340738116244301	1.8	6.6	-0.9	0.5	0.6

To distinguish between denitrification and simple mixing, plots of the $\delta^{15}N$ -NO₃ composition vs the natural log and inverse (1/NO₃) concentrations can be used. Denitrification in this aquifer might be disregarded since the plot of " $\delta^{15}N$ -NO₃ versus NO₃ and natural log of

nitrate" (Fig. 18) does not indicate the drop in NO_3 concentration caused by the " $\delta^{15}\text{N}-\text{NO}_3$ enrichment" to imply fractionation by denitrification (Yin et al., 2020). Additionally, the lack of a link between the inverse nitrate concentration and the $\delta^{15}\text{N}-\text{NO}_3$ indicates the role that denitrification played in the Mojave aquifer's nitrate pollution.

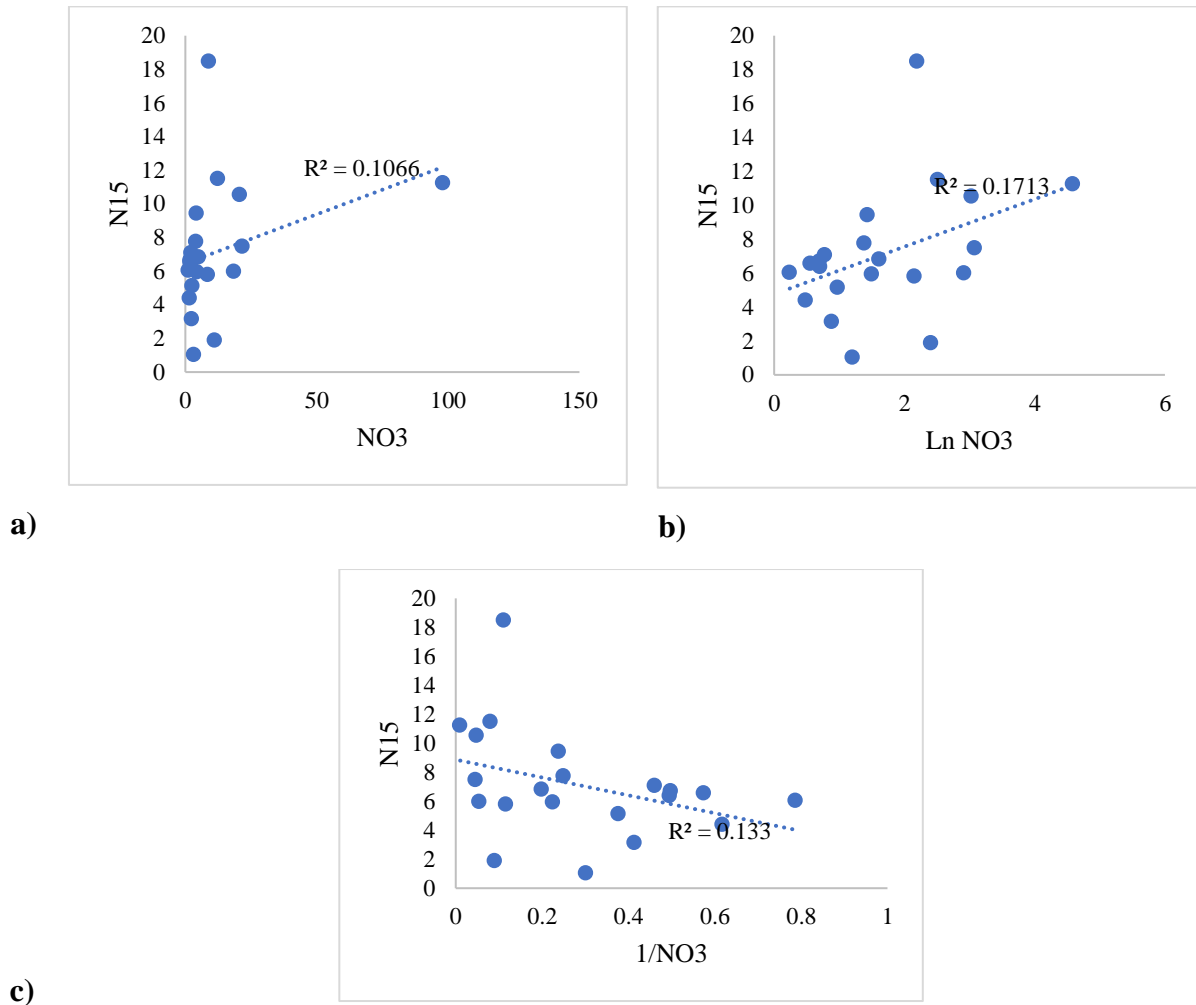


Fig.18. a) Nitrate versus $\delta^{15}\text{N}-\text{NO}_3$, b) natural log of nitrate concentration versus $\delta^{15}\text{N}-\text{NO}_3$, and c) inverse nitrate concentration ($1/\text{NO}_3$) versus $\delta^{15}\text{N}-\text{NO}_3$

2.3 Heavy Metals Evaluation in Groundwater

Because of the world's rising population and economic growth, heavy metal pollution in groundwater has become a severe problem, with metals entering through a variety of natural and

manmade processes. In contrast to human sources, such as mining and mineral extraction, household, agricultural, and industrial wastes, natural processes include the weathering of rocks and soils, the decomposition of living things, and the influence of the atmosphere (Kabir et al., 2020; Singh et al., 2017; Dede, 2016). Micronutrients that are classified as heavy metals can be hazardous to human health if their concentration exceeds the set limits. As a result, it is crucial to assess the presence of heavy metals with a relatively high concentration in groundwaters in dry and semiarid regions like southern California, which is the major emphasis of this research. For instance, more than 13 million Americans, mostly in Western states, are exposed to arsenic in drinking water at quantities more than 10 $\mu\text{g/L}$. (Adelaju et al., 2021). As a result, monitoring them in groundwater used for drinking purposes is critical for human health (Singh et al., 2014).

According to Musgrove (2021), strontium (Sr) distribution and abundance data from groundwater samples taken from 32 major aquifers (PAs) in the United States were used to examine factors that impact the concentration of Sr. The common trace element strontium was detected in 99.8% of groundwater samples ($n = 4,824$; median = 225 $\mu\text{g/L}$), and it is present in soils, rocks, and water. Concentrations in 2.3 percent of the samples above the 4,000 $\mu\text{g/L}$ health-based screening threshold. The groundwater type has a role in determining the proportionate influence of regulating variables on Sr concentration, which is regionally variable. As it has a relatively high concentration in the Mojave aquifer in the southern part of California due to the carbonate water type of this aquifer, the majority of high concentrations ($>4,000 \mu\text{g/L}$) in drinking-water supply wells were observed in samples from carbonate aquifers that were the result of "water-rock interaction with Sr-bearing rocks and minerals" (Hassanvand and Hays, 2022). High Sr concentrations from monitoring wells were more common in unconsolidated sand and gravel aquifers in dry or semi-arid regions where shallow groundwater is affected by irrigation and

evaporative concentration of dissolved elements together with lithologic or applied Sr sources. A high concentration of total dissolved solids always denotes a high Sr content. With 86 percent reliant on carbonate aquifers, an estimated 2.2 million people in the southeast of the United States may receive their water from public supply wells with high Sr concentrations.

As a result, there are several indices available to measure the quantity of heavy metals in groundwater. WQI could only examine physical characteristics and major ion chemistry; it does not include all potential contaminants, such as heavy metal and trace element toxicity (Sahoo and Khaoash, 2020). However, the Heavy metals Pollution Index (HPI), Heavy Metals Evaluation Index (HEI), and Cd (Contamination Index) indices are frequently used to define the general condition of water quality with regard to heavy metals and to evaluate the quality of water for drinking and irrigation uses (Kabir et al., 2020). (table 11).

HPI evaluates the combined impact of individual heavy metals on overall water quality. Its calculation method is based on a rating system (value ranges between 0 and 1) that can be used to rank particular heavy metals according to how important quality concerns they are to society as a whole. It can also be used to calculate values that are inversely proportional to the maximum permissible (Si) and maximum desirable limits (Ii) for each heavy metal. The amount of heavy metal ions present and their concentrations in relation to the permitted water quality criteria are the two elements that define the HPI in water (Prasanna et al., 2012).

HPI is represented by following equation, where "n" is the number of evaluated elements, and Qi is the sub-index of each parameter. It is calculated by following equation:

$$HPI = \frac{\sum_{i=1}^n WiQi}{\sum_{i=1}^n Wi}$$

$$Qi = \sum_{i=1}^n \frac{|Mi - Ii|}{Si - Ii} \times 100$$

"Ii is the ideal value of the ith parameter, and Mi is the monitored value of heavy metal for

that parameter" (Herojeet et al, 2015).

HEI index represents an "overall quality of the water" in terms of heavy metals concentration. It is calculated as the equation (Prasanna et al., 2012):

$$HEI = \sum_{i=1}^n \frac{M_i}{S_i}$$

Where M_i and S_i are the monitored value and maximum concentration permissible of the i th parameter (heavy metal). High concentrations of metal compared to S_i value indicate poor water quality. The contamination index (Cd) computes the combined effects of many aspects of water quality that are regarded as potentially dangerous components for drinking water (Prasanna et al., 2012; Backman et al., 1998). It is written as the equation below:

$$Cd = \sum_{i=1}^n cfi$$

$$Cfi = \frac{Cai}{Cni} - 1$$

Where "Cfi is the contamination factor, Cai is the analytical value, and Cni is the upper permissible concentration of the i th parameter (heavy metal)". These indices are used for As, B, Cr, Fe, Mn, and Sr in Mojave aquifer (table 10).

Table 10) values used to HPE, HEI, and Cd indices

Heavy metals	"W"	"S"	"T"	"MAC"
As	0.02	50	10	50
B	0.002	500	0	500
Cr	0.02	50	50	50
Fe	0.005	300	200	200
Mn	0.02	100	500	50
Sr	0.0003	4000	0	4000

Table 11) Indices for groundwater assessment for drinking water use

Indices	Formula	Category	Ranges
Heavy metals pollution index Parsad (2001)	$HPI = \frac{\sum_{i=1}^n WiQi}{\sum_{i=1}^n Wi}$ $Qi = \sum_{i=1}^n \frac{ Mi - Ii }{Si - Ii} \times 100$	Suitable Threshold risk unsuitable	<100 =100 >100
Heavy metals evaluation index Edet and Offiong (2002)	$HEI = \sum_{i=1}^n \frac{Mi}{Si}$	Low High	<1 >1
Contamination index Al-Ami et al. 1987	$Cd = \sum_{i=1}^n cfi$ $Cfi = \frac{cai}{cni} - 1$	Low Medium High	1< 1-3 >3

Trace elements' distribution and existence in groundwater are based on their degree of weathering and movement. The pH of the aquifer is one of the factors that regulates metal solubility there. Metal solubility is reduced by a high pH, resulting in a low concentration in the water. On the other hand, a low pH or acidic condition in the water makes metals from the rock or soil more soluble, resulting in a high metal load in the water. 110 wells analyzed from 2000 to 2019 had water with a pH range of 7 to 9.4 that is neutral to alkaline in character. The sequence of the mean metals is as follows: Sr>B>Fe>Mn>As>Cr. With a mean of 10.14, the Sr concentration varies from 0.0047 to 12.9 µg/l. Seven wells (n=87) exhibit Sr pollution and their results are more than 4 mg/L when compared to EPA/WHO regulations. In nature, strontium is often found as the Sr²⁺ cation and exhibits geochemical behavior akin to that of Ca²⁺. The main factor limiting Sr²⁺ mobility in the subsurface at neutral to alkaline pH ranges is sorption to clay particles and iron oxide minerals. Sr²⁺ mobility rises as ionic strength rises because strontium bound by outer sphere sorption is susceptible to remobilization by ion exchange reactions with Ca²⁺ and Mg²⁺ (Wallace

et al., 2012). Interestingly, despite the considerable capacity of phosphate biominerals to sorb Sr^{2+} as outer sphere complexes, certain tests have shown that sorbed strontium is susceptible to remobilization in high ionic strength environments (Handley-Sidhu et al., 2014). Despite this, at high pH conditions or high phosphate concentrations, Sr^{2+} may be absorbed into calcium-carrying minerals like calcite (CaCO_3) and Ca-phosphate minerals like hydroxyapatite ($\text{Ca}_5(\text{PO}_4)_3\text{OH}$) (Thorpe et al., 2012).

With a mean of 0.3 mg/L, the boron content varies from 0.008 to 5.7 mg/L. According to the EPA, 0.5 mg/L of boron is the maximum permitted level, hence 47% of the 108 wells that were analyzed contain boron pollution. Increases in hazardous components like boron are typically seen in groundwater with high salt levels. There are several plausible explanations for the coexistence of this pollutant, including the salt effect, competing adsorption for the active sites on the adsorbent, microbiological activity, and cation exchange (Li et al., 2020). Therefore, the Mojave aquifer's comparatively high salinity may provide a conducive environment for boron (B) solubility. Additionally, boron and SO_4^{2-} show a high association, suggesting a geogenic origin, and SO_4^{2-} is shown to be a prominent anion in the investigated wells. The range of the Fe content is 0.022 to 0.771 mg/L (average 0.22 mg/L). The Fe content is larger than the preferred limit (0.3 mg/L) of the EPA/WHO among the examined wells (n=70), showing the influence of weathered granitic and metamorphic rock as a potential source. These three wells had Fe concentrations of 0.4, 0.42, and 0.7 mg/L. The range of arsenic in the sample is 0.001 to 0.17 mg/L (average: 0.00629 mg/L). Nevertheless, arsenic contamination is present in 17 wells, with a mean value of 0.0538 and a value more than 0.001 mg/L. These wells are mostly found in the Mojave River drainage basin, which contains a largely coarse granitic river channel, as well as in the area surrounding the floodplain, which contains alluvium formed from older stream deposits, locally derived alluvial

fans, playa lake deposits, and fractured bedrock.

Inorganic arsenic (iAs) found in groundwater and some foods is very hazardous, with well-documented health impacts. Recent studies of arsenic's great sensitivity to pH, redox conditions, and co-occurring elements in groundwater reveal a more complicated geochemical scenario for its formation and toxicity (Ali et al., 2019). According to Ali et al (2019) higher concentration of "sulfates (SO_4^{2-}), chloride (Cl^-), and carbonate (CO_3^{2-})", as well as elevated EC and pH, and increased presence of arsenic species, were all indicators of oxidizing conditions in groundwater.

Arsenic may be mobilized at pH 6.5–8.5, a common pH range in groundwater, under oxidizing and reducing circumstances. On the other side, common anthropogenic sources include agriculture, livestock, and industrial manufacturing. It has been proposed that the presence of nitrate in groundwater may play a significant role in the oxidation of arsenic to arsenate (V). It is more frequent for nitrate to act as a final electron acceptor in anoxic conditions (Adeloye et al., 2021).

With mean concentrations of 114 for 6 heavy metals (As, Sr, Fe, Mn, B, Cr) in 110 groundwater sample years between 2000 and 2019, the Mojave basin aquifer's HPI varies from 95 to 132. It is implied that all groundwater samples, with the exception of one well, are over the threshold value of 100 and are thus unsuitable for human consumption.

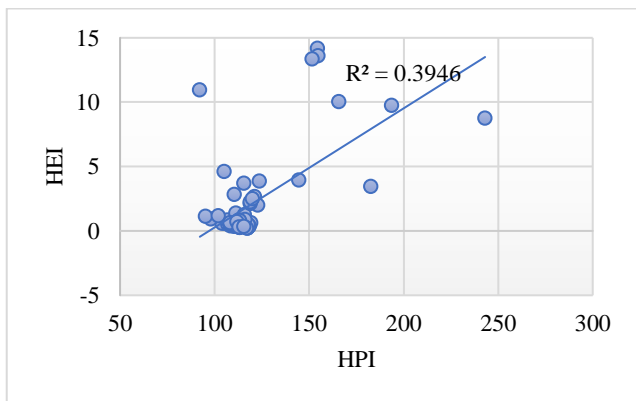
The range value and mean concentrations of HPI for the Mojave basin aquifer deviates from 96 to 132 and 114 respectively for 6 heavy metals (As, Sr, Fe, Mn, B, Cr) in 110 groundwater samples years between 2000-2019. It is inferred that, except on well, all the groundwater samples are above the critical value of 100, hence unfit for human consumption.

HEI has also been evaluated to gain a better knowledge of the pollutant loads; its range is

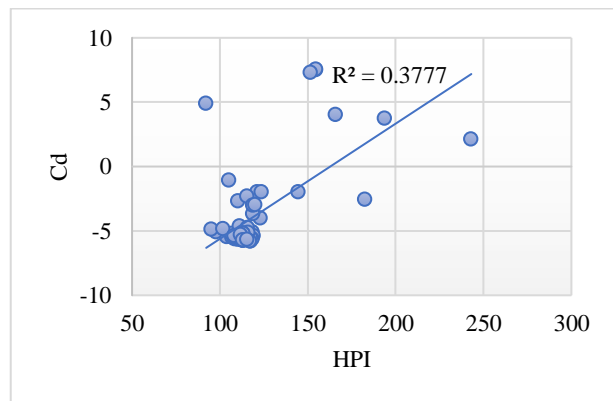
0.2 to 14.2, with a mean value of 2.0. where the monitored value and the maximum allowable concentration of the i th parameter, respectively, are M_i (heavy metal concentration) and S_i (standard value) (heavy metal). When compared to S_i values, high metal concentrations imply poor water quality. This index states that this water cannot be used if the concentration of each element is more than the standards' maximum allowable value (the M_i/S_i ratio is greater than 1). As a result, the HEI index defines a value of "one" as the threshold for pollution risk (Seifi and Riahi, 2018). As a result, nine out of the 70 studied wells have HEI values more than 1, making them unsuitable for home usage.

To determine the degree of metal pollution, the contamination index (Cd) is also used. The mean and range of Cd readings are -5.9 - 8.2 and -3.92 , respectively, and 4 wells ($n=70$) are classified as having substantial pollution. Surface runoff-derived heavy metal buildup in polluted wells mostly impacts samples that are positioned in the direction of the flow.

Alfalfa, small grains (for hay), onions, carrots, peaches, pears, and nectarines are the main crops in the study region. Farmers use a variety of chemical fertilizers, insecticides, fungicides, and weedicides extensively to increase crop productivity. Since intensive agriculture has been practiced for a long time, leaching mechanisms have sustained the metal buildup.



a)



b)

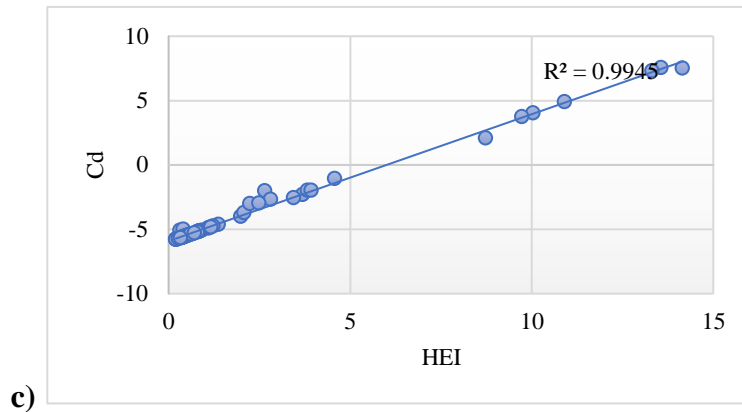
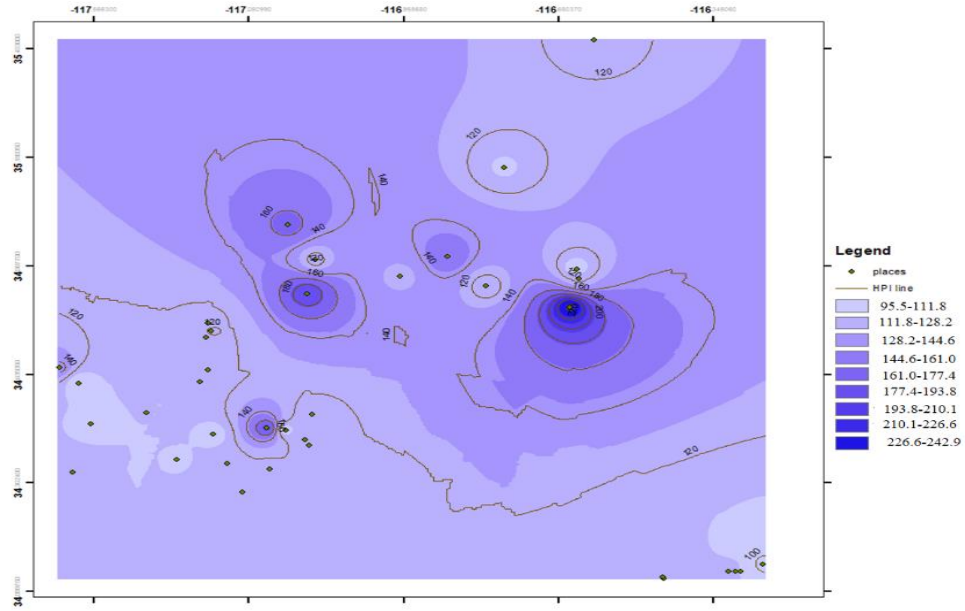


Fig. 19. Scatter plot of a) HPI versus HEI b) HEI versus Cd c) HPI versus Cd indices and their correlation of determination in the Mojave aquifer

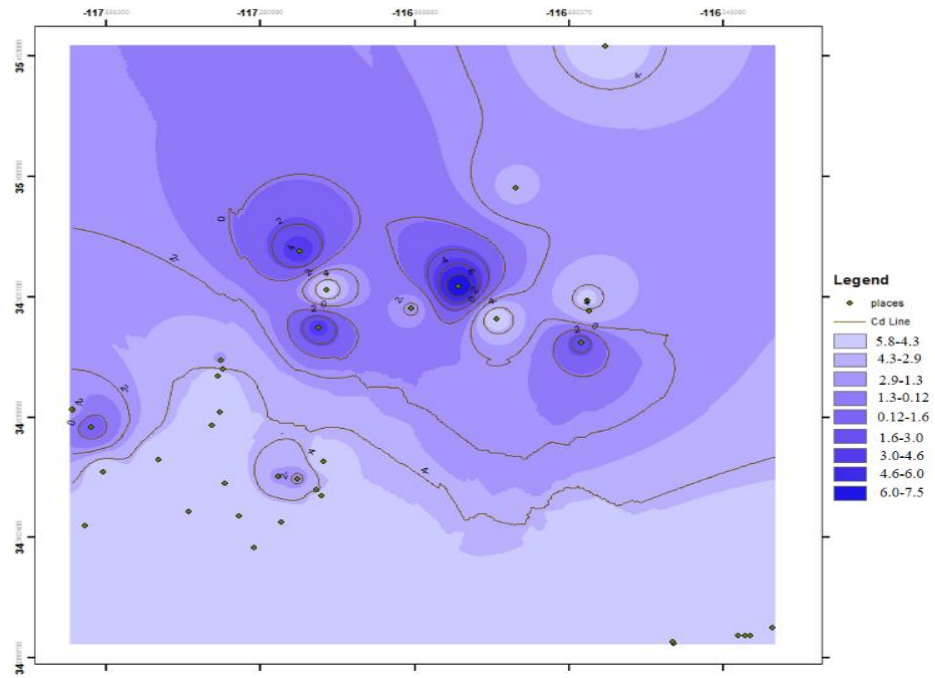
Different indices indicate various risk classifications. As a result, a scatter plot of HPI, HEI, and Cd against one another has been created and is displayed in Fig. 19, table 12, for more information. The scatter figure clearly shows a substantial association between HEI and Cd with a correlation coefficient value of $R^2 = 1$, while only weak correlations between HPI and HEI and between Cd and HPI are shown ($R^2 = 0.39$ and 0.39 , respectively). As a result, choosing between the HEI and Cd indices, or using both, may be a preferable alternative for classifying samples. Additionally, Fig. 20 illustrates the geographical distribution of these indices in the research region to visually identify the contaminated areas. It clearly shows the link between Cd and EHI, and the majority of the contaminated wells are in the cities of Helendale and Victorville.

Table 12) Spearman correlation between indices , studies heavy metal, nitrate, pH and Eh

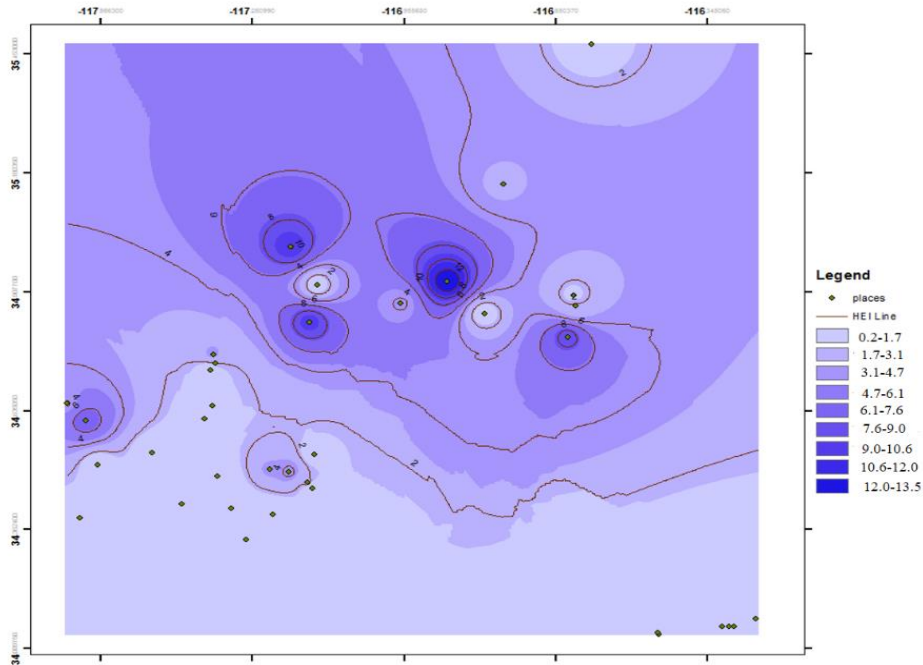
	HPI	HEI	Cd	As	Boron	Cr	Fe	Sr	Mn	NO3	ph	EC
HPI	1											
HEI	0.63	1.00										
Cd	0.63	1.00	1.00									
As	0.33	0.15	0.15	1.00								
Boron	0.18	0.08	0.08	0.44	1.00							
Cr	-0.11	-0.11	-0.11	-0.19	-0.18	1.00						
Fe	0.02	0.02	0.02	0.31	0.02	-0.21	1.00					
Sr	0.19	0.04	0.04	0.02	0.55	-0.20	0.00	1.00				
Mn	0.29	0.02	0.02	-0.05	-0.02	-0.11	-0.02	0.62	1.00			
NO3	0.06	0.05	0.05	-0.09	-0.10	0.13	-0.05	-0.11	-0.05	1.00		
ph	0.01	-0.16	-0.16	0.02	0.20	0.06	-0.21	0.14	0.10	-0.11	1.00	
EC	0.22	0.77	0.77	0.16	0.00	-0.17	0.03	-0.02	-0.06	0.02	-0.38	1.00



a)



b)



c)

Fig. 20. "Geographical distribution of studied parameters in the Mojave aquifer: a) HPI b) CD c) EHI"

Chapter 3: Central Valley-San Joaquin Valley- Tulare Basin

The aquifer system of the Central Valley is composed of unconfined, semi-confined, and confined aquifers that are mostly found in the upper 300 meters of alluvial deposits deposited by streams draining the nearby Sierra Nevada and Coast Ranges. The upper 300 meters of the deposits are where the majority of the groundwater in the Central Valley is found. However, groundwater with dissolved solids less than 2000 mg/L can be found at depths greater than 900 m in the southern San Joaquin Valley and in the alluvial deposits that fill the structural troughs along the west side of the Sacramento Valley (Faunt, 2009). Under these depths, thick marine sedimentary rocks trap saline water (Planert and Williams, 1995). The Central Valley aquifer's sediments are varied, with a range of 30% to 70% coarse-grained texture across the valley (Burow et al., 2013). In the western portion of the San Joaquin Valley, the Corcoran Clay, a geographically limiting unit, divides the

groundwater flow system into two zones: upper semiconfined and lower confined (Burow et al., 2004). The Sierra Nevada and Coast Ranges' respective source materials have different compositions, as shown by the aquifer's shifting texture from east to west. Contrary to the Coast Ranges' shale-rich composition, which results in finer-grained sediments on the valley's western side, the Sierra Nevada's crystalline composition provides a greater source of coarse material to the Central Valley (Faunt et al., 2010).

Agriculture is the Central Valley's main land use, making it one of the most profitable agricultural regions in the world with more than \$40 billion in earnings in 2013. (Great Valley Center, 2014; USDA, 2012). An extensive network of canals transports the water needed for agriculture from reservoirs in the Sierra Nevada and foothills (Faunt, 2009). Wells in the Central Valley are reportedly drying up because groundwater levels are dropping, according to Jasechko and Perrone (2020). Their investigation provided information on the southern Central Valley, where groundwater use and depletion were significant, and the study of dry wells was limited by the availability of well-constructed data. There are less groundwater supplies in many, but not all, of the areas where wells are drying up because those areas are classed as critically over drafted basins. By balancing groundwater recharge and losses in certain locations, either by supply augmentation or pumping reductions, the number of wells that run dry in the future can be decreased. Alarming rates of well drying are occurring in the home.

Two basins—the San Joaquin Basin in the north and the Tulare Basin in the south—make up the San Joaquin Valley, which makes up the southern two-thirds of the Central Valley (Fig. 21). Arid to semi-arid Mediterranean climate characterizes the San Joaquin Valley, with mean annual precipitation ranging from 15 to 20 inches between 1911 and 1960. (Gronberg et al., 1998).



["https://ca.water.usgs.gov/projects/central-valley/about-central-valley.html"](https://ca.water.usgs.gov/projects/central-valley/about-central-valley.html)

Fig. 21. The location of San Joaquin valley (San Joaquin & Tulare Basin aquifers)

The San Joaquin Valley's southernmost region includes the internally drained Tulare Basin, which is surrounded by mountains on three sides. The Tulare Basin was separated from the San Joaquin Basin's southern end by the convergence of alluvial fans to the east and west (Faunt, 2009). The Tulare Basin is home to Tulare Lake, which was formerly the largest freshwater lake west of the Mississippi River and the second largest lake in terms of surface area in the United States (Moore et al., 1990). The Tulare Basin aquifer's textures show that fine- and coarse-grained material predominates in the top 230 m and the ancient Tulare Lake-bed, respectively, northwest of the Corcoran clay (Faunt, 2009).

One of the most productive agricultural areas in the country is where Tulare County is situated. This county's main economic activity is agriculture, which contributes 35% of the state's total agricultural economy. With an estimated \$3.5 billion in yearly agricultural income, Tulare

County is the most economically successful county in the United States. Tulare has been the leading milk-producing county in the US since 2003. (California State Water Resources Control Board Groundwater Protection Section, 2016).

The Tulare Shallow Aquifer covers around 6,008.8 km² and is situated in the southern San Joaquin Valley (fig. 22) and the close-by Sierra Nevada mountains (Bennett et al., 2017). The alluvial and fluvial deposits from the Sierra Nevada to the east, which date to the Quaternary, make up the freshwater aquifer system in the groundwater basins. It has two zones, with The Corcoran Clay in the bottom zone and an upper zone with a clay-rich lacustrine unit (Faunt, 2009). Groundwater recharge in this aquifer is influenced by the Sierra Nevada snowfall, precipitation, river and stream seepage, irrigation water percolation, canal seepage, and intentional recharge (California, Department of Water Resource) (DWR, 2004).

The principal aquifer's boundaries are defined by the eastern alluvial fan's region in the eastern Tulare basin, which has been heavily farmed and irrigated since the early 1900s. The central and western portions of the Tulare Basin contain the nonmarine Tulare Formation, which is made up of relatively permeable unconsolidated layers of clay, silt, sand, and gravel that are mostly from the Coast Range, which marks the western edge of the basin.

years from 2001 to 2020 (table 13), to identify the groundwater classification for agricultural uses.

Table 13) water quality parameters in Tulare aquifer for irrigation uses years 2000 to 2020

parameter	Unit	Maximum	Minimum	Mean
Ca ²⁺	Mg/L	570	1.0	50.2
Mg ²⁺	Mg/L	128	0.02	11.0
Na ⁺	Mg/L	442	1.9	71.9
K ⁺	Mg/L	8.54	0.08	1.9
Cl ⁻	Mg/L	517	0.3	46.5
SO ₄ ²⁻	Mg/L	1730	0.2	61.6
HCO ₃ ⁻	Mg/L	848	56	233
CO ₃ ²⁻	Mg/L	19	0.001	1.2
EC	µS/cm	2970	35	637.5
pH	-	9.6	6.1	7.7
Na%	%	98.4	5.9	48.8
SAR	-	24.2	0.09	3.6
RSC	meq/L	11.5	-15.2	0.2
MH	%	88.9	0.9	21.9
PI	%	141.4	29.8	79.2
PS	meq/L	20.6	0.02	1.9

The pH range of the local groundwater samples is 6.1 to 9.6, with a mean of 7.7, indicating alkaline conditions. The average pH in 20 wells (n=143) is 6.6, however. As can be observed in Fig. 23, the majority of the water samples that have been investigated are situated in the Ca²⁺-Mg²⁺-HCO₃⁻ section where carbonate minerals might potentially impact them. In reality, the plot demonstrates that the majority of the groundwater samples fall into the category of alkaline earth metals (Ca²⁺, Mg²⁺), which predominate over alkalis (Na⁺, K⁺), and weak acids (CO₃²⁻, HCO₃⁻), which outweigh strong acids (Cl⁻, SO₄²⁻). However, 12 wells (HLS02, HLS09, HLS14, KAW03, KAW04, KAW05, KAW07, KAW08, KAW09, KAW10, KAW11, KAW12) located on the east

and central part of Tulare aquifer are Na+K type (fig. 23). "The freshwater aquifer system in the groundwater basins is composed of Quaternary-age alluvial and fluvial sediments primarily derived from the Sierra Nevada to the east and is divided into upper and lower zones by a clay-rich lacustrine unit, the Corcoran Clay" (Faunt, 2009). The granitic rocks from the Mesozoic era make up the majority of the fractured rock aquifers in the highlands. Overall, ion exchange, evaporation, and concentration mostly impacted the hydrochemical facies of Tulare aquifer samples.

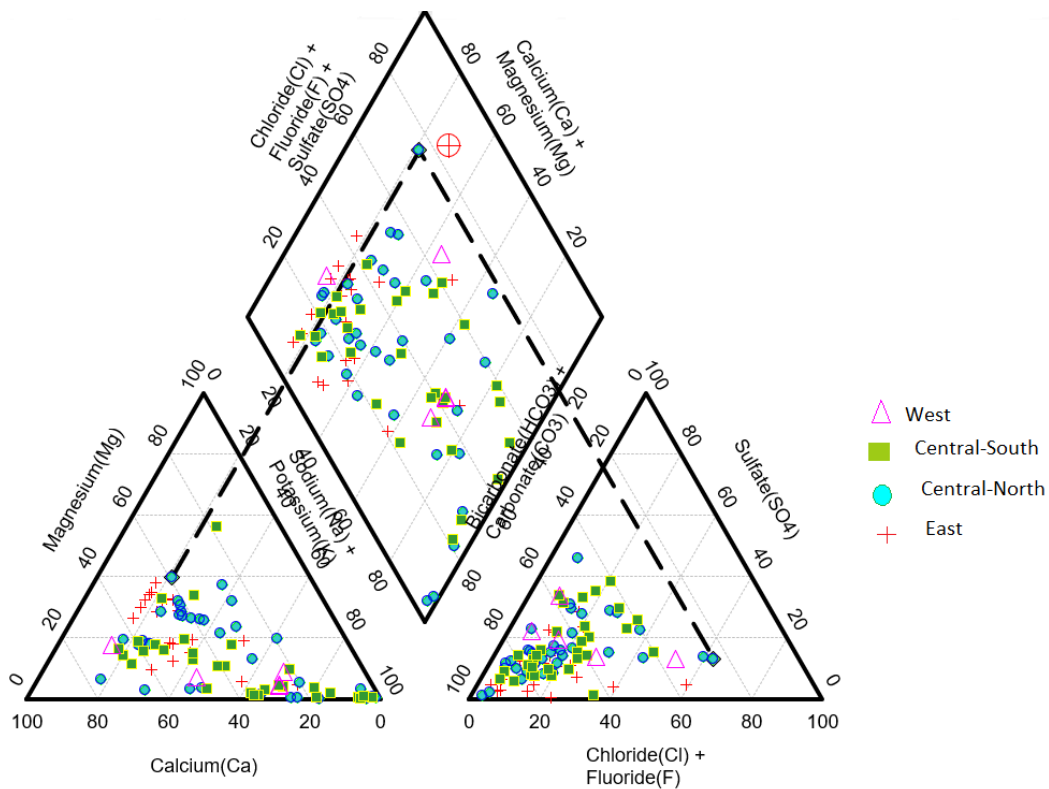


Fig.23. Piper diagram showing water type in the Tulare aquifer

3.1.1 Salinity Index and Salinity Hazard

The number of dissolved solids in the water has a strong correlation with its electrical conductivity (EC), a critical component in categorizing the utility of water.

With the exception of one well in the east section of the aquifer, where the electrical

conductivity was 38 $\mu\text{s}/\text{cm}$, the electrical conductivity values varied from 120 to 2,670 $\mu\text{s}/\text{cm}$, with a mean of 641.9 $\mu\text{s}/\text{cm}$ (table 14).

Table 14) Classification of water salinity based on EC (Handa1969)

EC ($\mu\text{S}/\text{cm}$)	Water salinity	EC range (no. of sample)	Percent
0-250	Low (excellent quality)	120-246 (18 samples)	9.9
251-750	Medium (good quality)	256-743 (118 samples)	65.1
751-2,250	High (permissible quality)	751-2,040 (43 samples)	23.8
2,251-6,000	Very high	2,650-2,970 (2 samples)	1.2
6,001-10,000	Extensively high	-	-
10,001-20,000	Brine weak concentration	-	-
20001-50000	Brine moderate concentration	-	-
50001-100000	Brine high concentration	-	-
>100000	Brine extremely high concentration	-	-

Approximately 9.95% of the total groundwater samples (n=181) had low EC and high quality for irrigation, as determined by the EC classification. 23.8% had high salinity, 65.16 percent have medium salt enrichment, and 1.11 percent of the samples have extremely high salinity. The central and western portions of the Tulare aquifer are where more than 90% of examined wells with EC greater than 750 $\mu\text{s}/\text{cm}$ are found. Alluvial and river deposits from the Sierra Nevada make up the majority of the geological formations in these regions, which date to the Quaternary.

Groundwater salinization assessment is critical in the assessment of water quality for irrigation purposes because salinization may result in the loss of soil productivity. It is crucial to express the total amount of dissolved salts in irrigation water in terms of the electrical conductivity of water for diagnostic and categorization reasons. Water samples are divided into four categories based on their electrical conductivity (table 15).

Table 15: Water categorization for the research region based on salinity risk

Salinity hazard class	EC (µS/cm)	Quality	range (no. of sample)	Percent
C1	100-250	Excellent	120-246 (18 samples)	9.9
C2	250-750	Good	256-743 (118 samples)	65.1
C3	750-2,250	Medium	751-2,040 (43 samples)	23.8
C4	>2,250	Unsuitable	2,650-2,970 (2 samples)	1.2

In the groundwater of the Tulare aquifer, 135 samples, or 75% of all samples, are appropriate for irrigation, whereas 43 samples, or 23.8% of all samples, have questionable water quality.

3.1.2 "Sodium Percent (%Na) and Sodium Absorption Ratio (SAR)"

Since the mineralization of the water and its effects on plants and soil determine whether groundwater is suitable for irrigation, Wilcox's (1955) classification and understanding techniques were applied to categorize and understand the fundamental chemical characteristics of groundwater. When irrigation water contains a lot of sodium, the soil's clay particles take up the sodium and push out the Mg^{2+} and Ca^{2+} ions, which reduces soil permeability and internal drainage. Due to this, air and water flow are constrained in wet conditions, and these soils harden when they are dried (Ravikumar et al. 2011). Based on the percent levels of sodium, groundwater samples from the area are categorized into five categories (table 16).

The categorization of water samples according to salt percent is shown in Table 16. Accordingly, the results show that 18.4% of the samples are acceptable, 20.33 % are "dubious", and 15.39 % are "inappropriate".

Table 16) "Water classification based on the sodium percent (Wilcox,1955)"

"Sodium (%)"	"Water class"	Range	Percent
<20	"Excellent"	5.9-19.6 (24 samples)	13.2
20-40	"Good"	20.2-38.6 (60 samples)	32.9
40-60	"Permissible"	40.2-59.7 (33 samples)	18.1
60-80	"Doubtful"	60.3-79.7 (37 samples)	20.4
>80	Unsuitable	80.9-98.4 (28 samples)	15.4

The relation between soluble Na⁺ and soluble divalent cations (Ca²⁺ and Mg²⁺) is described by the sodium adsorption ratio (SAR). A quantitative chemical analysis of the water in contact with the soil yields a measurement of its salt levels.

Table 16 presents the SAR classification of the groundwater samples from the Tulare aquifer. In the salt danger classification for irrigation, 91.76% of the water samples have sodium absorption ratios lower than 10 and are classified as S1 (Excellent) classes, 5.5% as good and classified as S2, and 2.75% (5 samples) as S3 with questionable quality.

To classify the water samples in the Tulare aquifer according to their irrigational suitability quotient, SAR is plotted against EC on the US salinity map (fig. 25). Accordingly, the majority of water samples with somewhat salinity to salinity are in the C2S1, C3S1, C2S2, and C3S2 classes, according to the Wilcox diagram. But 7 of the water samples fall into the category of being extremely salty and unfit for agriculture (table 17).

Table 17) water danger classes based on USSL classification and sodium hazard classes based on SAR values (Ravikumar et al., 2011)

"SAR values"	"Sodium hazard class"	Quality	Range	Percent
<10	S1	"Excellent"	0.09-9.3 (167 samples)	91.8
10-18	S2	"Good"	10.4-17.4(10 samples)	5.5
19-26	S3	"Doubtful"	19.5-24.1(5 samples)	2.7
>26	S4 and S5	"Unsuitable"	-	-

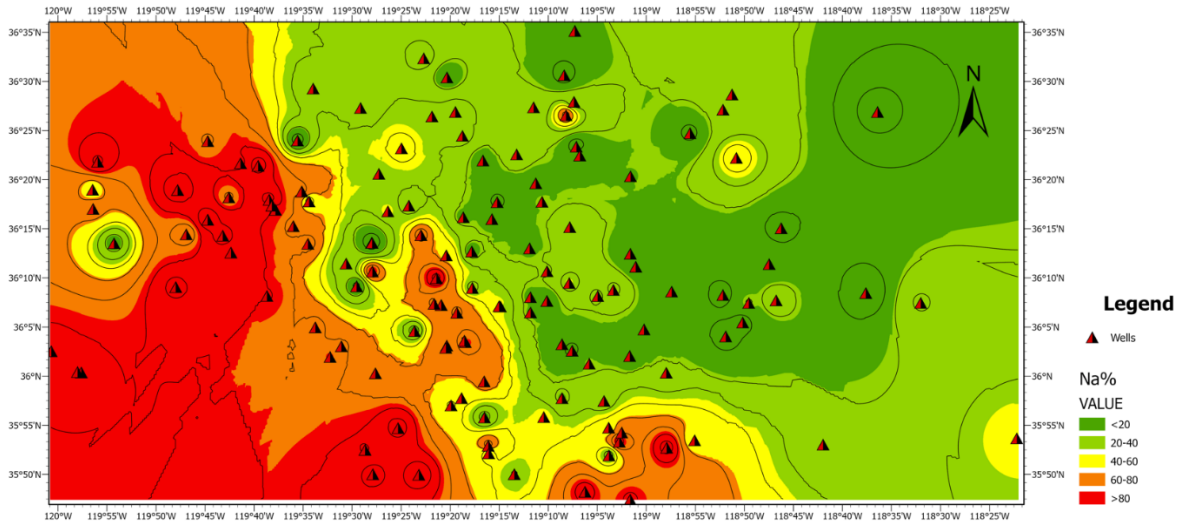


Fig. 23 "Spatial distribution of sodium percent (Na%)" in Tulare aquifer

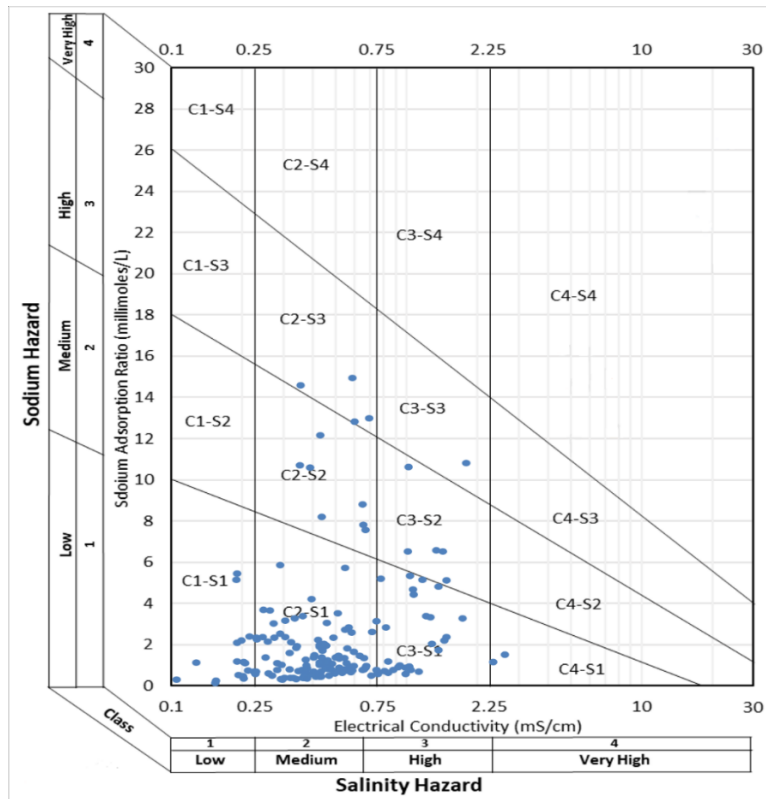


Fig. 25. Groundwater in the Tulare Aquifer is classified according to salinity and sodium adsorption ratio for irrigation usage

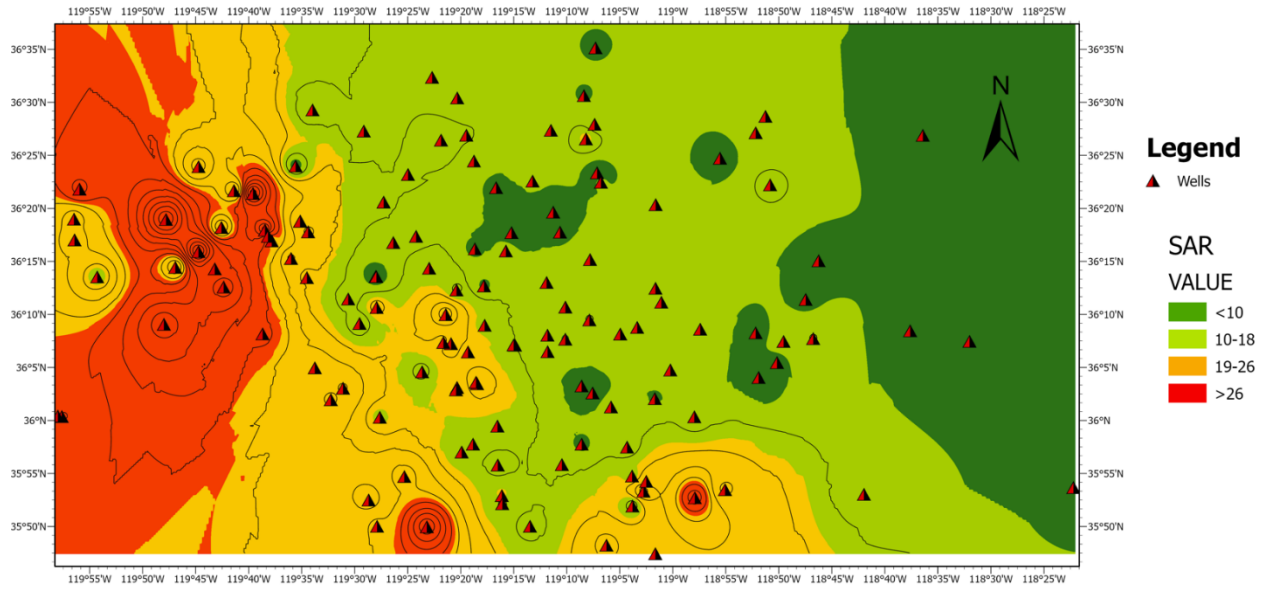


Fig. 26. Spatial distribution of sodium adsorption ratio (SAR) in Tulare aquifer

The western side of the research region, which is mostly agricultural and has a large density of residential areas, has high salinity, according to the spatially distributed map of Na% and SAR, whereas the center of the study area has moderate salinity (Fig. 24 and 26). The major causes of the low water quality in these areas may be overuse of groundwater and agricultural activities. The Tulare aquifer's easternmost region has the area with the best water quality.

3.1.3 Residual Sodium Carbonate

Water quality is impacted by carbonate ions ($\text{HCO}_3^- + \text{CO}_3^{2-}$), alkaline earths ($\text{Ca}^{2+} + \text{Mg}^{2+}$), and finally an increase in the proportion of Na^+ (Eaton 1950). The situation gets worse when there are more carbonates present than alkaline earths. NaHCO_3 , which is created when more carbonates mix with Na^+ , has an impact on the soil's structure.

The residual sodium carbonate is what it is known as (RSC). The appropriateness of water for irrigation can therefore be explained by a relation between the concentration of carbonates and the concentration of alkaline earths.

The investigated groundwaters were subsequently categorized based on the RSC values (fig. 27). The findings show that 80% of the water samples have RSC less than 1.25 and are good for irrigation, 11.58% of the samples fall into the questionable water category, and 8.4% of the samples have RSC greater than 2.5 and are not suitable for irrigation usage. On the western side of the Tulare aquifer, there are wells with a high RSC value (Table 18).

Table 18) "Groundwater quality based on RSC"

"RSC"	"Quality"	Range	Percent
<1.25	"Good"	-15.2-1.1 (76 samples)	80
1.25-2.5	"Doubtful"	1.3-2.4 (11 samples)	11.6
>2.5	"Unsuitable"	2.9-11.5 (8 samples)	8.4

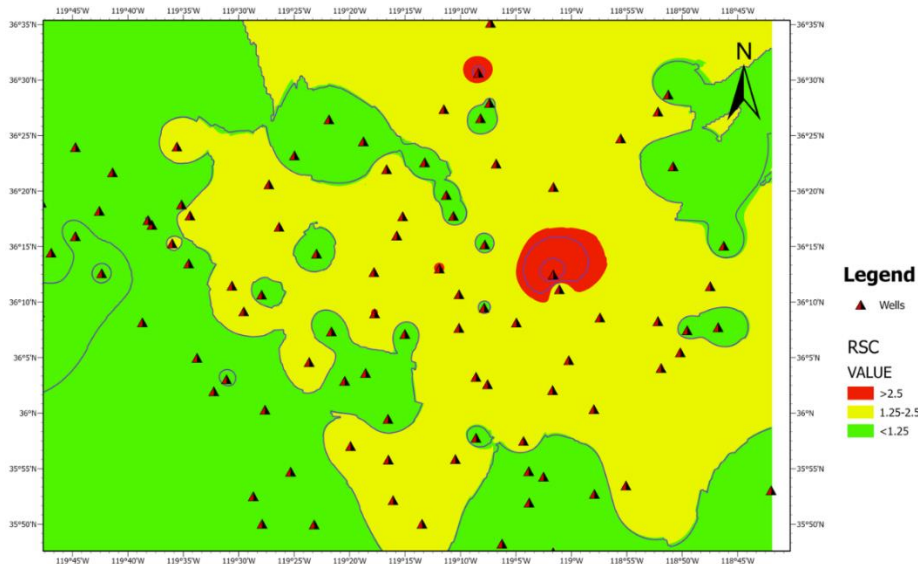


Fig. 27. Spatial distribution of Residual sodium carbonate (RSC) in Tulare aquifer

3.1.4 Magnesium Ratio and Magnesium Hazard

In contrast to how they normally operate in water, where they typically maintain an equilibrium condition, Ca^{2+} and Mg^{2+} behave differently in the soil system. Magnesium weakens the structure of soil in very salty, high Na^+ water. The higher amounts of Mg^{2+} are caused by exchangeable Na^+ in irrigated soils. More Mg^{2+} can degrade soil quality in equilibrium by making

it alkaline. As a result, it affects agricultural productivity. The risk associated with magnesium is indicated as a magnesium ratio (MR) (Ravikumar et al. 2011).

If the MR value is higher than 50, the water associated with that number is considered dangerous and should not be used for irrigation since it reduces agricultural yields. The Tulare Aquifer's MR has a mean of 21.9 and a range of 0.9 to 88.9. In around 5% of the groundwater samples (n=182), which are unsuitable for irrigation and are mostly found on the east section, the MR surpasses the value of 50. (fig. 28). The MR is less than 50 in the remaining 95% of the groundwater samples, making them appropriate for irrigation. High magnesium ration could be due to the presence of granitic and metamorphic formations of Sierra Nevada mountain ranges.

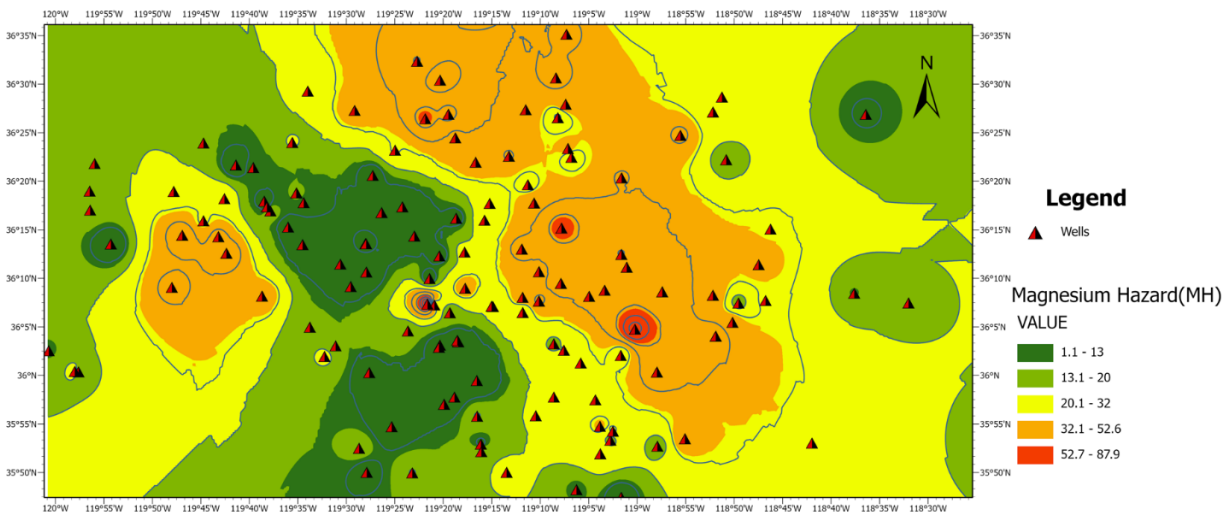


Fig. 28 "Spatial distribution of magnesium hazard (MH)" in Tulare aquifer

3.1.5 "Permeability Index"

The soil's Na^+ , Ca^{2+} , Mg^{2+} , HCO_3^- , and Cl^- concentrations have a significant impact on permeability, and long-term irrigation with high salt water has an impact as well.

Water quality may be divided into three categories based on this index: class I, with a maximum permeability of 75%, appropriate for irrigation; class II, with a permeability index between 25 and 75%, marginally suitable; and class III, with a permeability index less than 25%,

unsuitable for irrigation.

PI varies in the Tulare aquifer from 29.8 to 141.4 (n=95). In the Tulare aquifer, almost 50.5% of the samples are classified as class I (PI > 75%) and 49.48% as class II (PI = 25-75%), which is moderately appropriate (fig. 29).

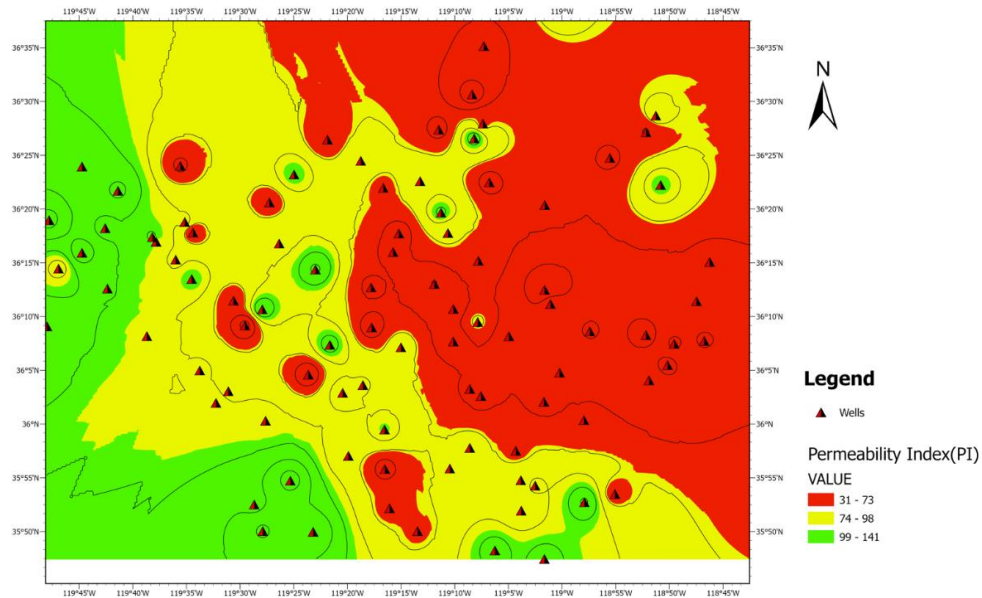


Fig. 29. Spatial distribution of permeability index (PI) in Tulare aquifer

3.1.6 "Potential Salinity"

Based on this characteristic, there are three categories for water: suitable (PS<3 meq/L), medium (3–15 meq/L), and unsuitable (>15 meq/L) (Delgado et al., 2010). According to this classification, about 85.6% of water samples in Tulare aquifer have PS less than 3, 6.6% placed in good to injurious class with PS ranged 3-5, and 7.7 % are unsuitable for irrigation (table19) located on the east part (fig. 30).

Table 19) the groundwater classification based on potential salinity

"Potential Salinity"	"Water class"	Range	Percent
<3.0	"Excellent to good"	0.02-2.9 (155 samples)	85.6
3.0-5.0	"Good to injurious"	3.3-4.6 (12 samples)	6.6
>5.0	"injurious to unsatisfactory"	5.2-20.5 (14 samples)	7.7

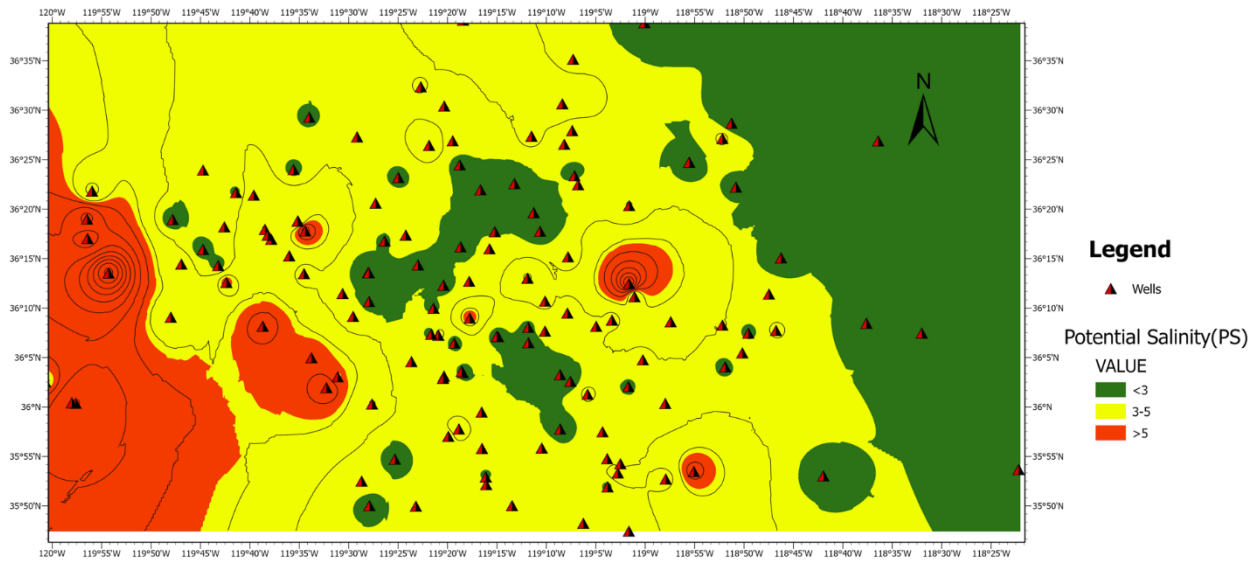


Fig. 30. Spatial distribution of potential salinity (PS) in Tulare aquifer

3.2 Nitrate Assessment and its Stable Isotopes

The Tulare aquifer's nitrate content varied from 0.038 to 48.6 mg/L, with a mean value of 8.98 mg/L. In the Tulare aquifer, around 33.5% (n=161) of water samples contain nitrate concentrations that are higher than the Maximum Contaminant Level (MCL) established by the Environmental Protection Agency (fig. 31). In addition, 70% of the examined wells contain nitrate levels more than 3 mg/L. Although there hasn't been a baseline assessment on the amount of naturally occurring NO_3^- concentrations in groundwater in this area, NO_3^- levels above 3 mg/L are believed to be the result of anthropogenic sources (Babiker et al., 2004). The range of NO_3^- readings from 0.038 to 48.6 mg/L makes it impossible to assume that the NO_3^- comes from organic nitrogen in the soil. Water samples are collected from 161 wells in this research region between the years of 2001 and 2020. The average nitrate value for each year between 2001 and 2020 shows a generally rising trend (fig. 31).

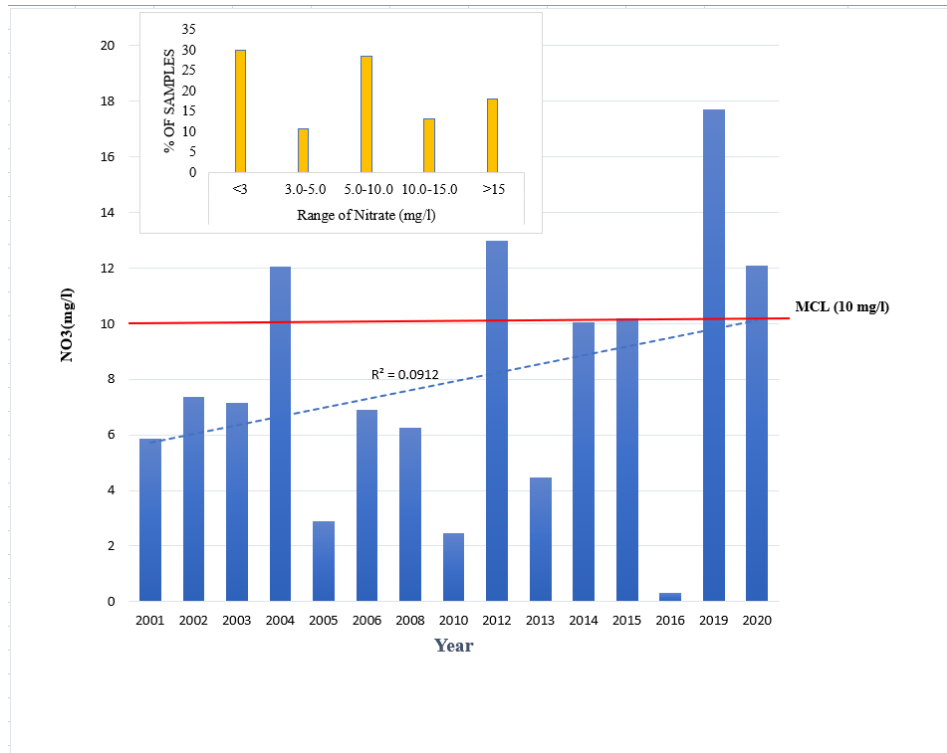


Fig. 31. Nitrate concentration of Tulare aquifer in the range date of 2001-2020

For assessment of nitrate concentration and identify its potential sources using stable isotopes, Tulare aquifer is divided to 4 sub-regions: west part, central-north part, central-south part, and East part (fig. 22), table 21.

In the east part of Tulare aquifer (HLS), the mean concentrations of NO_3^- is 6.46 mg/L (n=18), and $\delta^{15}\text{N}-\text{NO}_3^-$ values ranged from +1.66 to +14.5‰ with a mean of 6.59‰. The highest nitrate content (11.74 mg/L) was found in the central-north portion (KAW) of the Tulare aquifer (n=31). The range of this component's $\delta^{15}\text{N}-\text{NO}_3^-$ and $\delta^{18}\text{O}-\text{NO}_3^-$ values was +2.43 to +43.02 with a mean of 7.71 and -3.21 to 20.52 with a mean of 1.53, respectively.

Similar to the central-north region, the south part (TLE) also has a high nitrate content, with a mean value of 9.04 mg/L (n=27). The ranges of $\delta^{15}\text{N}-\text{NO}_3^-$ and $\delta^{18}\text{O}-\text{NO}_3^-$ values were respectively +2.13 to +19.67‰ and -1.94 to +6.99‰. West portion (TLA) nitrate concentration is

3.95 mg/L (n=6). The isotope values in this region may be found in a very wide range; for example, the west part's $\delta^{15}\text{N-NO}_3^-$ and $\delta^{18}\text{O-NO}_3^-$ values varied from -10.46 to +57.51‰ with a mean of +15.18‰ and -6.42 to +18.09‰ with a mean of +3.32‰ respectively. The usual ranges of $\delta^{15}\text{N-NO}_3^-$ and $\delta^{18}\text{O-NO}_3^-$ values for the main sources of NO_3^- that may have an impact on the Tulare aquifer are shown in Fig. 32 for these sources.

All areas of this aquifer's isotopic nitrate signatures fall within the acceptable range for sewage and manure, soil organic matter, and chemical fertilizers. Although a distinct relationship between $\delta^{15}\text{N-NO}_3^-$ versus $\delta^{18}\text{O-NO}_3^-$ is not always found when a single site is taken into account (for example, the central-south section), a somewhat positive relationship was discernible for the entire data set. The presence of nitrate attenuation brought on by microbial denitrification at the aquifer site is shown by the linear relationship between the $\delta^{15}\text{N-NO}_3^-$ and $\delta^{18}\text{O-NO}_3^-$ values and a drop in NO_3^- concentration (Kendall 1998). Denitrification is probably occurring in the central-north (KAW) and eastern (HLS) portions of the aquifer (fig. 32), although it may not be the only factor affecting the concentration of nitrate in this area. On the other hand, the non-linear relation between the $\delta^{15}\text{N-NO}_3^-$ and $\delta^{18}\text{O-NO}_3^-$ values in some wells located on the central-north (KAW) part shows mixing might be happening. The difference in the average value of wells depth could be a reason for these kinds of various reactions affecting nitrate concentration in the Tulare aquifer. For example, average depth of the wells in on the central-north (KAW) part is lower than the other parts indicating more influence of waste waters produced from farming land and urban areas.

Since the concentrations of $\delta^{15}\text{N-NO}_3^-$ and $\delta^{18}\text{O-NO}_3^-$ are primarily found in soil organic matter, manure, and sewage, as well as chemical fertilizers, it is likely that these three sources contributed to the nitrate contamination or that it originated from a single variable source inside the common composition area. As a result, there is no common groundwater circulation pattern

throughout the research area's many groundwater sites, making it difficult to explain this pattern only in terms of microbial denitrification or mixing.

In other words, it is possible to discern between denitrification and simple mixing using plots of the $\delta^{15}\text{N-NO}_3$ composition against the natural log and inverse ($1/\text{NO}_3$) concentrations. The negative relationship between $\delta^{15}\text{N-NO}_3$ and the inverse of nitrate concentration ($R= 0.22$) (fig. 33b) is consistent with mixing, while the positive relationship between $\delta^{15}\text{N-NO}_3$ and the natural log of nitrate ($R=0.14$) (fig. 33a) shows the decrease in NO_3 concentration as the result of the enrichment in $\delta^{15}\text{N-NO}_3$ to suggest the effect of denitrification in nitrate concentration in the Tulare aquifer.

Another factor to evaluate nitrate sources in groundwater is the correlation between nitrate and major cations or anions (table 20). There is a strong link between nitrate and Cl^- , SO_4^{2-} , and Na^+ in the Tulare aquifer, which points to two possibilities. 1) NO_3 , Cl , and SO_4^{2-} come from diverse sources. Since the increase in Cl^- concentration in the study area is not accompanied by an increase in NO_3^- concentration, it indicates that the inputs of Cl^- and NO_3^- into the Tulare aquifer have become decoupled. For instance, SO_4^{2-} may have a natural origin as opposed to nitrate, which is most likely of anthropogenic origin. This decoupling, according to Xing et al. (2013), may be caused by the mixing of several water sources with different Cl^- and NO_3^- concentrations, but it may also be due to denitrification taking place inside the aquifer. For instance, chloride can come from a variety of sources, such as road salts, water supply systems, and atmospheric depositions. Contrarily, denitrification in the subsurface will result in a decrease in the amount of reactive N while having no impact on the concentrations of Cl^- .

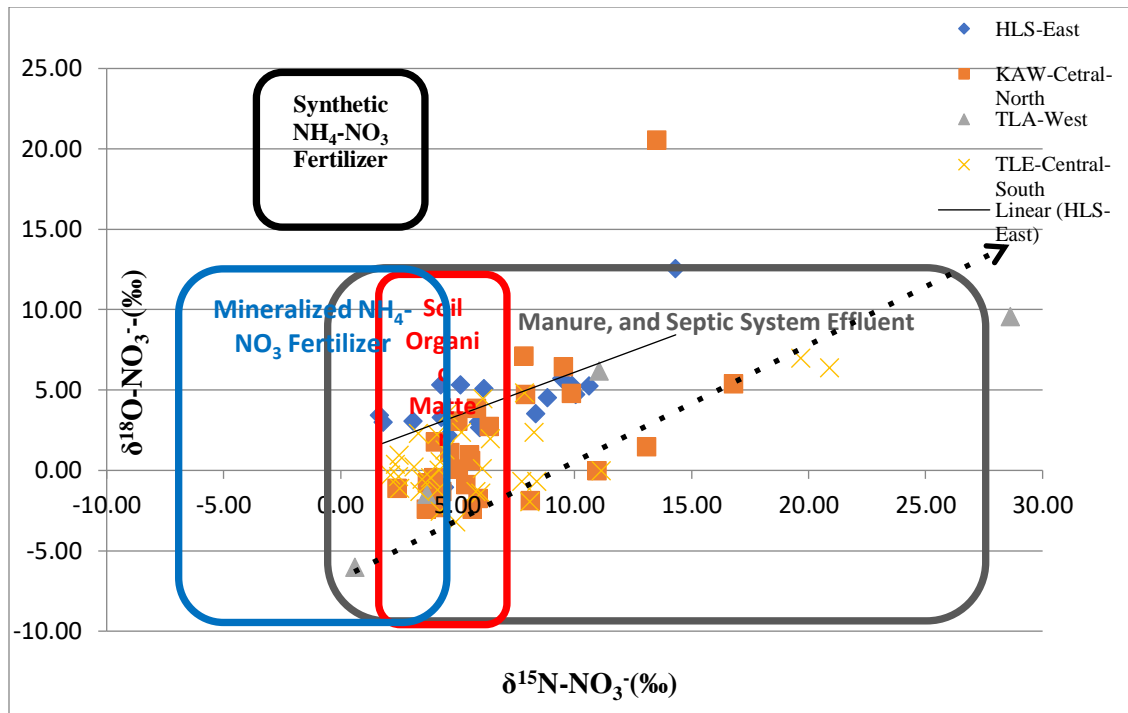


Fig. 32. Expected " $\delta^{15}\text{N}-\text{NO}_3^-$ versus $\delta^{18}\text{O}-\text{NO}_3^-$ " ranges for natural and anthropogenic nitrate sources in Tulare aquifer.

Tulare is a shallow aquifer and average depth of studies well in this region is about 48m. as a result, it should be noted that evaporation may affect the isotopic composition of NO_3^- generated by nitrification due to enrich H_2O in $\delta^{18}\text{O}$ isotopes (Hoefs and Hoefs, 2015). The well samples are also the most isotopically enriched, mapping following an evaporative trend away from the global meteoric waterline (fig. 33c). The penetration of irrigation water contaminated with NO_3^- is supported by isotopic evidence. The enriched H and $\delta^{18}\text{O}$ values of wells with high NO_3^- concentrations, including wells HLS01, HLS03, HLS09, HLS10, HLS12, TLE25, TLE27, and TLE28 (table 21), suggest that irrigation canals were used to recharge the groundwater or that groundwater that was pumped from the aquifer may have evaporated at the surface before infiltrating back into the aquifer system.

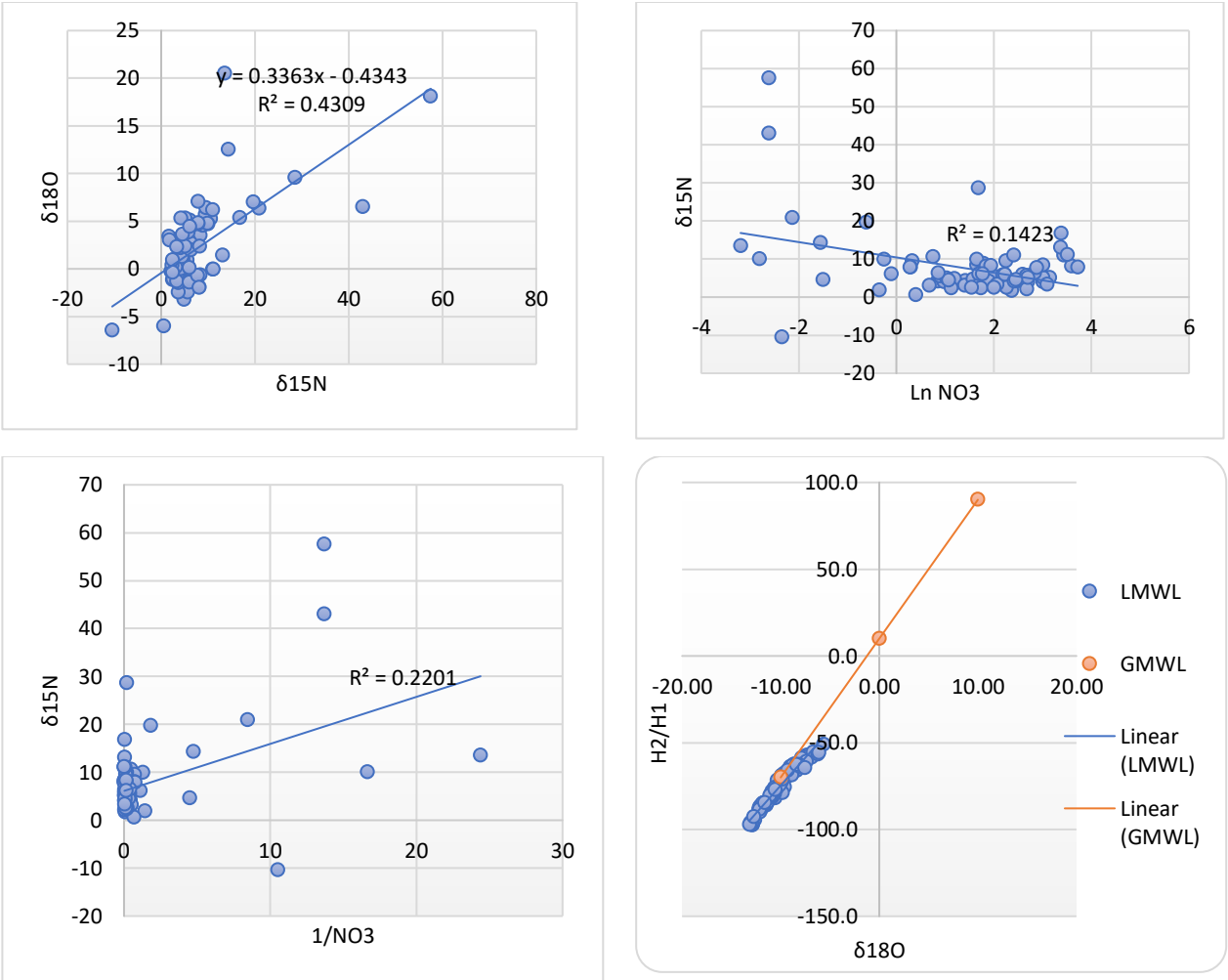


Fig. 33 a. Nitrate versus $\delta^{15}\text{N} - \text{NO}_3$, b) natural log of nitrate concentration versus $\delta^{15}\text{N} - \text{NO}_3$, and c) inverse nitrate concentration ($1/\text{NO}_3\text{N}$) versus $\delta^{15}\text{N} - \text{NO}_3$

Table 20) the correlation between nitrate and ions

Parameters (mg/L)	NO_3^-	Ca^{2+}	Mg^{2+}	Na^+	K^+	Cl^-	SO_4^{2-}
NO_3^-	1						
Ca^{2+}	0.37	1.00					
Mg^{2+}	0.51	0.41	1.00				
Na^+	-0.04	0.24	0.06	1.00			
K^+	0.25	0.24	0.66	-0.12	1.00		
Cl^-	0.22	0.34	0.53	0.56	0.14	1.00	
SO_4^{2-}	-0.04	0.77	0.08	0.48	0.01	0.21	1.00

The Tulare aquifer is where the areas of nitrate pollution are indicated by dark colors on the geographical distribution map (Fig. 34). The center of the basin is where most of the polluted regions are located. In the rural area of the research region, there is a greater concentration of nitrate due to a significant input of chemical or mineral fertilizer.

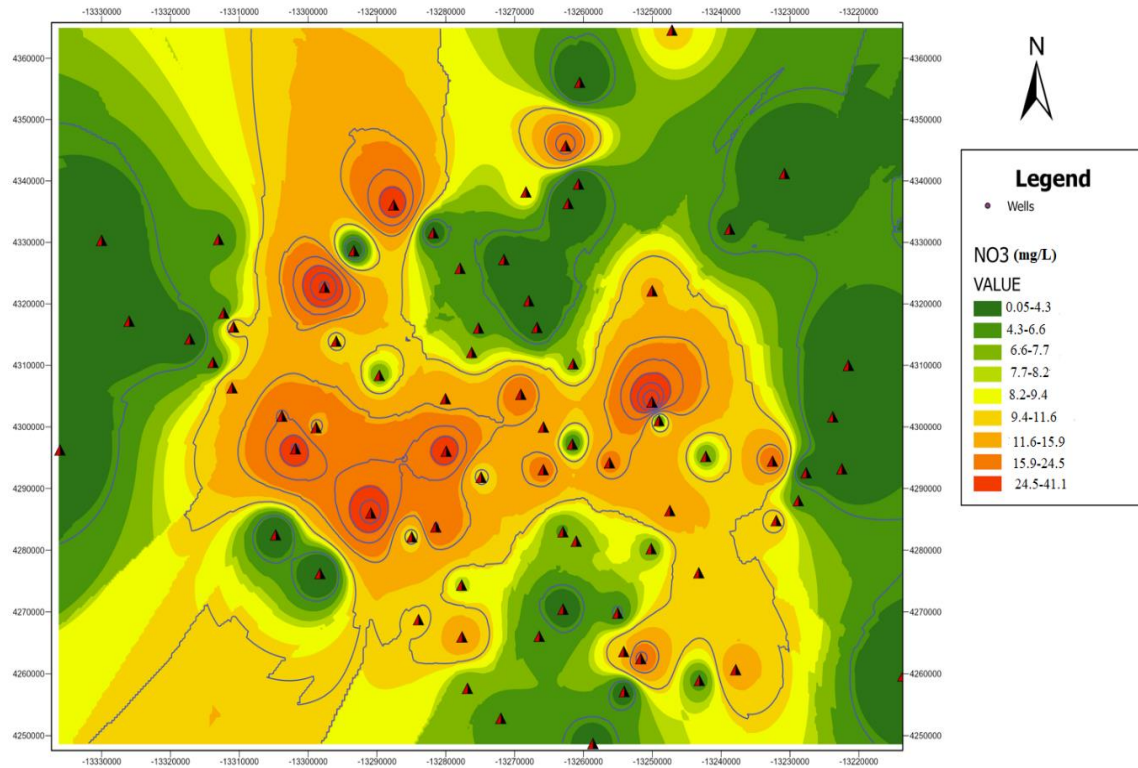


Fig. 34. Spatial distribution of nitrate in Tulare aquifer

Table 21) Stable isotopes values in Tulare aquifer

GAMA_ID	$\delta^{15}\text{N}$ of nitrate	$\delta^{18}\text{O}$ of nitrate	$\delta^{18}\text{O}$ of water	$\delta^2\text{H}$ of water	Nitrate (mg/l)
S4-TUSK-HLS01	4.30	3.30	-7.47	-57.5	11.9
S4-TUSK-HLS02	6.12	5.10	-8.58	-64.8	0.897
S4-TUSK-HLS03	5.12	5.33	-7.29	-57.3	23.1
S4-TUSK-HLS04	9.88	5.28	-7.86	-58.7	0.777
S4-TUSK-HLS05	4.43	-1.05	-10.36	-71.6	9.97
S4-TUSK-HLS06	3.09	3.06	-9.04	-64.0	4.04
S4-TUSK-HLS07	8.35	3.53	-8.36	-66.1	5.19
S4-TUSK-HLS08	4.28	5.32	-5.68	-51.1	6.67
S4-TUSK-HLS09	5.91	3.01	-6.88	-58.6	13.3
S4-TUSK-HLS10	1.66	3.42	-7.61	-58.5	10.6
S4-TUSK-HLS11	5.94	2.67	-7.90	-59.0	19
S4-TUSK-HLS13	1.83	3.01	-9.66	-70.3	0.7
S4-TUSK-HLS15	10.62	5.25	-8.84	-67.8	2.11
S4-TUSK-HLS16	8.85	4.54	-9.11	-67.0	5.99
S4-TUSK-HLS17	14.32	12.55	-6.70	-55.4	0.211
S4-TUSK-HLS18	9.46	5.72	-9.94	-69.1	1.38
S4-TUSK-HLS19	10.05	4.71	-8.94	-64.2	0.06
S4-TUSK-HLS20	4.60	2.16	-9.70	-67.9	0.222
S4-TUSK-KAW01	10.98	-0.06	-11.24	-83.7	30.8
S4-TUSK-KAW02	4.02	-2.34	-11.59	-85.3	20.2
S4-TUSK-KAW03	4.36	-1.35	-11.68	-84.8	12.1
S4-TUSK-KAW04	9.90	4.77	-11.63	-85.9	5.18
S4-TUSK-KAW05	43.02	6.51	-11.49	-86.3	0.073
S4-TUSK-KAW06	16.82	5.36	-9.86	-73.9	29.3
S4-TUSK-KAW07	4.00	-0.50	-10.10	-74.7	2.66
S4-TUSK-KAW08	8.14	-1.92	-11.03	-80.9	36.1
S4-TUSK-KAW09	4.01	-1.10	-11.60	-85.5	9.2
S4-TUSK-KAW10	5.89	-1.79	-12.17	-88.7	6.69
S4-TUSK-KAW11	5.37	-0.92	-11.99	-88.5	14.3
S4-TUSK-KAW13	13.10	1.44	-9.39	-70.0	29.1
S4-TUSK-KAW14	5.66	-2.45	-12.09	-87.7	14.4
S4-TUSK-KAW15	3.70	-2.44	-12.07	-88.4	7.43
S4-TUSK-KAW16	5.58	0.57	-12.23	-88.6	5.92
S4-TUSK-KAW17	3.74	-0.82	-12.04	-87.0	5.74
S4-TUSK-KAW18	2.43	-1.15	-9.90	-73.3	3.06
S4-TUSK-KAW19	9.55	6.41	-10.16	-77.5	9.46
S4-TUSK-KAW20	5.54	0.95	-12.08	-86.5	2.44
S4-TUSK-KAW21	13.53	20.52	-12.18	-87.3	0.041
S4-TUSK-KAW22	5.03	3.04	-11.83	-84.9	2.78
S4-TUSK-KAW23	5.06	0.04	-10.61	-78.0	20.1
S4-TUSK-KAW24	4.08	1.73	-6.23	-56.8	14.7
S4-TUSK-KAW25	6.38	2.71	-9.60	-75.6	16.9
S4-TUSK-KAW26	4.70	1.06	-10.19	-76.4	4.8
S4-TUSK-KAW27	7.86	7.09	-7.40	-61.0	41.2
S4-TUSK-KAW28	5.83	3.83	-10.20	-77.4	7.07
S4-TUSK-KAW30	7.92	4.69	-8.63	-62.5	1.34

Table 21 (Cont.)

GAMA_ID	$\delta^{15}\text{N}$ of nitrate	$\delta^{18}\text{O}$ of nitrate	$\delta^{18}\text{O}$ of water	$\delta^2\text{H}$ of water	Nitrate (mg/l)
S4-TUSK-TLA01	-10.46	-6.42	-8.99	-65.5	0.095
S4-TUSK-TLA04	0.62	-6.03	-12.62	-94.6	1.48
S4-TUSK-TLA05	57.51	18.09	-12.87	-97.3	0.073
S4-TUSK-TLA11	3.70	-1.48	-13.17	-97.4	5.6
S4-TUSK-TLA12	28.62	9.57	-11.10	-81.9	5.35
S4-TUSK-TLA13	11.06	6.19	-11.39	-84.8	11.1
S4-TUSK-TLE03	19.67	6.99	-10.62	-75.8	0.54
S4-TUSK-TLE04	7.85	4.81	-10.85	-81.5	1.32
S4-TUSK-TLE05	11.14	-0.03	-10.99	-81.7	33.1
S4-TUSK-TLE06	5.78	-1.30	-10.99	-79.9	8.83
S4-TUSK-TLE07	2.52	-1.10	-9.68	-68.9	9.53
S4-TUSK-TLE10	4.22	0.02	-9.95	-73.0	6.65
S4-TUSK-TLE11	2.13	-0.28	-9.68	-69.4	14.5
S4-TUSK-TLE12	3.40	-1.31	-10.40	-76.6	7.83
S4-TUSK-TLE13	8.39	-0.67	-11.02	-81.0	20.2
S4-TUSK-TLE14	6.00	-1.40	-11.12	-80.4	9.24
S4-TUSK-TLE15	7.75	-0.68	-12.18	-88.7	17.8
S4-TUSK-TLE16	8.08	-1.94	-11.65	-84.8	6.3
S4-TUSK-TLE17	3.14	0.20	-12.72	-92.7	1.97
S4-TUSK-TLE18	2.35	0.39	-9.78	-69.8	5.65
S4-TUSK-TLE19	6.05	0.12	-10.10	-74.5	5.44
S4-TUSK-TLE20	4.46	1.26	-8.90	-68.7	2.92
S4-TUSK-TLE21	6.40	1.97	-8.77	-62.9	2.36
S4-TUSK-TLE22	4.13	2.22	-8.17	-62.6	11.2
S4-TUSK-TLE23	2.50	0.95	-9.31	-66.0	4.65
S4-TUSK-TLE24	2.48	-0.39	-10.57	-77.0	7.34
S4-TUSK-TLE25	5.18	2.36	-8.03	-64.0	14.8
S4-TUSK-TLE26	8.26	2.36	-9.85	-71.1	6.95
S4-TUSK-TLE27	4.61	3.60	-8.40	-62.8	11.6
S4-TUSK-TLE28	3.33	2.31	-6.16	-55.8	21.9
S4-TUSK-TLE29	6.08	4.45	-7.54	-64.6	5.83

3.3 Heavy Metals Evaluation in Groundwater

Pollution indices are often established to assess whether water is suitable for a certain intended application. In this work, the indices Heavy Metal Contamination Index (HPI), Heavy Metal Evaluation Index (HEI), and Degree of Contamination (Cd) are computed to assess the level of groundwater pollution. The ratios between the observed values of the parameters and the permitted concentrations of the corresponding parameters are used to assess these indices.

The HPI is created in two steps: first, creating a grading scale for each chosen parameter (heavy metal); and second, choosing the pollutant parameter on which the index is to be based. The HPI is based on the "weighted arithmetic quality" mean technique. Heavy metals evaluation index (HEI) will also be evaluated in order to have a better knowledge of the pollutant loads in the aquifers. Contamination degree is the last index for evaluation of heavy metals concentration in the aquifers (table 21). It sums up the combined impacts of a number of quality characteristics that are thought to be hazardous to domestic water (Backman et al., 1998). For Tulare aquifer HPI is calculated for As, Ba, B, Mo, Sr, V, and U based on the equations (table 22).

Table 22) values used to HPE, HEI, and Cd indices

Heavy metals	The weightage (1/MAC)	S	I	MAC
As	0.02	50	10	50
Ba	0.0005	2000	700	2000
B	0.002	500	0	500
Mo	0.014	70	0	70
Sr	0.0003	4000	0	4000
V	0.05	20	0	20
U	0.05	30	0	20

MAC: maximum admissible concentration

I: Highest permissible in ppb

S: standard permissible (EPA)

182 examined wells between 2000 and 2020 had groundwater samples with pH values ranging from 6.1 to 9.6, with a mean of 7.7, indicating mild acid to alkaline conditions. The Tulare aquifer's mean concentration of As, Ba, B, Mo, Sr, V, and U was determined to be 0.01, 0.09, 0.16, 0.01, 0.41, 0.02, and 0.22 mg/L from 2000 to 2020, respectively. Moreover, the mean concentrations were observed in decreasing order of Sr > U > B > Ba > Mo > As whereas the

concentration of As, Mo, and U in 13.8, 4.4, and 12.7% of the studied wells (n=182) respectively are more the standard level reported by EPA and WHO. These polluted wells are mostly located on the central part of Tulare aquifer with more agricultural lands.

Arsenic fluctuation in the Central Valley may potentially be influenced by increasing groundwater residence time and introducing oxidizing recharge water (through irrigation) with high dissolved solids contents (Anning et al., 2012).

(Ayotte et al., 2016) have identified two causes for increased arsenic in anoxic and oxic environments by study of arsenic in groundwater in the San Joaquin Valley and based on prior studies. The first is arsenic that is produced when iron or manganese oxyhydroxides are reduced under iron- or manganese-reducing conditions (anoxic conditions). The second is an increase in the concentration of dissolved arsenic brought on by desorption or suppression of sorption to aquifer sediments when pH increases in an oxic environment. Additionally, between 1980 and 2019 Haugen et al (2021) assessed the arsenic content in 7870 wells situated inside the San Joaquin valley limit. They discovered that since 2010, 10% or so of San Joaquin Valley drinking water wells had had arsenic concentrations higher than the country's 10 $\mu\text{g/L}$ maximum contamination standard. High pH (more than 7.8) or changed geological conditions are commonly connected to high arsenic concentrations. They discovered that these wells typically showed elevated nitrate and sulfate trends, indicating oxic groundwater that was probably recharged by agriculture.

High level of salinity in groundwater also is frequently accompanied with an increase in toxic elements such as arsenic and boron. The coexistence of various contaminants is conceivably explained by the salt effect, competing adsorption for the active sites on the adsorbent, microbiological activities, and cation exchange (Li et al., 2020).

Nearly 24% of the household wells in the eastern San Joaquin Valley that were evaluated

had uranium contents over the US EPA MCL and were located in agriculturally-dominated areas (Rosen et al., 2019). According to research by Jurgens et al. (2010), shallow aquifers with high bicarbonate concentrations are strongly related to groundwater with high U contents. They claimed that the creation of uranylcarbonato complexes, which are desorbed from mineral surfaces and transmitted to shallow aquifers by irrigation recharge, is favored by crop production and increases P_{CO_2} in oxic surface soils.

Nolan and Weber (2015) discovered a reasonably significant association between nitrate and uranium contents in the Central Valley and High Plain aquifers in the United States in addition to bicarbonate alkalinity. The fertilizer nitrate can change U(IV) to U(VI) by oxidative dissolution or a variety of other indirect mechanisms. By reacting with complexing ligands like carbonate and then with alkaline earth metal ions like Ca^{2+} , nitrate-generated U(VI) can be transported into shallow aquifers.

The impact of HCO_3 and NO_3 on the U mobilization of groundwaters in the San Joaquin Valley was also validated by Rosen et al. in 2019. They expanded their knowledge of U's geologic genesis to include alluvial fan sizes. The location of high concentrations is determined by the combination of geological U sources from fluvial fans that start in the Sierra Nevada to the east and seepage of irrigation water with high concentrations of HCO_3 , which leaches U from the sediments.

Molybdenum (Mo) content in groundwater is affected by redox and pH conditions. Mo concentrations in groundwater are typically modest ($2 \mu\text{g/L}$), and when they are increased, they are due to anthropogenic pollution, however geogenic sources have also been found. In oxic and anoxic aquifers, Mo is soluble in groundwater when the pH is more than 7.5. The mobilization of Mo and As is controlled by the reductive dissolution of iron and manganese oxides and the

precipitation of sulfide minerals under highly reducing circumstances. "Mo is often plentiful in sulfide-organic-rich sediments, and another possible source of the metal for groundwater is the oxidative breakdown of sulfide minerals like pyrite" (Harkness et al, 2017).

The HPI values for the Tulare aquifer deviate from 4.33 to 1,300.7 with mean of 63.9 for 7 heavy metals (As, Ba, B, Mo, Sr, V, and U) in 182 groundwater samples years between 2001-2020. It is inferred that, 24 wells have HPI more than 100 with mean value of 217.46, hence unfit for human consumption. These wells are: HLS10, 11, 15, 16, KAW1, 5, 6, 7, 13, 15, 16, 18, 20, 23, 26, 25, 29, TLA5, 9, 12, 13, and TLE 4,5 (fig. 35).

HEI, which has also been evaluated for a better understanding of the pollutant loads, has a range of 0.04 to 36.01 and a mean value of 2.33. High concentrations of metal compared to Si value indicate poor water quality. According to this index, this water cannot be utilized if the concentration of each metal exceeds the maximum permissible value in the standards (i.e. the Mi / Si ratio is more than one). As a result, based on the HEI index, a value of "one" is defined a pollution risk threshold (Seifi and Riahi, 2017). Accordingly, among 182 studies well, 137 wells (75%) have HEI more than 1 and consequently are considered inappropriate for residential usage.

To determine the degree of metal pollution, the contamination index (Cd) is also used. Cd readings vary from -6.96 to 29.01 and -4.67, respectively, and all wells—aside from three (HLS15, KAW05, and TLA09)—are classified as low contaminated with Cd levels of less than 1. (fig. 36).

Different indexes indicate various risk classifications. Consequently, a scatter plot of HPI, HEI, and Cd against one another has been created and is displayed in Fig. 36, table 12, in order to provide more information. The scatter figure clearly shows that HEI and Cd have a significant link with a correlation coefficient of $R^2 = 0.99$, whilst HPI and HEI and Cd and HPI have weak correlations with $R^2 = 0.7499$ and 0.7487 , respectively. As a result, choosing between the HEI and

Cd indices, or using both, may be a preferable alternative for classifying samples.

Different indices represent different classes of risk levels. Therefore, for more information, a scatter plot of HPI, HEI and Cd versus each other have been prepared and are shown in Fig. 36, table 12. It is obvious from the scatter plot that there is a strong correlation between HEI and Cd with correlation coefficient value of $R^2 = 0.99$, whereas poor correlations between HPI and HEI ($R^2 = 0.7499$), and Cd and HPI ($R^2 = 0.7487$) are observed. Therefore, a selection of either HEI and Cd indices or both could be a better option for the classification of samples.

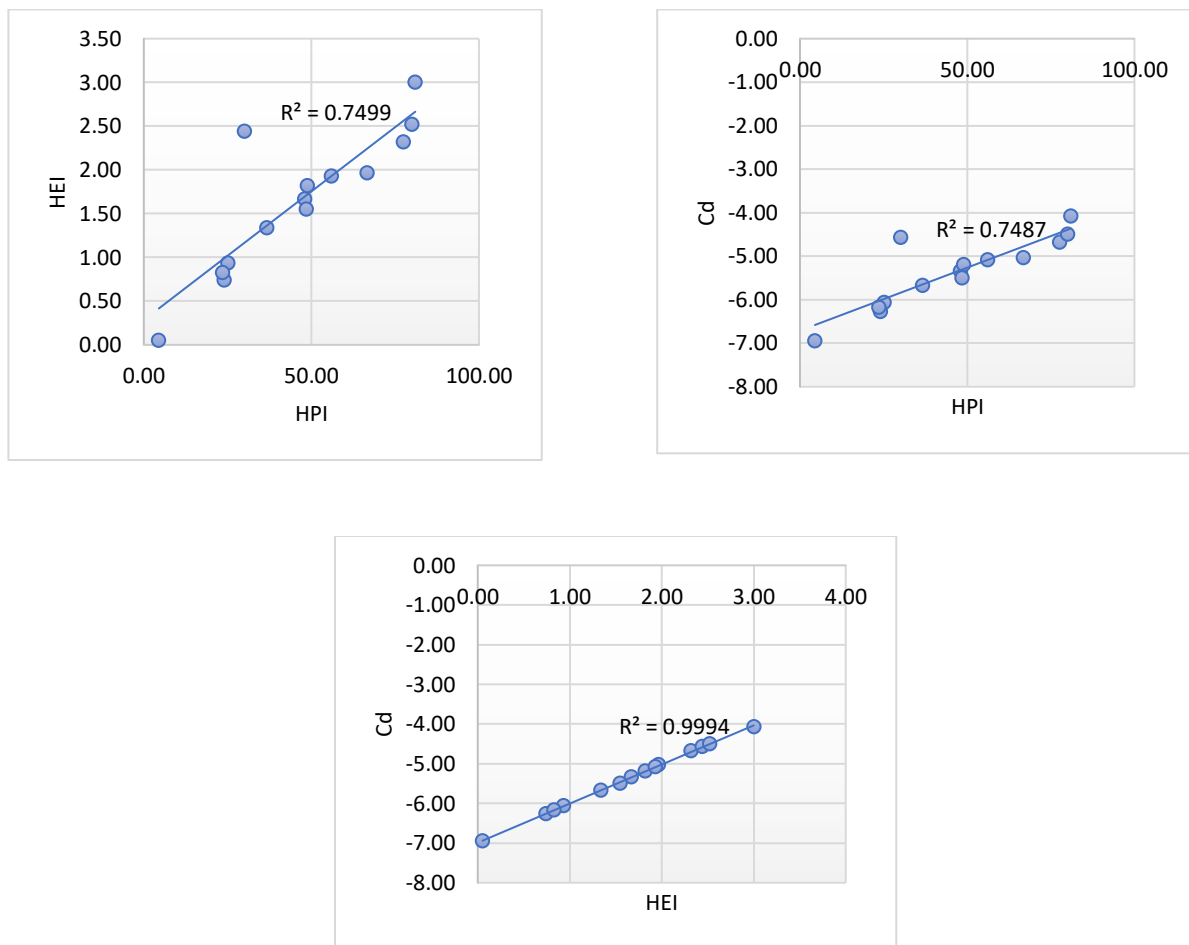
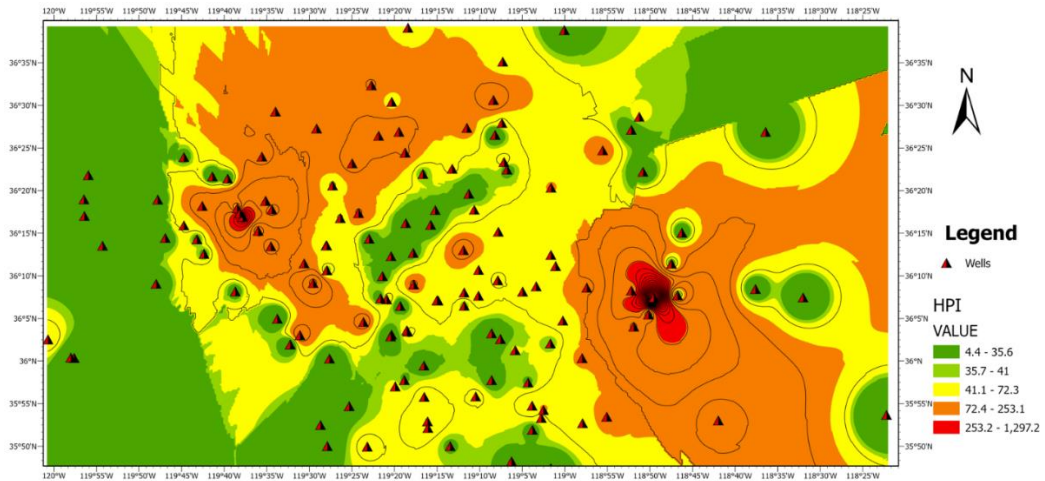
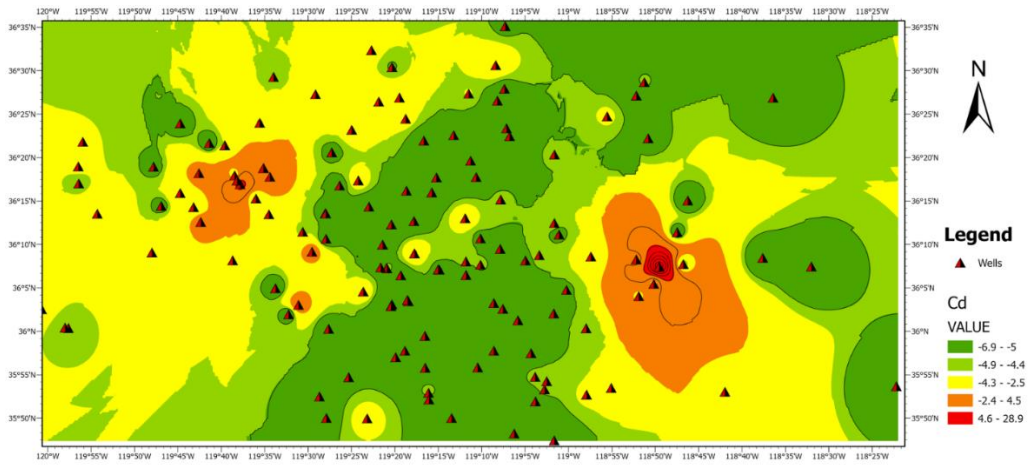


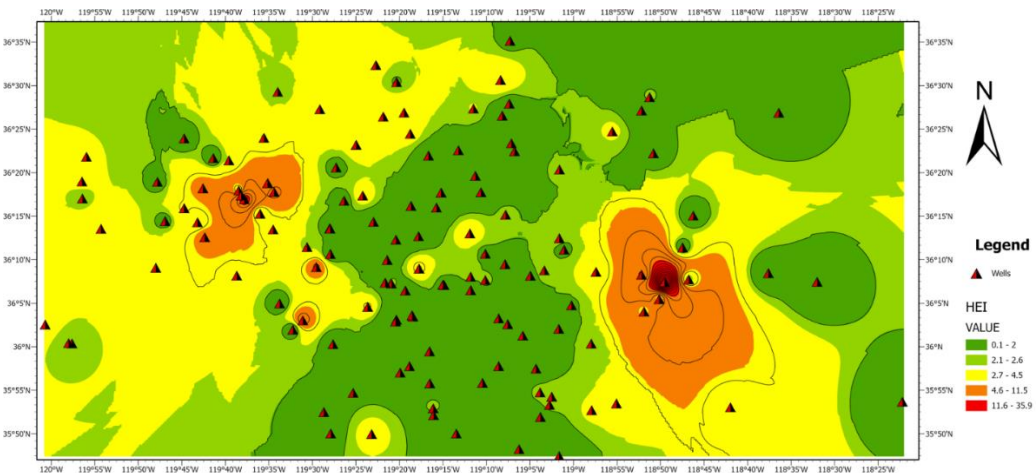
Fig. 36. "Scatter plot of a) HPI versus HEI b) HEI versus Cd c) HPI versus Cd indices and their correlation of determination in the Tulare aquifer"



a)



b)



c)

Fig. 35. Geographical distribution of studied parameters in the Tulare aquifer: a) HPI b) Cd c) EHI

Chapter 4: San Joaquin Aquifer

One of the most agriculturally productive regions in the world is the Central Valley of California, which has a total area of 51,799.8 km². More than 250 different crops worth a combined \$17 billion are grown in the Central Valley each year. For California's rapidly expanding metropolitan population, the Central Valley is likewise emerging as a crucial location. This region's population has increased from 2 million to 3.8 million since 1980, almost doubling. Due to the increase in population, there is more competition for water resources in the Central Valley (Claudia et al., 2009).

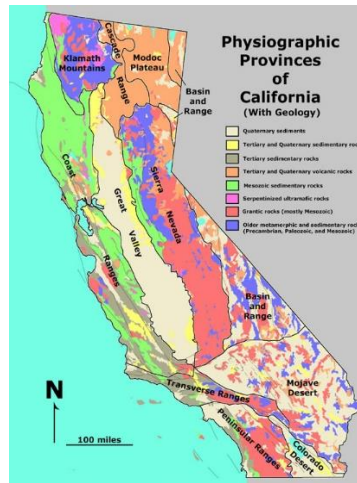
Two basins make up the San Joaquin Valley, which makes up the southern two-thirds of California's Central Valley: the San Joaquin Basin to the north and the Tulare Basin to the south (Fig. 37). An arid to semi-arid Mediterranean climate characterizes the San Joaquin Valley, with mean annual precipitation ranging from 15 to 20 inches between 1911 and 1960. (Gronberg et al., 1998). The majority of the unconsolidated alluvial, fluvial, and lacustrine deposits from the Quaternary to Pliocene age make up the upper 500 m of the freshwater San Joaquin aquifer. The aquifer is typically unconfined, but as it descends, various clay lenses cause it to become somewhat confined. Wells lose their impermeability and are more susceptible to vertical flow where they have been drilled through clay layers, such as the Corcoran Clay component that covers a sizable portion of the SJV (Weissmann et al., 2005). Since the development of the groundwater system for agriculture and public water supply, irrigation, seepage from rivers and streams, precipitation, urban runoff, and runoff from the nearby Sierra Nevada (in the east) have been the dominant sources of recharge where groundwater withdrawals from wells have been the main source of discharge in the San Joaquin aquifer (Faunt et al., 2009, California Department of Water Resources, 2003). Groundwater is largely used for agriculture in this region, especially during dry

years when surface water supplies are constrained (California Department of Water Resources, 2003).



<https://ca.water.usgs.gov/projects/central-valley/about-central-valley.html>

a



<https://geologycafe.com/california/maps/provinces1.htm>

b

Fig. 37. a) Location Map of San Joaquin and Tulare aquifers in Central Valley-California b) location of central valley in California

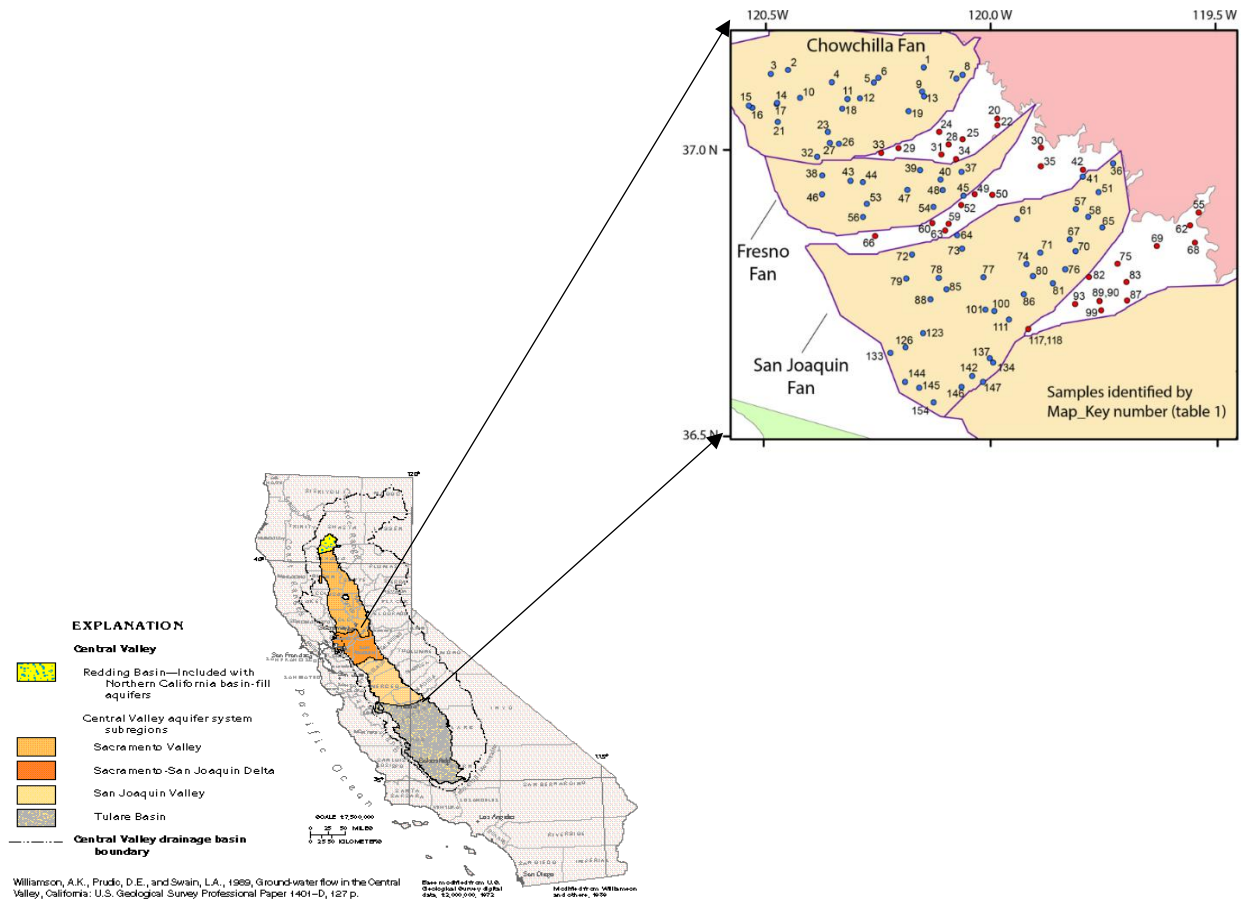


Fig. 38. The location of San Joaquin Valley in California (USGS, 2019)

4.1 Water Quality Assessment for Irrigation in San Joaquin Aquifer

To assess the groundwater quality and potential anthropogenic causes of groundwater contamination, 450 water samples is collected (USGS). These samples are years between 2000 to 2019 from 154 domestic and public supply wells (fig. 38).

The effects of chemical interactions between groundwater and lithologic framework's minerals are reflected in hydrogeochemical types. When combined with distribution maps and hydrogeochemical types, hydrogeochemical diagrams are intended to make it easier to identify evolutionary tendencies, especially in groundwater systems. It is possible to characterize the hydrogeochemical data as a whole by distinguishing the various hydrogeochemical kinds of water—commonly referred to as water type—using various plots, such as the trilinear Piper plot. The Piper trilinear diagram (Fig. 39), which includes cations and anions, shows the various geochemical patterns of the different types of groundwater that are prevalent in the research region. Similar to the cation triangle, the majority of the samples are concentrated to the right, indicating groundwater of the Ca^{2+} and Na^+ types. The anion field shows that the majority of the samples are concentrated to the left of the triangle, indicating that anions such as Cl^- and HCO_3^- predominate in the groundwater. The general characteristics of groundwater are shown by the diamond field. It reveals that the alkaline earths (Ca^{2+} and Mg^{2+}) predominate over the alkalis (Na^+ and K^+) in the San Joaquin aquifer, and the Ca-HCO_3 facies demonstrates the predominance of weak acids (HCO_3^-) over strong acids (SO_4^{2-} and Cl^-). As a consequence, $\text{HCO}_3\text{-Ca_Mg}$ was the most prevalent compound, followed by $\text{HCO}_3\text{-Na}$, which is connected to aquifers' carbonate-rich minerals. The strong correlation between alkali and alkaline earth metals and HCO_3^- ions lends credence to the hypothesis that weathering is caused by natural processes. The bacterial dissolution

of organic pollutants, the mineral dissolution of carbonates, or soil CO₂ can all result in the production of HCO₃.

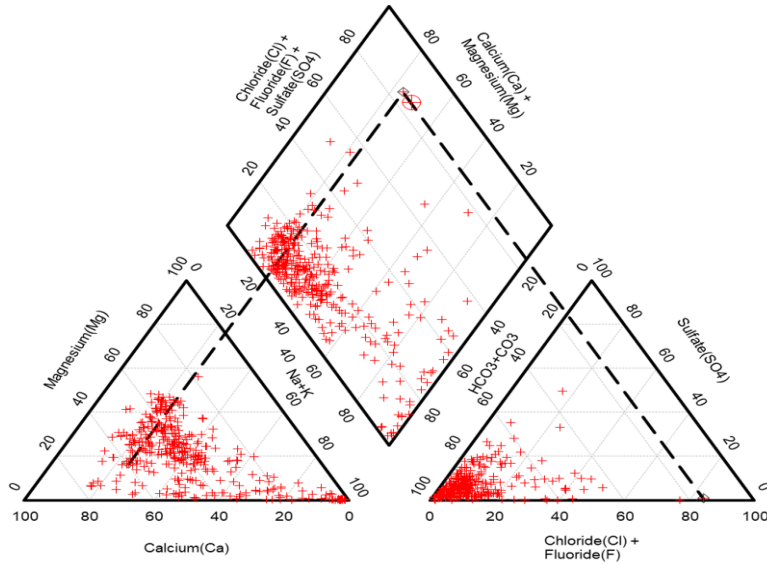


Fig. 39. Piper diagram for the groundwater in San Joaquin Valley

4.1.1 Salinity Index and Salinity Hazard

According to the EC values, 52% of the samples are classified as having low water salinity, 44.5% as having medium salinity, and 3.08% as having high salinity with allowable quality (table 23).

Table 23) Classification of water salinity based on EC (Handa,1969)

EC (µS/cm)	Water salinity	EC range (no. of sample)	Percent
0-250	Low (excellent quality)	53.6-250 (152 sample)	52
251-750	Medium (good quality)	255-716.9 (130 samples)	44.5
751-2,250	High (permissible quality)	850-1,058 (9 samples)	3.08
2,251-6,000	Very high	2,907 (1 sample)	
6,001-10,000	Extensively high	-	-
10,001-20,000	Brine weak concentration	-	-
20,001-50,000	Brine moderate concentration	-	-
50,001-100,000	Brine high concentration	-	-
>100,000	Brine extremely high concentration	-	-

The electrical conductivity (EC) measurements made in this area's calculations classified the salinity threat into four categories (Table 24). Among the investigated samples, 152 samples (n=292) are assigned to the C1 category for exceptional quality, 130 samples to C2 for good quality, 18 samples to C3 for question, and one sample to C4 for inappropriate for irrigation (Table 24).

Table 24) Salinity hazards used to classify the water in the research region

Salinity hazard class	EC (µS/cm)	Quality	range (no. of sample)	Percent
C1	100-250	Excellent	53.6-250(153 sample)	52
C2	250-750	Good	255-716.9(130 samples)	44.5
C3	750-2,250	Medium	850-1,058 (9 samples)	3.08
C4	>2,250	Unsuitable	2,907 (1 sample)	-

4.1.2 Sodium Percent (%Na) and Sodium Absorption Ratio (SAR)

The categorization of water samples according to salt percent is shown in Table 25. Accordingly, the results show that 53.8% of the samples fall into the "Good" category, 20.2% are "Permittable," 6.5% are "Doubtful," and 9.6% are "Unsuitable for Irrigation Use" (table 25).

Table 25) categorization of water depending on the percentage of sodium (Wilcox,1955)

"Sodium (%)"	"Water class"	"Range (no. of sample)"	Percent
<20	"Excellent"	10.7-19.8 (29 samples)	9.9
20-40	"Good"	20.0-39.8 (157 samples)	53.8
40-60	"Permittable"	40.0-57.8(59 samples)	20.2
60-80	"Doubtful"	60.9-78.7 (19 samples)	6.5
>80	"Unsuitable"	80.1-98.8 (28 samples)	9.6

Table 26 presents the SAR classification of the groundwater samples from the San Joaquin aquifer. Approximately 91.5% of the samples have sodium absorption ratios under 10 and are classified as having excellent sodium hazard for irrigation (S1), 3.8% of the samples are classified

as having good sodium hazard for irrigation (S2), and 4.8% are classified as having relatively unsuitable sodium absorption ratios (SAR) for irrigation (S3). fig. 40 and 41 show wells with more salinity are located on west part of San Joaquin aquifer. These wells are drilled on Mesozoic and marine sediments.

Table 26) categorization of the San Joaquin aquifer's waters based on SAR ratings and USSL sodium danger classifications (Ravikumar et al. 2011)

SAR values	Sodium hazard class	Quality	Range	Percent
<10	S1	Excellent	0.2-8.6 (267 samples)	91.5
10-18	S2	Good	10.4-17.8 (11 samples)	3.8
19-26	S3	Doubtful	18.0-25.9 (14 samples)	4.8
>26	S4 and S5	Unsuitable	-	-

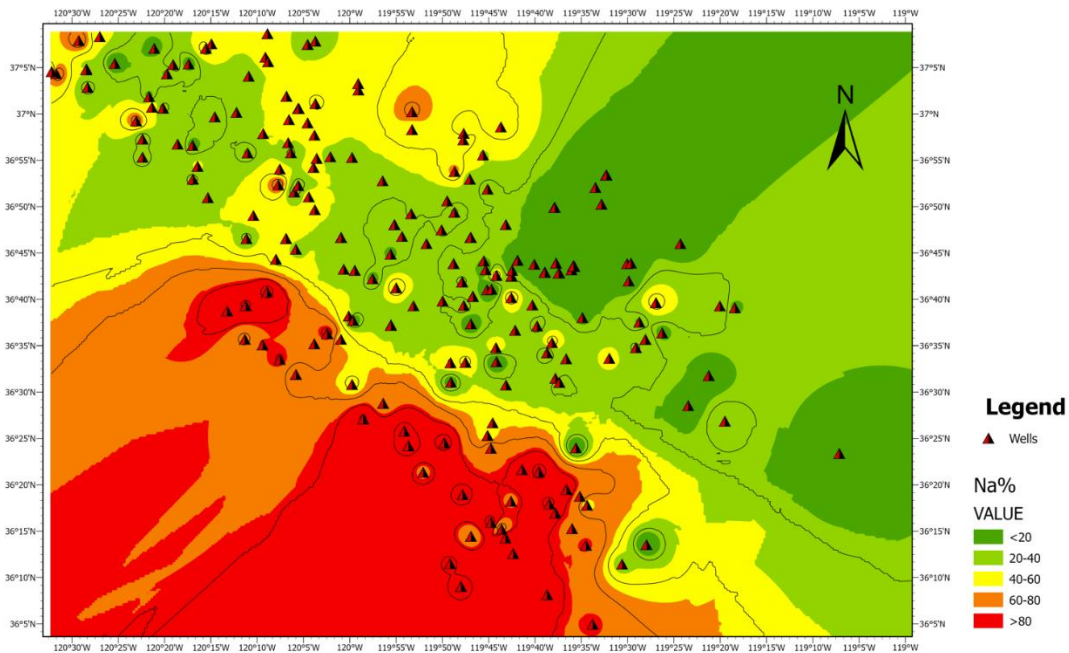


Fig. 40. Spatial distribution of sodium percent (Na%) in San Joaquin aquifer

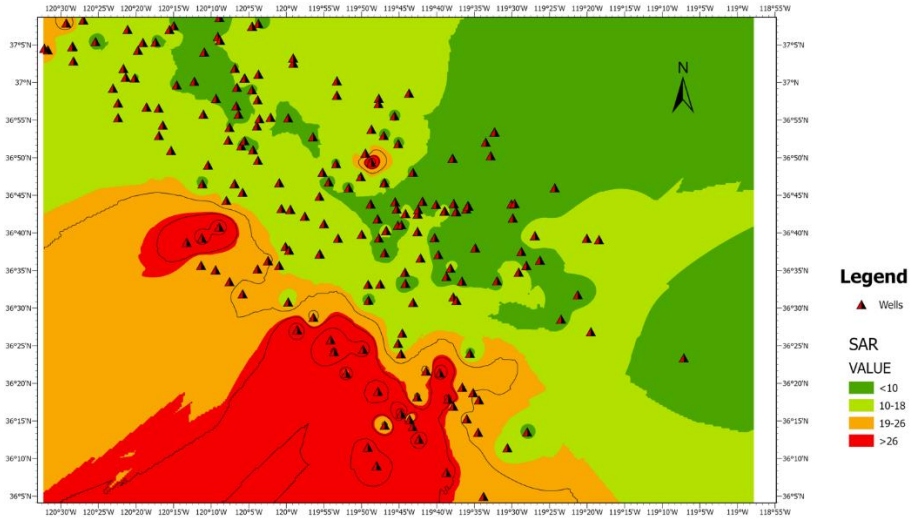


Fig. 41. Spatial distribution of sodium adsorption ratio (SAR) in San Joaquin aquifer

The majority of samples (88%) plot in the C1S1 and C2S2 zones of "the U.S. Salinity Laboratory (USSL)" map, which suggests that these water samples are risk-free. With the exception of one sample, 12% of samples fall into the classification C3S1, which denotes water with high salinity (C3) and low sodium (S1) hazards. This water may be used for irrigation on nearly all soil types with little risk of exchangeable sodium (fig. 42).

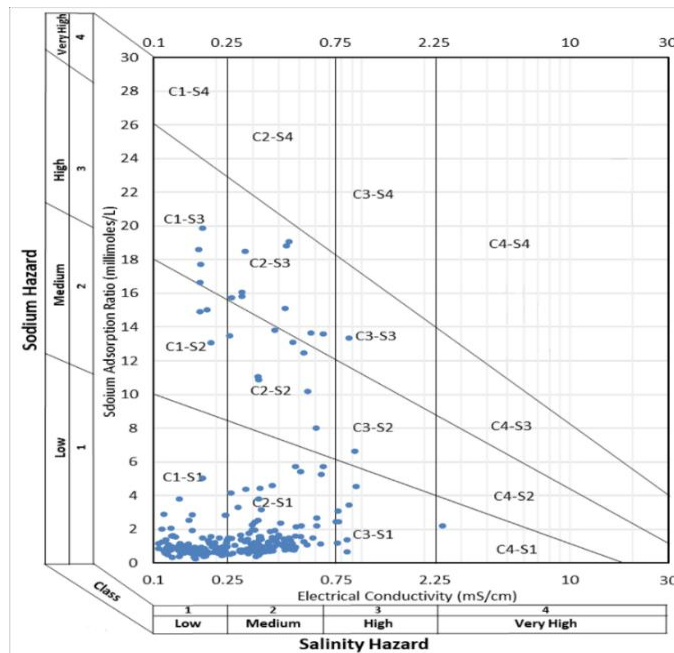


Fig. 42. Diagram of sodium adsorption ratio and salinity for classification of groundwater in San Joaquin aquifer for irrigation uses

4.1.3 Residual Sodium Carbonate

Because it's important to keep the equilibrium between these two ions, the excess of carbonate (CO_3^{2-}) and bicarbonate (HCO_3^-) over the alkali earth metals (Ca^{2+} and Mg^{2+}) might have an effect on the soil. High RSC concentrations in irrigation water speed up the adsorption of salt in soil (Eaton, 1950). RSC levels more than 5 hinder plant development, while RSC values greater than 2.5 are inappropriate for irrigation.

The dominating ion in the groundwater was bicarbonate, in accordance with the kind of water in the San Joaquin aquifer. As a result, just 1.7% of samples fell into the good group, 8.5% into the questionable category, and 87.2% into the inappropriate category for irrigation usage (fig. 43). (Table 27). In this area, RSC has an average value of 6.6 meq/L.

Table 27) Groundwater quality of San Joaquin aquifer based on (residual sodium carbonate)
RSC

RSC	Quality	Range	Percent
<1.25	Good	-32.6-0.6 (5 samples)	1.7
1.25-2.5	Doubtful	1.4-2.4 (25 samples)	8.5
>2.5	Unsuitable	1.3-1.7 (262 samples)	89.8

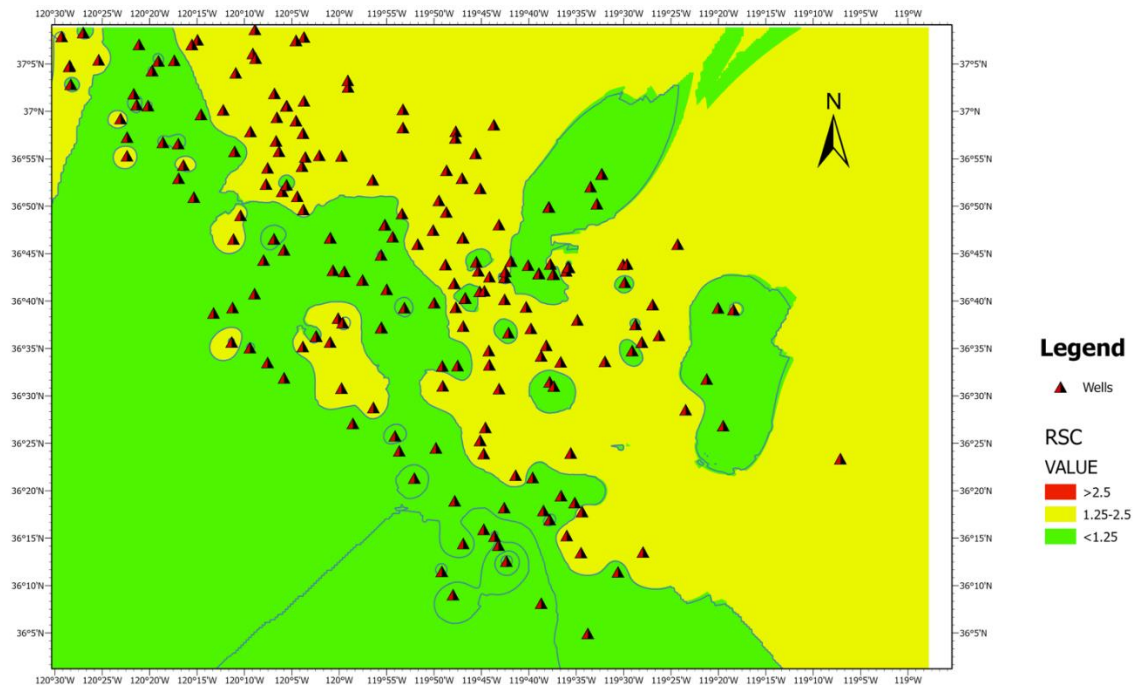


Fig.43. Spatial distribution of residual sodium carbonate (RSC) in San Joaquin aquifer

4.1.4 Magnesium Hazard

In most waters, Ca^{2+} and Mg^{2+} generally maintain an equilibrium condition, but they act differently in soil systems. Magnesium damages soil structure, especially in extremely salty and Na^+ -dominated groundwater. Typically, irrigated soils with exchangeable Na^+ have high Mg^{2+} concentrations. Increased Mg^{2+} levels in water will, in equilibrium, have a detrimental effect on soil quality and lead it to become alkaline, which will have a detrimental effect on crop yield (Ravikumar et al., 2011). Magnesium hazard (MH) levels more than 50% would be detrimental to agricultural development as soils become more alkaline. MH values in the San Joaquin aquifer ranged from 0.9 to 60.9. The majority of the samples (84.9%) in the study had MH values below 50, making them appropriate for irrigation, whereas 15.0% of the samples had MH values above 50, which may have a negative impact on the soil and cause it to become more alkaline. These wells are situated on the eastern edge of the San Joaquin aquifer, similar to the Tulare aquifer,

suggesting that granitic deposits in the Sierra Nevada Mountain range with high magnesium values may have an impact (fig. 44).

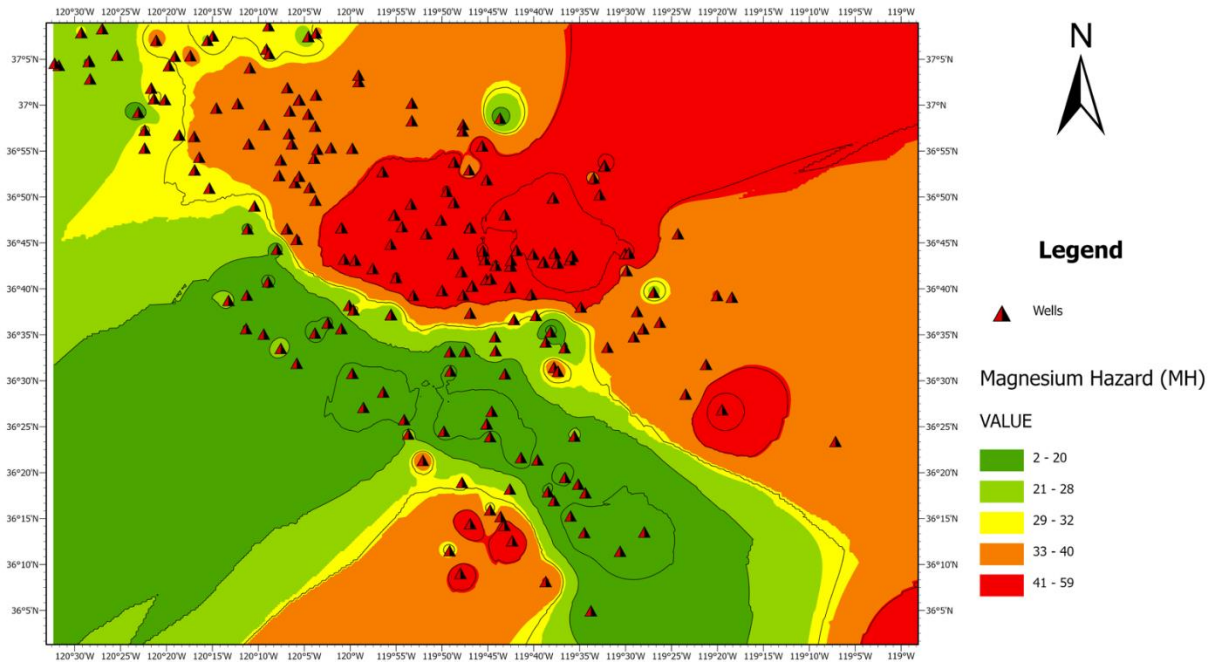


Fig. 44. Spatial distribution of magnesium hazard (MH) in San Joaquin aquifer

4.1.5 Permeability Index

The PI, which is impacted by extended contact to irrigation water having high concentrations of Na^+ , Ca^{2+} , Mg^{2+} , and alkalinity ions, is widely used to assess the appropriateness of irrigation water. The appropriateness of groundwater for irrigation has been categorized into three categories based on the permeability index. The San Joaquin aquifer's PI index is found to range from 20.63 to 144.0, and 46.3% of the samples are classified as acceptable (class I) for irrigation (PI more than 75%) whereas 53.8% of the samples are classified as class II (PI between 25-75%). (fig. 45).

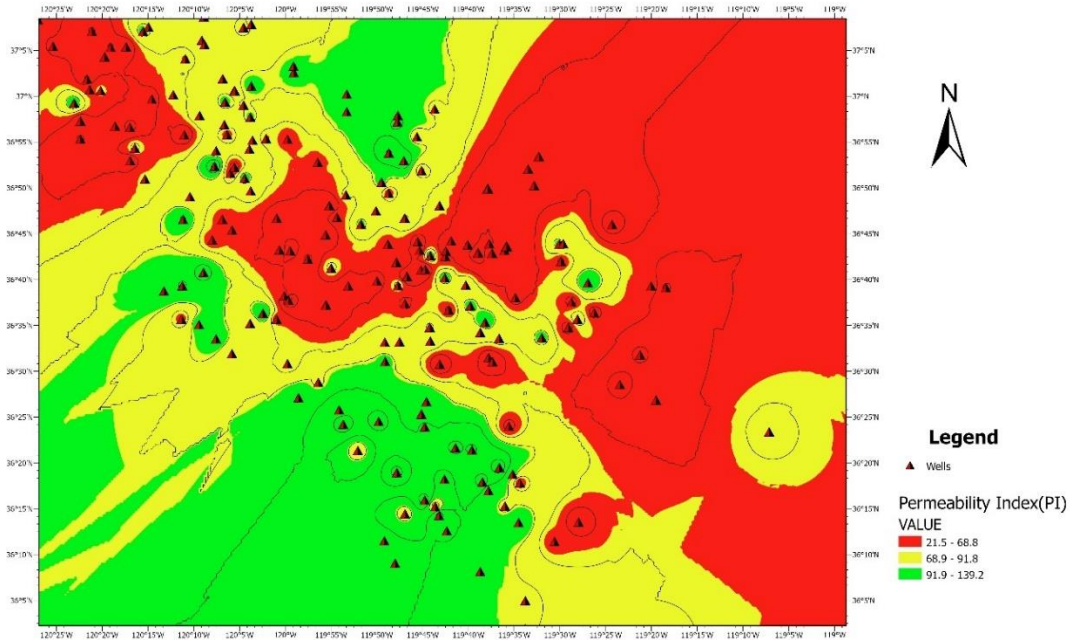


Fig. 45. Spatial distribution of permeability index (PI) in San Joaquin aquifer

4.1.6 Potential Salinity

Another accurate indicator of the suitability of irrigation water is the potential salinity, which is computed as the sum of the chloride ion concentration and half of the sulfate ion concentration. A lot more hazardous than SO_4^{2-} salts are Cl salts. As a result, when calculating potential salinity, only half of the SO_4^{2-} salt is considered.

Table 28) the division of groundwater according to potential salinity

Potential Salinity	Water class	Range	Percent
<3.0	Excellent to good	0.04-2.9 (247samples)	84.6
3.0-5.0	Good to injurious	3.0-4.5 (22samples)	7.5
>5.0	injurious to unsatisfactory	5.0-52.5 (23samples)	7.9

Table 28 shows that, in the east portion of the San Joaquin aquifer (fig. 46), 84.6% of water samples fall in the excellent to good category for irrigation, 7.5% fall in the good to harmful category, and only 7.9% of samples fall in the injurious to unsatisfactory class for irrigation (table 28).

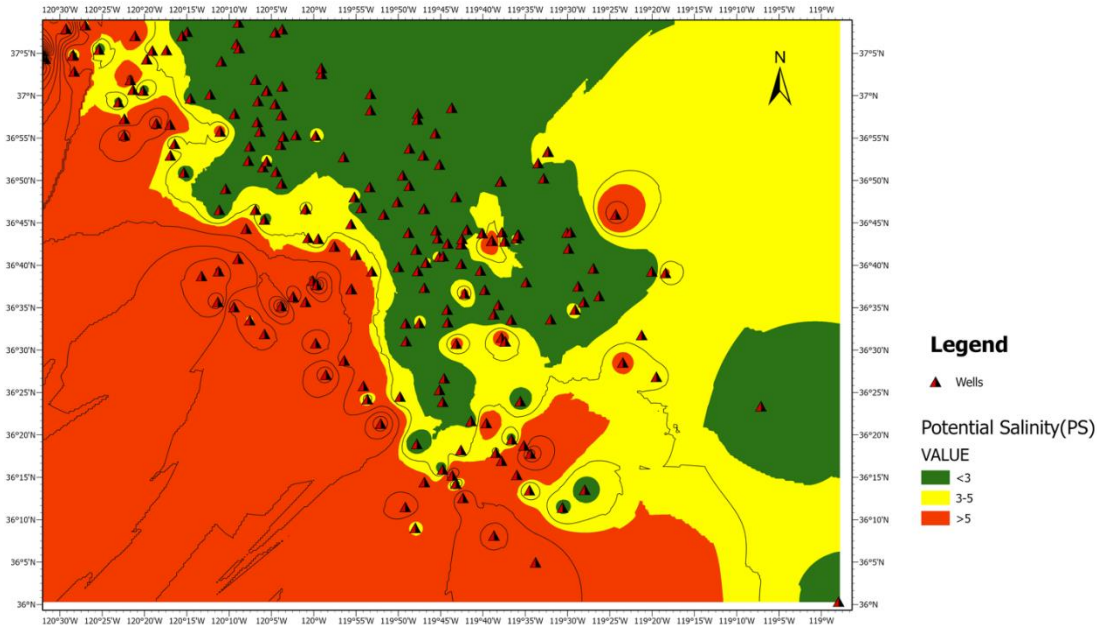


Fig. 46. Spatial distribution of potential salinity (PS) in San Joaquin aquifer

4.2 Heavy Metals Evaluation in San Joaquin Aquifer

For the San Joaquin aquifer, the Heavy metals Pollution Index (HPI), Heavy metals Evaluation Index (HEI), and Contamination Index (CI) (table 4) are taken into account. These indices are used in this aquifer for the elements U, As, Ba, B, Mo, Sr, and V. (table 29).

Table 29) values used to HPE, HEI, and Cd indices

Heavy metals	W	S	I	MAC
U	0.05	30	0	20
As	0.02	50	10	50
Ba	0.0005	2,000	700	2,000
B	0.002	500	0	500
Mo	0.014286	70	0	70
Sr	0.0003	4,000	0	4,000
V	0.05	20	0	20

With a pH range of 6.1 to 9.4 and a mean value of 7.5, the water in the San Joaquin aquifer is neutral to alkaline in nature in the 259 examined wells from 2000 to 2019. Sr, Ba, B, U, V, As, and Mo are the order of mean metals, accordingly. However, the water samples are contaminated

with V, U, and B when compared to EPA/WHO limits. With a mean of 1.16 mg/L, the boron content varies from 0.007 to 1.7 mg/L. Based on EPA, the standard permissible for boron is 0.5 mg/L, accordingly about 6.1% of the studied wells (n=259) have boron contamination with mean of 9.9 mg/L. The concentrations of B in domestic and certain industrial wastewater effluents range from several hundred $\mu\text{g/L}$ to several mg/L. According to earlier research, either treated or untreated wastewater releases practically all anthropogenic B burden into urban ecosystems. The most typical cause of this enrichment is sodium perborate, a bleaching chemical used in detergents and cleaning goods that is routinely dumped into home wastewater (Neal et al., 2010). Additionally, boron is a crucial element for plants, thus many fertilizers include it. As a result, the San Joaquin Valley, which has a high concentration of both urban and agricultural activity, may be a good area for boron poisoning of the groundwater. With a mean of 0.017 mg/L, the vanadium (V) content varies from 0.00005 to 1.08 mg/L. Since 0.02 mg/L of boron is the maximum allowed threshold, 35% of the wells under study (n=259) contain vanadium contamination with a mean of 0.03 mg/L.

There has been relatively little research on vanadium (V) in groundwater, despite the possibility that drinking vanadium-contaminated water might have harmful consequences on human health. Potential sources of V in groundwater include waste streams from industrial operations and the dissolution of V-rich rocks. Geochemical processes such adsorption/desorption, precipitation/dissolution, and chemical reactions control the amounts of vanadium in groundwater. Based on thermodynamic data and laboratory study, it is projected that samples collected from oxic and alkaline groundwater will contain the highest V concentrations. The relationship between thermodynamic data and laboratory results and the actual distribution of V in groundwater is not obvious, though. Analysis of 8,400 groundwater samples collected in California revealed that high

(50 mg/L) and intermediate (25 to 49 mg/L) V contents were more frequently detected in regions with source rock and favorable geochemical conditions. Groundwater samples' V content distribution shows that mafic and andesitic rock are major sources of V. (Wright and Belitz, 2010).

With a mean of 0.036 mg/L, the uranium content varies from 0.000012 to 0.556 mg/L. According to the EPA, 0.03 mg/L is the maximum permitted level for U, hence 24.7% of the examined wells (n=259) exhibit U contamination, with a mean value of 0.127 mg/L.

In the Central Valley of California, Lopez et al. (2021) identified the biogeochemical constraints on local groundwater uranium contamination by combining machine learning and geochemical modeling. They discovered that soil pH, groundwater calcium, nitrate, and sulfate concentrations, as well as clay content (weighted average between 0 and 2 m depths), are the most significant determinants of groundwater uranium concentrations. These groundwater U levels were also shown to be closely related to bicarbonate concentrations, with the highest U concentrations occurring in the shallow aquifer zone (Jurgens et al., 2010). Based on solid-phase measurements and geochemical modeling, they claimed that crop production increases PCO₂ in oxic surface soils and encourages the development of uranylcarbonato complexes, which are desorbed from mineral surfaces and transmitted to shallow aquifers by irrigation recharge.

In the United States, groundwater with a uranium content of more than 30 µg/L is exceptional for drinking water, but it can be dangerous in areas where Uranium is mobilized by complicated interactions between aquifer components and human-induced modifications to the natural flow regime. The procedures for mobilizing uranium in the San Joaquin Valley were examined by Rosen et al. in 2019. They expanded their knowledge of the geologic origins of uranium to the size of individual alluvial fans and confirmed mobilization by HCO₃ and disproved mobilization by NO₃. The interplay of high HCO₃ irrigation water seepage that leaches U from the

sediments and geological U sources from fluvial fans that start in the Sierra Nevada (east portion of the San Joaquin aquifer) to the west. Additionally, reactions with PO_4 from fertilized irrigated crops may cause U to be sequestered in the aquifer. The location and concentration of U in each individual fluvial fan are typically controlled by the interaction of high-U natural geological sources, anthropogenically induced HCO_3 additions, and possibly phosphate fertilizer, but the addition of nitrate to fertilizer does not appear to control the location of high U. Although these geochemical interactions are complex, they can be used to identify the causes of elevated U levels in alluvial aquifers.

Uranium (U), which is naturally rich in the soils and aquifer sediments of the eastern San Joaquin Valley, is unconnected to fertilizers or pesticides, in contrast to the agricultural contaminants. It comes from the east side of the San Joaquin Valley's Sierra Nevada granitic rocks (Jurgens et al., 2008). Additionally, because the aquifer in this region is oxic, uranium is predicted to stay mobile in groundwater, posing a major threat to its long-term sustainability as a source of drinking water (Jurgens et al., 2010).

The HPI for the San Joaquin aquifer deviates from 3.8 to 705.9 with mean concentrations 80 for 7 heavy metals (Sr, Ba, B, U, V, As, and Mo) in 259 groundwater samples years between 2000-2019. It may be assumed that 19.7% of the groundwater samples are unsafe for human consumption since they are over the threshold value of 100.

HEI, which has also been evaluated for a better understanding of the pollutant loads, has a range of 0.3 to 20.3 with a mean value of 2.59. As a result, according to 85% of studies, wells had HEI values more than 1, making them unsuitable for residential usage. To determine the degree of metal pollution, the contamination index (Cd) is also used. Cd has a range of -6.5 to 33.3 with a mean value of -2.6. About 12% of the samples have Cd more than 3, and 1.15% (3 samples) range

between 1-3 (table 30).

Table 30) water quality parameters in San Joaquin aquifer for irrigation uses years 2000 to 2020

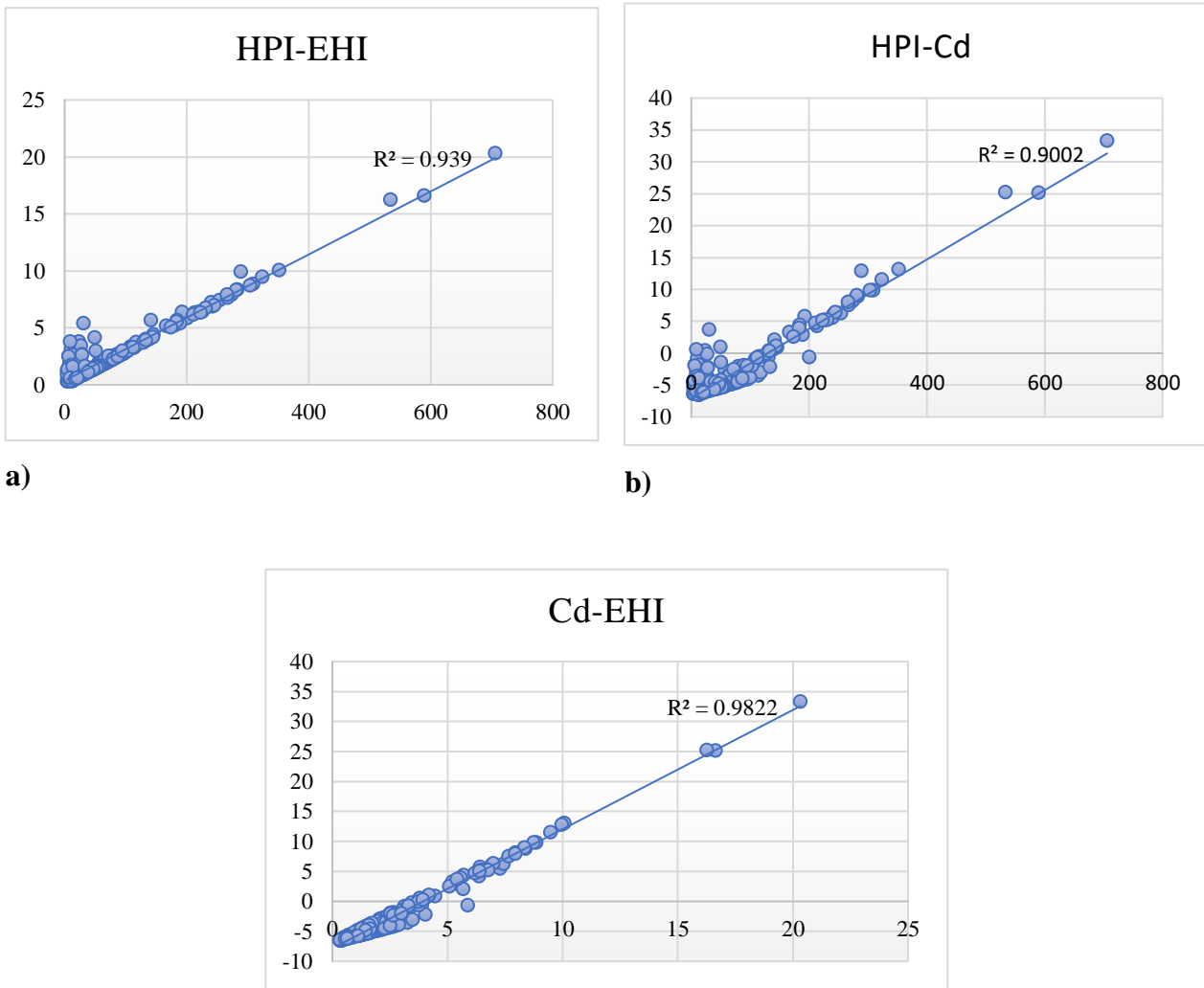
parameter	Unit	Maximum	Minimum	Mean
Ca ²⁺	Mg/L	654	0.79	54.2
Mg ²⁺	Mg/L	112	0.025	19.44
Na ⁺	mg/l	442	5.04	64.47
K ⁺	Mg/L	18.95	0.1	3.85
Cl ⁻	Mg/L	1850	0.82	52.3
SO ₄ ²⁻	Mg/L	703	0.18	50.52
HCO ₃ ⁻	Mg/L	822	50	247.3
CO ₃ ²⁻	Mg/L	676	41	204.18
EC	μS/cm	2907.8	53.6	300
pH	-	9.4	6.11	7.44
Na%	%	98.85	10.74	39.95
SAR	-	25.93	0.25	3.08
RSC	meq/L	33.56	-32.63	6.55
MH	%	60.97	0.97	34.12
PI	%	144.02	20.63	74.14
PS	meq/L	52.52	0.04	2

The high correlation between uranium and these indices (table 31) indicates that among studied heavy metals, U have the most effect on groundwater contamination in San Joaquin aquifer. Furthermore, the relatively high correlation of Sr, Ca, Mg, and Cl with EC shows that they are more solubility in alkaline groundwater.

Table 31) Spearman correlation between indices , studies heavy metal, nitrate, Ph and Eh

	EC	pH	Ca	Mg	Na	K	CaCO ₃	HCO ₃	Cl	SO ₄	NO ₃	U	As	Ba	B	Mo	Sr	V	HPI	HEI	Cd	
EC	1.00																					
pH	-0.18	1.00																				
Ca	0.86	-0.38	1.00																			
Mg	0.62	-0.46	0.73	1.00																		
Na	0.70	0.23	0.28	0.08	1.00																	
K	0.35	-0.39	0.49	0.49	0.02	1.00																
CaCO ₃	0.59	-0.23	0.51	0.66	0.49	0.40	1.00															
HCO ₃	0.59	-0.26	0.52	0.67	0.48	0.41	1.00	1.00														
Cl	0.83	-0.02	0.75	0.36	0.49	0.29	0.15	0.15	1.00													
SO ₄	0.56	-0.11	0.34	0.36	0.63	0.05	0.46	0.46	0.15	1.00												
NO ₃	0.38	-0.42	0.54	0.60	0.00	0.29	0.48	0.49	0.10	0.21	1.00											
U	0.41	-0.18	0.41	0.31	0.35	0.34	0.54	0.54	0.13	0.48	0.26	1.00										
As	0.01	0.42	-0.16	-0.21	0.26	-0.19	-0.02	-0.03	0.05	0.02	-0.21	-0.07	1.00									
Ba	0.67	-0.22	0.74	0.42	0.22	0.29	0.25	0.25	0.77	-0.04	0.30	0.03	-0.07	1.00								
B	0.27	0.34	-0.12	-0.18	0.71	-0.18	0.27	0.26	0.14	0.31	-0.19	0.04	0.25	-0.12	1.00							
Mo	0.25	0.13	-0.07	-0.06	0.56	-0.13	0.25	0.24	0.05	0.45	-0.16	0.07	0.22	-0.07	0.52	1.00						
Sr	0.86	-0.34	0.97	0.66	0.31	0.48	0.47	0.47	0.80	0.25	0.49	0.38	-0.14	0.80	-0.11	-0.06	1.00					
V	-0.18	-0.03	-0.06	0.11	-0.32	-0.02	-0.08	-0.08	-0.15	-0.21	0.11	-0.14	-0.01	0.03	-0.33	-0.18	-0.08	1.00				
HPI	0.36	-0.17	0.39	0.33	0.28	0.32	0.52	0.53	0.09	0.43	0.28	0.96	-0.04	0.03	-0.03	0.04	0.35	0.13	1.00			
HEI	0.46	-0.08	0.39	0.30	0.47	0.28	0.58	0.59	0.16	0.51	0.23	0.95	0.07	0.04	0.20	0.20	0.35	0.04	0.97	1.00		
Cd	0.48	-0.08	0.39	0.28	0.51	0.28	0.59	0.59	0.18	0.54	0.22	0.96	0.07	0.04	0.25	0.22	0.36	-0.09	0.95	0.99	1.00	

The scatter plot clearly shows that the link between HEI and Cd is larger than the correlations between HPI and HEI and between Cd and HPI (both of which have R^2 values of 0.93). As a result, choosing between the HEI and Cd indices, or both, may be a preferable alternative for classifying samples (fig. 47). Additionally, the geographical distribution of the indices is shown in fig. 48 (a, b, and c).



a)

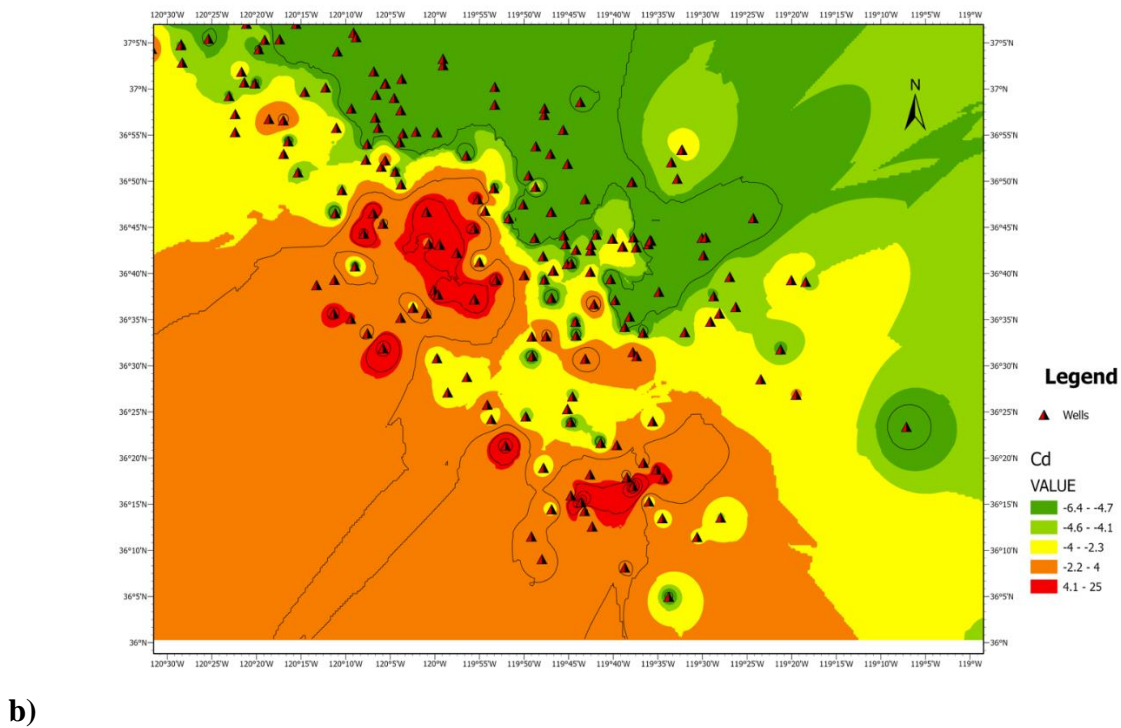
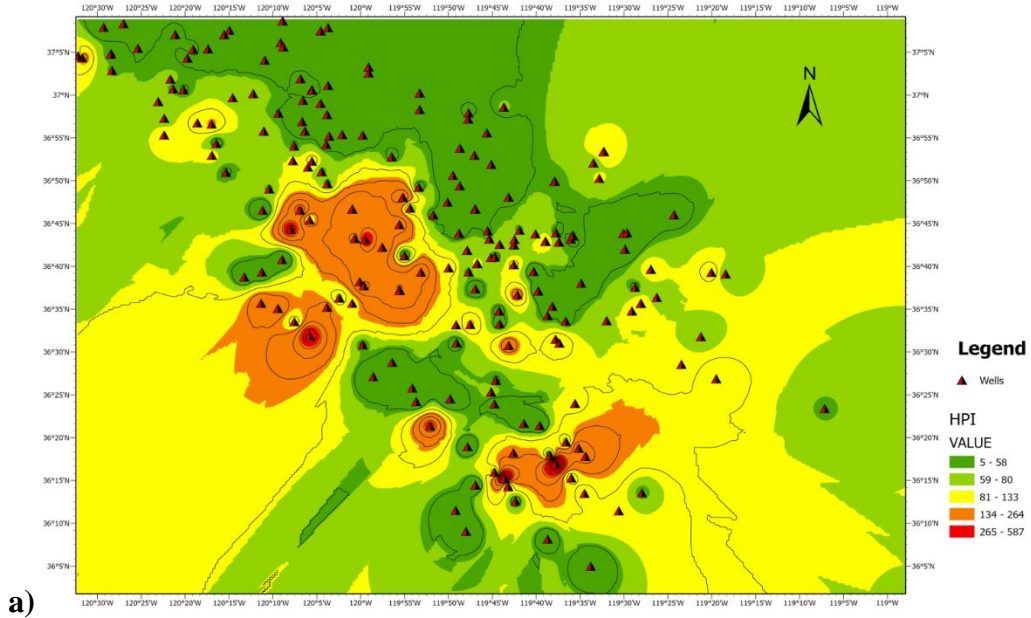
b)

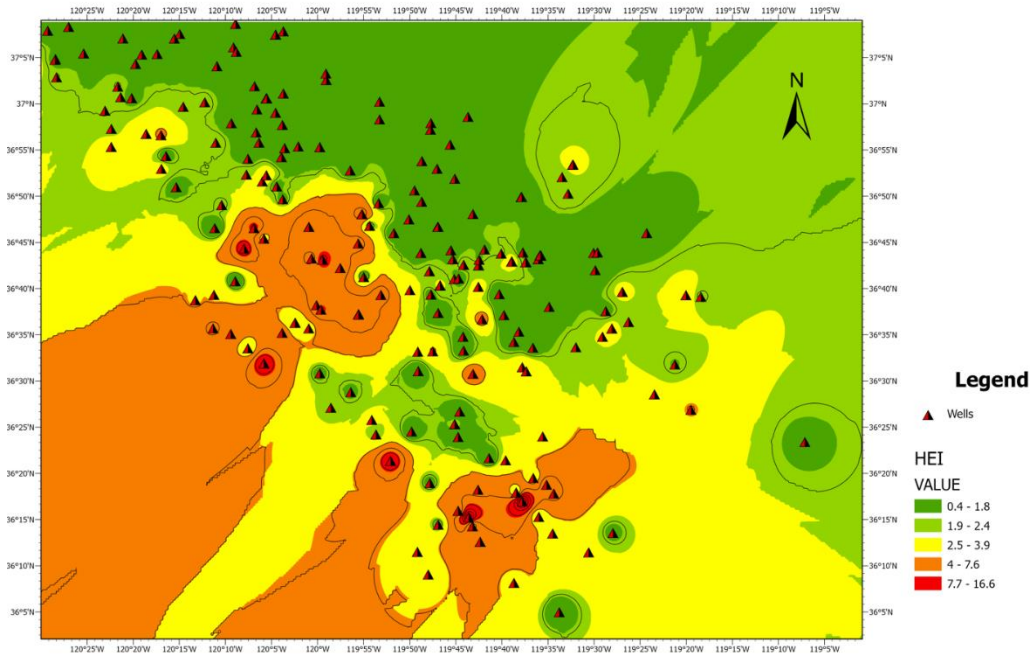
c)

Fig 47. Scatter plot shows the San Joaquin aquifer's a) HPI vs HEI, b) HPI versus Cd, and c) HEI versus Cd indices and their correlation of determination

The San Joaquin aquifer's central and western parts have the greatest contamination in

shallow groundwater, according to a comparison of HPI, HEI, and Cd assessment methodologies. Furthermore, study findings suggested that the main source of heavy metal pollution in the area may be wastewater from the region's densely populated metropolitan regions, agricultural land, and other enterprises.





c)

Fig. 48. Spatial distribution of heavy metals indices in San Joaquin aquifer a)HPI b) Cd c) HEI

4.3 Nitrate Evaluation in San Joaquin Aquifer

The San Joaquin and Tulare Basins are prone to groundwater nitrate pollution in the central valley because of excessive fertilizer use and other possible contaminations (Shrestha and Luo 2017). The SJV's coarse sediments can facilitate the fast penetration of nitrogen inputs into the groundwater system since the groundwater system is predominately oxic, and nitrate has a tendency to persist (Mcmahon and Chapelle, 2008, Jurgens et al., 2009).

In 292 groundwater samples taken between 2000 and 2019, the San Joaquin aquifer's nitrate content varied from 0.03 to 60.2 mg/L as nitrogen, with a mean value of 6.7 mg/L. (fig. 49). The Environmental Protection Agency's Maximum Contaminant Level (MCL) for nitrate is exceeded in almost 22% of samples (fig. 50), and 58.9% of the investigated wells have nitrate concentrations over 3 mg/L, demonstrating the impact of human causes on water quality. Additionally, from 200 to 2019, the mean value of nitrate for each year shows a gradually rising

trend. Using the concentrations of dissolved oxygen (DO), iron (Fe), and manganese (Mn), the oxic status of the valley was evaluated. Elevated Fe and Mn levels are found under anoxic conditions, and they are inversely related to DO. In several wells in the eastern parts of CV, high DO and low Fe and Mn values have been found, suggesting a higher nitrate presence in the groundwater. The eastern fans subregion had the highest groundwater nitrate concentrations, whilst the basin subregion had the lowest, according to Burow et al's (2013) findings, which were supported by their findings. This might be the result of nitrate moving from more oxic conditions in the alluvial fans to less oxic conditions in the centre of the basin. However, a study of the Central Eastside of the San Joaquin Valley did not deem denitrification to be significant (fig. 49).

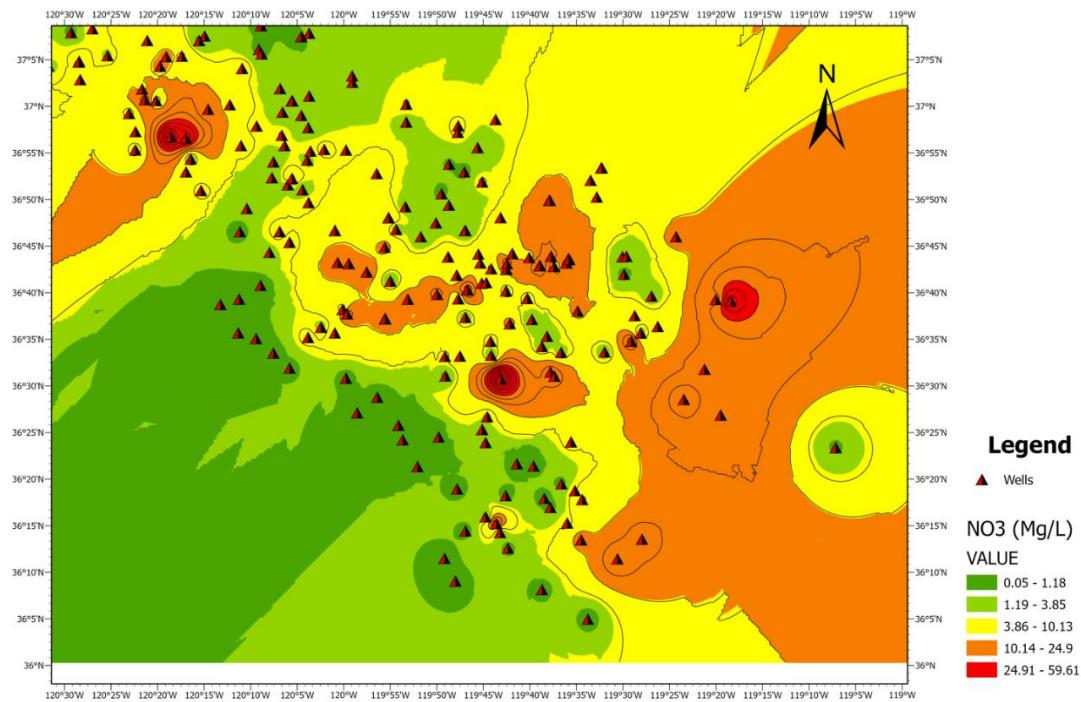


Fig. 49. Spatial distribution of nitrate(mg/L) in San Joaquin aquifer

4.3.1 The Correlation Between Nitrate and Major Ions

The link between nitrate and man-made cations/anions in the San Joaquin aquifer revealed that, similar to the Tulare aquifer, there is no discernible relationship between $\text{NO}_3\text{-Cl}$ and NO_3^- SO_4^{2-} (table 29). Chlorine may come from a number of places, including water supply systems, air

depositions, and road salts, as was previously described. While having no effect on the amounts of Cl^- , denitrification in the subsurface will reduce the quantity of reactive N. However, the San Joaquin aquifer's link between NO_3^- and cations (Ca^{2+} and Mg^{2+}) shows that they came from the same sources (table 29). Chemical fertilizers (NH_4NO_3 , $(\text{NH}_4)\text{SO}_4$, $\text{Ca}(\text{NO}_3)_2$, $(\text{Ca}, \text{Mg})\text{CO}_3$, and KCl) and manure may both be used to produce certain species, including Ca^{2+} , NO_3^- , and Mg^{2+} . In other words, as a result of processes that emerged following the application of N fertilizers, Ca^{2+} and Mg^{2+} are likely exchanged with NH_4^+ and added to the water, resulting from a cation exchange between Mg^{2+} and Ca^{2+} . By oxidizing ammonium N to NO_3^- , microorganisms in the unsaturated zone produce nitrification. Groundwater nitrate levels are frequently higher when there is greater mineralization. Additionally, increased acidity during nitrification causes carbonate to dissolve, enriching Ca^{2+} (Stumm, 1996).

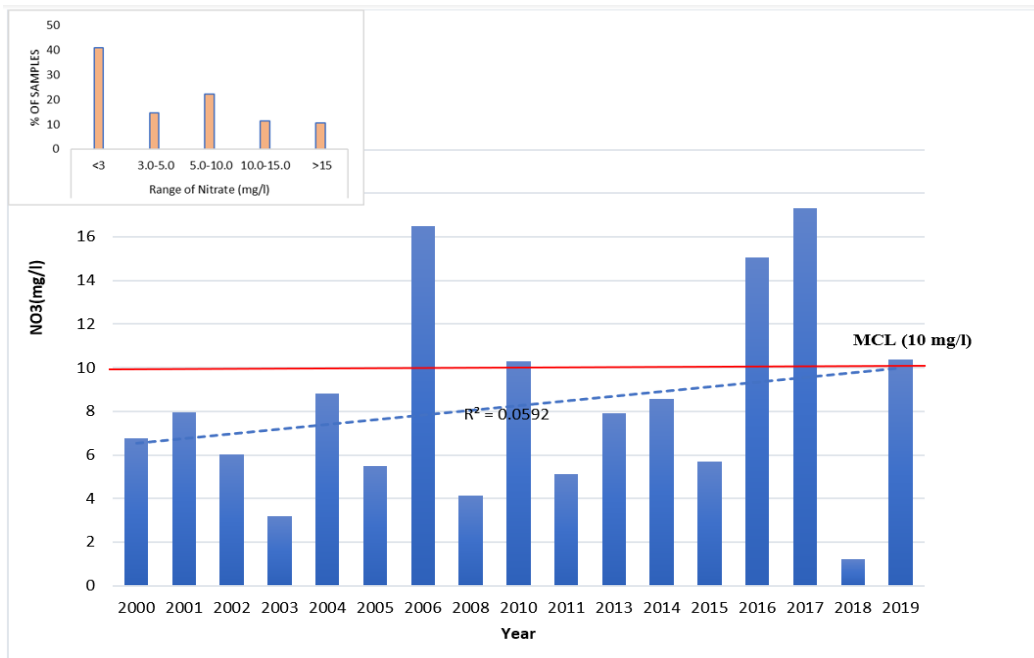


Fig. 50. Nitrate concentration of San Joaquin aquifer in the range date of 2000-2019 (the average value of all sampled well in each year)

4.3.2 Evaluation of Nitrate Sources Using Stable Isotopes

From 2003 to 2019, the San Joaquin aquifer's $\delta^{15}\text{N-NO}_3$ fluctuated from +0.73 to +14.66‰ and its $\delta^{18}\text{O-NO}_3$ ranged from -4 to 14.76‰, respectively (Fig. 51). (table 32). The usual ranges of $\delta^{15}\text{N-NO}_3^-$ and $\delta^{18}\text{O-NO}_3$ values for the main sources of NO_3^- that may have an impact on the San Joaquin aquifer are shown in Figure 25 based on Kendall (1998). The soil nitrogen, chemical fertilizers, and sewage/manure are the major sources of nitrate in the aquifer. Cl^- is a conservative ion, therefore it may be used to show biological activity or the mixing of NO_3^- sources (Yue et al. 2017). Low Cl^- concentrations, high $\text{NO}_3^-/\text{Cl}^-$ ratios, and low values of $\delta^{15}\text{N-NO}_3^-$ point to chemical fertilizer being the primary source of NO_3^- in the San Joaquin aquifer (fig. 52). In addition, the $\delta^{18}\text{O-NO}_3^-$ values by nitrification have a range of - 5‰ to + 15‰ indicating NO_3^- in the San Joaquin aquifer is mainly produced by nitrification (Kendall,1998).

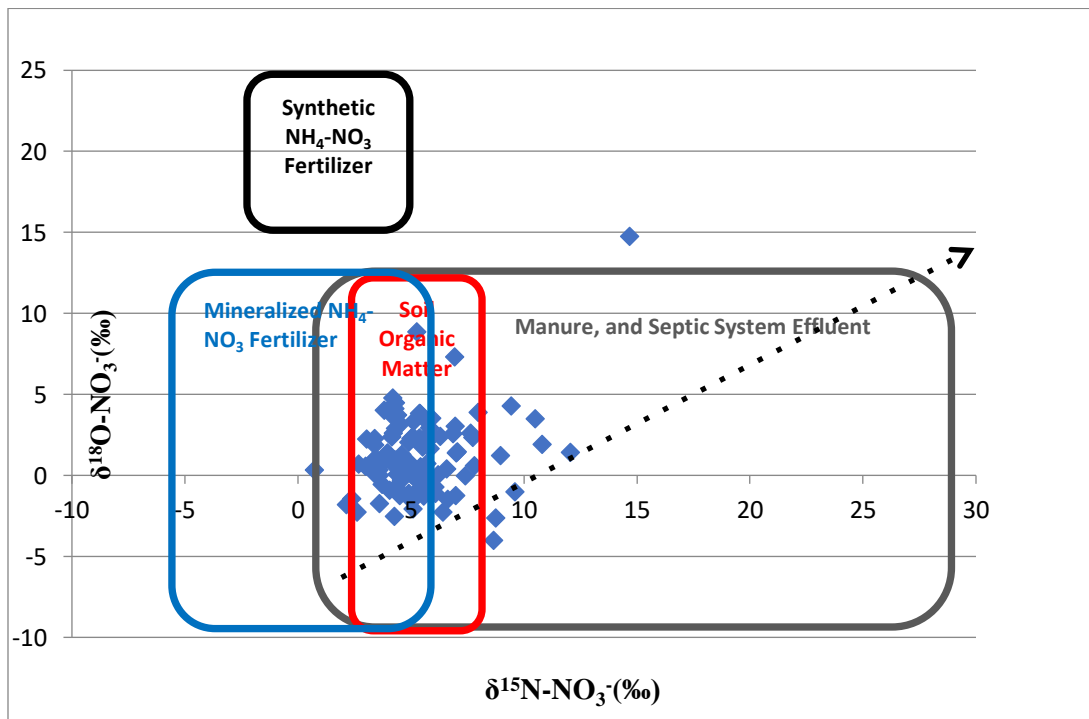


Fig. 51. Expected $\delta^{15}\text{N-NO}_3$ versus $\delta^{18}\text{O-NO}_3$ ranges for natural and anthropogenic nitrate sources

The enrichment ratios of $\delta^{15}\text{N}$ and $\delta^{18}\text{O}$ are positively associated by a factor ranging from

1.3:1 to 2.1:1, and the nitrification raises the values of $\delta^{15}\text{N}$ and $\delta^{18}\text{O}$ nitrate. Denitrification does not appear to be a major factor in the concentration of nitrate in the San Joaquin aquifer, nevertheless. If denitrification were to blame for the rising $\delta^{15}\text{N}\text{-NO}_3$ and $\delta^{18}\text{O}\text{-NO}_3$ values, the nitrate concentration in the wells with heavier values would be lower (Fig. 51). Furthermore, denitrification is impacted by the amount of dissolved oxygen (DO) (Yue et al. 2018). The San Joaquin aquifer may not have undergone considerable denitrification as 60% of investigated wells had DO concentrations more than 5 mg/L, which is not an optimal environment for denitrification.

Denitrification and simple mixing may also be distinguished using graphs of the $\delta^{15}\text{N}\text{-NO}_3^-$ composition against the natural log and inverse ($1/\text{NO}_3$) concentrations. Denitrification might be disregarded in this aquifer since the plot of " $\delta^{15}\text{N}\text{-NO}_3^-$ vs. natural log of nitrate" (Fig. 53) does not indicate the rise in NO_3 concentration as a consequence of " $\delta^{15}\text{N}\text{-NO}_3^-$ enrichment" to infer fractionation by denitrification (Yin et al., 2020). Also, the negative correlation between inverse nitrate concentration and the $\delta^{15}\text{N}\text{-NO}_3^-$ confirms the lack of denitrification role in nitrate contamination of San Joaquin aquifer, and this is consistent with mixing in the aquifer.

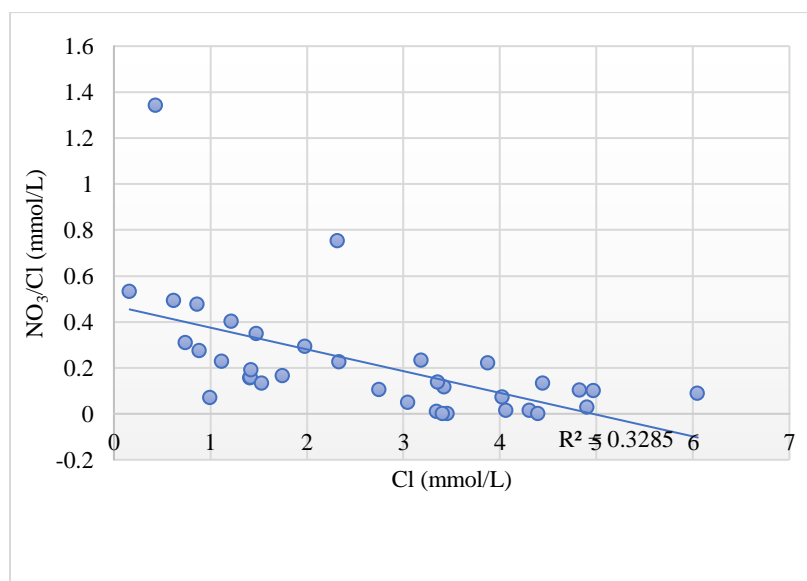
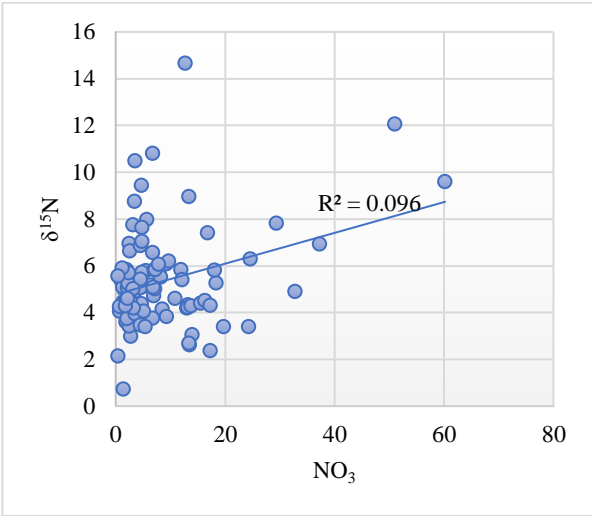
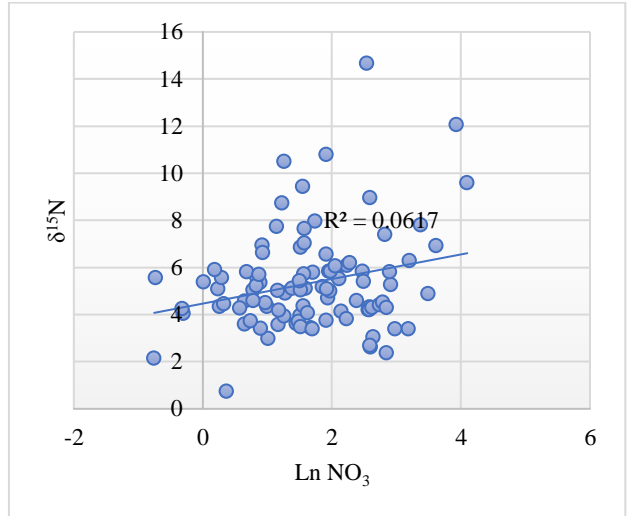


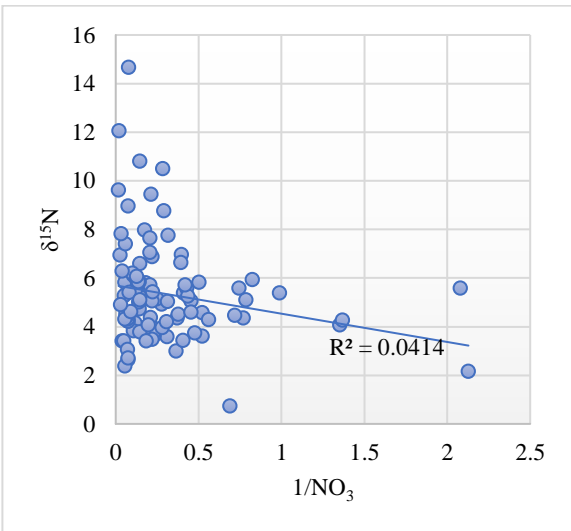
Fig. 52. The relation between Cl^- and $\text{NO}_3^-/\text{Cl}^-$ in San Joaquin aquifer



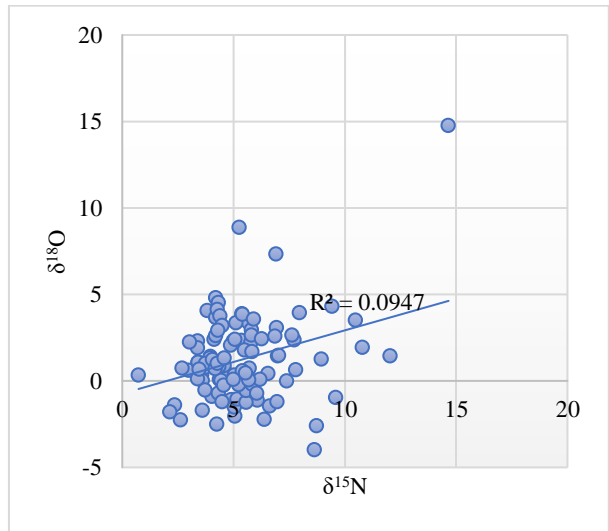
a)



b)



c)



d)

Fig. 53. a) Nitrate versus $\delta^{15}\text{N} - \text{NO}_3$, b) natural log of nitrate concentration versus $\delta^{15}\text{N} - \text{NO}_3$, c) inverse nitrate concentration ($1/\text{NO}_3$) versus $\delta^{15}\text{N} - \text{NO}_3$ and d) $\delta^{15}\text{N} - \text{NO}_3$ vs $\delta^{18}\text{O} - \text{NO}_3$

Table 32) The stable isotopes values of San Joaquin Aquifer

Well-no	$\delta^{15}\text{N}$ (air) ‰	$\delta^{18}\text{O}$ (V-SMOW) ‰	$\delta^2\text{H}$	$\delta^{18}\text{O}(\text{H}_2\text{O})$	NO_3 (mg/L)	$\text{Ln}(\text{NO}_3)$	$1/\text{NO}_3$
USGS 363000119430001	9.6	-0.99	-9140	-11.91	60.2	4.10	0.02
USGS 362600119440001	8.74	-2.62	-100	-13.55	3.42	1.23	0.29
USGS 363900119180001	6.92	7.32	-72.1	-9.26	37.3	3.62	0.03
USGS 363700119280001	4.14	2.39	-86.9	-11.52	8.54	2.14	0.12
USGS 364300120000001	2.62	-2.27	-89.2	-12.02	13.5	2.60	0.07
USGS 364200119570001	8.95	1.23	-80.5	-10.46	13.4	2.60	0.07
USGS 365200119330001	3.82	4.04	-52.5	-6.47	9.26	2.23	0.11
USGS 364200119420003	4.2	4.79	-64.6	-8.26	13	2.56	0.08
USGS 364200119420003	4.32	4.5	-64.4	-8.23	13.2	2.58	0.08
USGS 364200119420003	4.21	3.64	-64.8	-8.38	13.2	2.58	0.08
USGS 364200119420003	4.29	4.12	-66.3	-8.43	13.8	2.62	0.07
USGS 363900119500001	2.37	-1.42	-91.6	-12.56	17.3	2.85	0.06
USGS 363500119280001	3.58	0.36	-61.7	-8.1	3.21	1.17	0.31
USGS 363900119260001	2.98	0.59	-75	-10.22	2.75	1.01	0.36
USGS 364359119293601	5.38	3.85	98.8	-13.39	1.01	0.01	0.99
USGS 363712119394801	4.05	-0.92	-99.5	-13.53	0.74	-0.30	1.35
USGS 364156119475201	3.96	1.4	-61.2	-7.71	4.54	1.51	0.22
USGS 364600119510001	5.08	-2.06	-89.4	-11.97	1.27	0.24	0.79
USGS 363600120020001	6.95	3.06	-72.2	-9.41	2.52	0.92	0.40
USGS 363100119490001	2.14	-1.81	-98	-13.35	0.47	-0.76	2.13
USGS 363325119440901	6.4	-2.25	-98.4	-13.24	0.89	-0.12	1.12
USGS 363100119370001	7.4	-0.01	-94.1	-12.66	16.8	2.82	0.06
USGS 363400119440001	4.9	-1.09	-96.5	-13.1	3.59	1.28	0.28
USGS 363900119200001	5.26	8.87	-89.3	-11.6	18.4	2.91	0.05
USGS 364600119240001	5.84	2.38	-57.7	-7.62	11.9	2.48	0.08
USGS 363300119310001	3.6	-1.72	-96.2	-13.08	1.91	0.65	0.52
USGS 364900119470001	6.63	-1.46	-90	-12.06	2.54	0.93	0.39
USGS 365100119450001	3.43	1.06	-77.1	-10.32	5.33	1.67	0.19
USGS 364600119540001	5.05	-1.55	-82.5	-11.11	2.19	0.78	0.46
USGS 364355119484601	4.71	0.42	-64.5	-8.56	6.95	1.94	0.14
USGS 364600119410001	8.65	-4	-77.4	-9.76	0.66	-0.42	1.52
USGS 363900119470001	3.61	0	-66.4	-8.58	4.28	1.45	0.23
USGS 365000119320001	5.68	3.38	-63.4	-7.99	7.92	2.07	0.13
USGS 364400120070001	7.74	2.34	-85.8	-11.37	3.15	1.15	0.32
USGS 364258119380204	5.81	2.94	-81.9	-10.97	18.1	2.90	0.06
USGS 364015119420001	3.42	1.04	-62	-8.1	2.45	0.90	0.41
USGS 364500120050001	10.49	3.5	-94.9	-12.83	3.53	1.26	0.28
USGS 364338119354603	5.37	2.31	-86.3	-11.71	2.44	0.89	0.41
USGS 364338119354603	5.12	3.35	-88.6	-11.5	4.01	1.39	0.25
USGS 364100119450001	5.88	-0.01	-79.2	-10.45	7.59	2.03	0.13
USGS 364316119360801	4.21	2.6	-86.6	-11.56	23	3.14	0.04
USGS 364306119364402	9.44	4.3	-81.5	-10.79	4.71	1.55	0.21
USGS 364255119372505	3.71	0.75	-66.7	-9.24	4.41	1.48	0.23
USGS 364259119385404	5.79	2.21	-61.2	-8.06	5.51	1.71	0.18
USGS 365322120401203	14.66	14.76	-61.9	-8.04	12.7	2.54	0.08
USGS 364700119500001	3.73	-0.56	-73.2	-9.95	2.09	0.74	0.48
USGS 363700119550002	6.09	-1.12	-74.8	-9.83	9.35	2.24	0.11
USGS 364239119440901	3.94	1.29	-59	-7.56	3.54	1.26	0.28
USGS 364315119451801	5.18	-1.07	-71.8	-9.43	6.41	1.86	0.16

Table 32 (Cont.)

USGS 363600119260001	5.51	1.77	-77.1	-10.27	8.24	2.11	0.12
USGS 363339119363501	6.97	-1.22	-96.7	-13.29	1.69	0.52	0.59
USGS 364200119420002	5.4	3.84	-63.3	-8.12	12.1	2.49	0.08
USGS 364200119420002	4.4	3.73	-64.8	-8.32	15.5	2.74	0.06
USGS 364200119420002	4.51	3.17	-65.8	-8.43	16.3	2.79	0.06
USGS 364200119420002	4.3	2.91	-66.3	-8.48	17.3	2.85	0.06
USGS 364300119420001	3.39	2.29	-79.6	-10.31	24.3	3.19	0.04
USGS 364400119450002	6.57	0.42	-68.6	-9.18	6.78	1.91	0.15
USGS 363800120000001	7	1.41	-66.7	-8.98	1.77	0.57	0.56
USGS 363700119590001	3.4	0.11	-59.7	-7.19	19.7	2.98	0.05
USGS 364600119460002	5.57	-1.26	-95.7	-12.7	1.34	0.29	0.75
USGS 364100119440001	7.97	3.91	-98.3	-13.41	5.7	1.74	0.18
USGS 364300119400001	5.1	0.26	-75.8	-10.07	4.93	1.60	0.20
USGS 365200119560001	3.76	0.99	-63.2	-8.09	6.78	1.91	0.15
USGS 365500119590001	7.64	2.63	-67.8	-9.2	4.83	1.57	0.21
USGS 364900120030001	5.05	0.31	-86.8	-11.6	4.55	1.52	0.22
USGS 370400120100001	5	2.29	-57.5	-7.63	7.16	1.97	0.14
USGS 365700120220001	4.37	0.08	-66.2	-8.81	4.75	1.56	0.21
USGS 365700120090001	3.47	0.64	-85.2	-11.65	4.56	1.52	0.22
USGS 365900120140001	4.6	0.86	-69.5	-9.23	10.9	2.39	0.09
USGS 365400120070001	4.33	-0.72	-75.8	-10.39	1.3	0.26	0.77
USGS 365500120110001	10.8	1.91	-70.7	-9.66	6.81	1.92	0.15
USGS 370100120060001	4.35	0.81	-61.9	-8.63	2.7	0.99	0.37
USGS 365600120180001	12.05	1.43	-59.8	-7.78	51	3.93	0.02
USGS 365900120040001	5.58	-0.59	-70.2	-9.78	2.32	0.84	0.43
USGS 370000119530001	4.06	1.2	-57.1	-7.51	5.09	1.63	0.20
USGS 365100120060001	4.5	-1.24	-79.2	-10.87	2.64	0.97	0.38
USGS 370200119590001	4.46	0.02	-72.3	-9.85	1.39	0.33	0.72
USGS 365800119530001	4.18	0.69	-57.6	-7.38	3.26	1.18	0.31
USGS 365400120160001	4.26	-2.53	-70.7	-9.79	0.73	-0.31	1.37
USGS 365700119470002	3.4	1.88	-57.8	-7.69	5.45	1.70	0.18
USGS 370102120535903	5.82	2.62	-43.3	-5.15	1.98	0.68	0.51
USGS 365800120510001	4.89	2.04	-66.9	-8.62	32.8	3.49	0.03
USGS 370800120270001	5.71	0.73	-66.3	-9.02	4.79	1.57	0.21
USGS 371000121010001	5.84	1.66	-66.4	-8.98	7.06	1.95	0.14
USGS 374109121000101	5.84	-0.21	-66.7	-9.25	7.23	1.98	0.14
USGS 374109121000101	6.19	0.06	-69.6	-9.62	9.73	2.28	0.10
USGS 374109121000101	5.42	0.55	-63.2	-8.77	4.5	1.50	0.22
USGS 374109121000101	5.23	-0.24	-68.6	-9.23	2.3	0.83	0.43
USGS 374109121000101	4.56	-0.27	-67.2	-9.28	1.91	0.65	0.52
USGS 374109121000101	5.01	0.07	-64.7	-8.87	3.2	1.16	0.31
USGS 374221120585903	4.28	0.98	-64.8	-8.98	1.78	0.58	0.56
USGS 371726121051501	3.04	2.24	-53.1	-6.67	14	2.64	0.07
USGS 374110121000304	5.7	0.05	-68.2	-9.39	2.39	0.87	0.42
USGS 374157120594303	0.73	0.33	-65.1	-8.87	1.45	0.37	0.69
USGS 372800121070001	6.86	2.58	-58.9	-7.88	4.56	1.52	0.22
USGS 372553121102503	2.69	0.72	-65.3	-8.75	13.4	2.60	0.07
USGS 371800121010001	7.04	1.47	-66.4	-8.75	4.84	1.58	0.21
USGS 374620120592901	6.06	-0.72	-77.6	-10.3	7.81	2.06	0.13
USGS 374635121040901	7.81	0.62	-71.6	-9.49	29.4	3.38	0.03
USGS 374909121110101	6.28	2.41	-74.2	-10.18	24.6	3.20	0.04
USGS 375422121095301	5.08	2.39	-50.8	-6.67	6.85	1.92	0.15
USGS 380136121025301	5.91	3.55	-56.2	-7.69	1.21	0.19	0.83
USGS 380524121115401	4.59	1.29	-58.7	-8.15	2.19	0.78	0.46
USGS 380843121205201	5.56	0.45	-79.3	-10.95	0.481	-0.73	2.08

Chapter 5: Discussion and Results

This study aims at the hydrogeochemical assessment of Mojave, Tulare, and San Joaquin aquifers located in south California, USA for agricultural and drinking water uses. For these three aquifers, USGS has published water quality data from 2000 to 2019. The study focuses on four main aspects: the first is chemical features of groundwater in relation to hydrogeochemical facies, genetic geochemical development of groundwater, and hydrogeochemical signatures to determine their suitability for different applications. These data include anions, cations, heavy metals, nitrate, and stable isotopes concentration. The second aspect is to investigate the sources and mechanisms impacting NO_3^- in three aquifers. This research employs a multiple-isotopic technique ($\delta^{15}\text{N}$, $\delta^{18}\text{O}$) in conjunction with chemical and hydrogeological data to figure out what's causing the rise in NO_3^- pollution in the aquifer, where it's coming from, and how it's related to land use so that future management choices can maintain groundwater quality. The third part is heavy metals assessment and evaluation of heavy metal mobility in groundwaters induced by salinity and nitrate. ArcGIS will also be utilized to create the map of Water Quality Index. Based on information on water quality, these maps seek to rapidly identify the areas of the study area where water is most and least suitable for drinking and agricultural use. This method has yet to be employed to evaluate the aquifer's groundwater quality, which is being threatened by rising population, industrial activity, and agricultural fields. Senior scholars, decision makers, and general public may quickly differentiate areas of high and bad water quality by mapping the index. Furthermore, an essential contribution is made to the knowledge of links between land use and groundwater quality.

The Mojave Aquifer's water is mostly alkaline, with Na-HCO_3^{2-} predominating. Most samples (90%) fall into the category of medium to high water salinity based on the EC values. Additionally, the Na% findings showed that 20% of the samples are somewhat inappropriate, 64%

are legal, and 16% of the samples fall into the category of good. The Wilcox diagram represented that 35.3% of samples fall in saline water category, 51% are slightly saline, and 9.8% of the samples are very saline. Furthermore, the Wilcox diagram indicated that while sodium threat is quite low, groundwater is enriched in salinity impacting soil structure and the loss of soil productivity. Based on the spatial distribution maps, wells with high Na% and sodium adsorption ratio (SAR) values are mostly located on north part of the aquifer. These contaminated wells are drilled in alluvium Pleistocene nonmarine sediment. Also, wells located on the cities of Barstow, Helendal, and Victorville have the most concentration showing the effect of anthropogenic sources on salinity beside the geological formation of Mojave aquifer. In Mojave aquifer, magnesium hazard (MH) values varied from 14.21 to 44.74. All examined samples had MH values below 50 and may be used for irrigation. Moreover, permeability index (PI) of all samples is more than 25% showing the lack of salinity impact on soil permeability.

With a mean value of 4.5 mg/L, the nitrogen content of nitrate in the Mojave aquifer varied from 1.3 to 21.8 mg/L. Nitrate levels in all water tests are below the Environmental Protection Agency's (10 mg/L) Maximum Contaminant Level (MCL). The average nitrate concentration in the aquifer is around 4.1 mg/L, and 30% of the examined wells have nitrate concentrations greater than 3 mg/L, demonstrating the impact of human causes on water quality. Furthermore, a positive correlation between EC and nitrate showed that the ionic strength of the Mojave aquifer's groundwater increases along with an increase in NO_3 . This illustrates that NO_3 , and certain significant ions come from the same source and that these ions have an impact on the groundwater's overall ionic strength.

From 2005 to 2019, the Mojave aquifer's $\delta^{15}\text{N-NO}_3$ levels varied from +1.0 to +11.5‰ and its $\delta^{18}\text{O-NO}_3$ levels from -1.7 to 7.7‰. As a result, the majority of samples in the analyzed wells

fell within the overlapping ranges of soil organic matter (from +3 to +8‰), manure (from +5 to +25‰), and chemical fertilizers (from -6 to +6‰). The overall trend of the data might also be provided by combining several sources. Therefore, the ratios of $\delta^{15}\text{N-NO}_3$ and $\delta^{18}\text{O-NO}_3$ were mostly distributed among the chemical fertilizer, soil-organic matter, and manure-septic wastewater, although the concentrations of $\delta^{15}\text{N-NO}_3$ and $\delta^{18}\text{O-NO}_3$ were moderately spread, suggesting that the nitrate contamination was generated by the three sources collectively. It is challenging to determine which of the sources is prominent due to the overlap. Manure is the most likely source of NO_3 in the polluted wells because active agricultural regions, metropolitan areas, and a small number of dairy farms are all present. The NO_3 pollution may result from manure being used as fertilizer to agricultural regions or from direct contamination of urban wastewater. Denitrification at levels that can be detected on dual-isotope plots in this aquifer may be discounted because the plot of " $\delta^{15}\text{N-NO}_3$ vs NO_3 and natural log of nitrate" did not show the decrease in NO_3 concentration as the result of the " $\delta^{15}\text{N-NO}_3^-$ enrichment" to suggest fractionation via denitrification. Additionally, the inverse relationship between nitrate content and $\delta^{15}\text{N-NO}_3^-$ showed a negative association, suggesting mixing may contribute to nitrate pollution of the Mojave aquifer.

The order of mean concentration of metals in Mojave aquifer is $\text{Sr} > \text{B} > \text{Fe} > \text{Mn} > \text{As} > \text{Cr}$ respectively. With a mean of 10.14, the Sr concentration varies from 0.0047 to 12.9 $\mu\text{g/l}$. Seven wells ($n=87$) exhibit Sr pollution and their results are more than 4 mg/L when compared to EPA/WHO regulations. With a mean of 0.3 mg/L, the boron content varies from 0.008 to 5.7 mg/L. According to the EPA, 0.5 mg/L of boron is the maximum permitted level, hence 47% of the 108 wells that were analyzed contain boron pollution. Increases in hazardous components like boron are typically seen in groundwater with high salt levels. The Fe content is larger than the preferred

limit (0.3 mg/L) of the EPA/WHO among the examined wells (n=70), showing the influence of weathered granitic and metamorphic rock as a potential source. These three wells had Fe concentrations of 0.4, 0.42, and 0.77 mg/L. The range of arsenic in water is 0.001 to 0.172 mg/L (average: 0.00629 mg/L). The majority of these wells are situated in the Mojave River drainage basin, which has a primarily coarse granitic river channel, and the area surrounding the floodplain, which contains alluvium formed from older stream deposits, locally derived alluvial fans, playa lake deposits, and fractured bedrock. With mean concentrations of 113.8 for 6 heavy metals (As, Sr, Fe, Mn, B, Cr) in 110 groundwater sample years between 2000 and 2019, the Mojave basin aquifer's HPI varies from 95.64 to 131.82. It is implied that all groundwater samples, with the exception of one well, are over the threshold value of 100 and are thus unsuitable for human consumption. HEI, which has also been evaluated for a better understanding of the pollutant loads, has a range of 0.22 to 14.2 with a mean value of 2.09. Nine of the 70 studied wells have HEI values greater than 1, making them unsuitable for residential usage. To determine the degree of metal pollution, the contamination index (Cd) is also used. The mean and range of Cd readings are -5.9-8.2 and -3.92, respectively, and 4 wells (n=70) are classified as having substantial pollution. Surface runoff-derived heavy metal buildup in polluted wells mostly impacts samples that are positioned in the direction of the flow.

Alkaline earth metals (Ca^{2+} , Mg^{2+}) predominate over alkalies (Na^+ , K^+) in the Tulare aquifer where the majority of groundwater samples are taken, while weak acids (CO_3^{2-} , HCO_3^-) outweigh strong acids (Cl^- , SO_4^{2-}). Additionally, the Na% data showed that 15.39% of the samples were inappropriate, 20.33% were questionable, and 18.4% fell into the category of allowed samples. The majority of the water samples, according to the Wilcox diagram, fall into the somewhat salinity to salinity range. Seven water samples, however, fall into the category of being

extremely salty and are not suited.

The Tulare aquifer's nitrate content varied from 0.038 to 48.6 mg/L, with a mean value of 8.98 mg/L. In the Tulare aquifer, 33.5% (n=161) of water samples had nitrate concentrations that exceeded the Maximum Contaminant Level (MCL) established by the Environmental Protection Agency. In addition, 70% of the examined wells contain nitrate levels more than 3 mg/L. Although there hasn't been a baseline assessment to determine the amount of naturally occurring NO₃⁻ concentrations in groundwater in this area, NO₃-N levels above 3 mg/L are generally considered to be the result of anthropogenic sources. The range of NO₃-N readings from 0.038 to 48.6 mg/L makes it impossible to assume that the NO₃⁻ comes from organic nitrogen in the soil. In this study area, the water samples are taken from 161 wells years between 2001 to 2020. The mean value of nitrate for each year indicates a relatively increasing trend from 2001 to 2020.

The mean NO₃⁻ concentrations in the HLS portion of the Tulare aquifer are 6.4 mg/L (n=18), and the mean δ¹⁵N-NO₃⁻ values varied from +1.6 to +14.5‰. The highest nitrate content (11.74 mg/L) was found in the central-north portion (KAW) of the Tulare aquifer (n=31). The range of this component's δ¹⁵N-NO₃⁻ and δ¹⁸O-NO₃ values was +2.43 to +43.02‰ with a mean of 7.7‰ and -3.2 to 20.52‰ with a mean of 1.53‰, respectively. Similar to the central-north region, the south part (TLE) also has a high nitrate content, with a mean value of 9.04 mg/L (n=27). The ranges for δ¹⁵N-NO₃⁻ and δ¹⁸O-NO₃ were respectively +2.1 to +19.7‰ and -1.9 to +6.9‰. West portion (TLA) nitrate concentration is 3.95 mg/L (n=6). There is a very wide range of isotope values in this region; for example, the west part's δ¹⁵N-NO₃⁻ and δ¹⁸O-NO₃ values varied from -10.4 to +57.5‰ with a mean of +15.1 and -6.4 to +18.0‰ with a mean of +3.3‰, respectively.

Since the concentrations of δ¹⁵N-NO₃⁻ and δ¹⁸O-NO₃⁻ are primarily found in soil organic matter, manure, and sewage, as well as chemical fertilizers, it is likely that these three sources

contributed to the nitrate contamination or that it originated from a single variable source inside the common composition area. As a result, there is no common groundwater circulation pattern throughout the research area's many groundwater sites, making it difficult to explain this pattern only in terms of microbial denitrification or mixing. To put it another way, the relationship between $\delta^{15}\text{N-NO}_3$ and the natural log of nitrate shows a decrease in NO_3 concentration as a result of $\delta^{15}\text{N-NO}_3$ enrichment, suggesting the effect of denitrification on nitrate concentration in the Tulare aquifer, while the negative relationship between $\delta^{15}\text{N-NO}_3$ and the inverse of nitrate concentration is consistent with mixing.

In 182 examined wells from 2000 to 2020, the pH value of groundwater samples from the Tulare Aquifer ranged from 6.1 to 9.6, with a mean of 7.7. This implies mild acid to alkaline conditions. The mean concentration of As, Ba, B, Mo, Sr, V, and U in the Tulare aquifer were found 0.01, 0.09, 0.16, 0.01, 0.41, 0.02, and 0.22 mg/L respectively years from 2000 to 2020. Moreover, the mean concentrations were observed in decreasing order of $\text{Sr} > \text{U} > \text{B} > \text{Ba} > \text{Mo} > \text{As}$ whereas the concentration of As, Mo, and U in 13.8, 4.4, and 12.7% of the studied wells (n=182) respectively are more the standard level reported by EPA and WHO. These polluted wells are mostly located on the central part of Tulare aquifer. The HPI values for the Tulare aquifer deviate from 4.33 to 1,300.7 with mean concentrations 63.97 for 7 heavy metals (As, Ba, B, Mo, Sr, V, and U) in 182 groundwater samples years between 2001-2020. It is inferred that, 24 wells have HPI more than 100 with mean value of 217.4, hence unfit for human consumption. The HEI has also been evaluated, and it has a mean value of 2.3 with a range of 0.04 to 36.0. As a result, of 182 study wells, 137 (75%) have HEI levels more than 1, and are consequently deemed inappropriate for residential usage. With the exception of three wells (HLS15, KAW05, and TLA09), all wells are classified as low contaminated with Cd levels of less than one. The Cd range

and mean readings are -6.9-29.0 and -4.6, respectively.

Alkaline earths (Ca^{2+} and Mg^{2+}) predominate over alkalis (Na^+ and K^+) in the San Joaquin aquifer's groundwater, and the Ca- HCO_3 facies demonstrates that weak acids (HCO_3^-) predominate over strong acids (SO_4^{2-} and Cl^-). As a consequence, HCO_3 -Ca_Mg was the most prevalent compound, followed by HCO_3 -Na, which is connected to the aquifer's carbonate-rich rocks. The majority of samples (88%) plot in the low salinity zones of the U.S. "Salinity Laboratory (USSL)" figure, which suggests that these water samples are risk-free. With the exception of one sample, 12% of samples come within the classification C3S1, which denotes water with high salinity (C3) and low sodium (S1) hazards and may be used to irrigate nearly all soil types with little risk of exchangeable sodium. Because it's important to keep the equilibrium between these two ions, the excess of carbonate (CO_3^{2-}) and bicarbonate (HCO_3^-) over the alkali earth metals (Ca^{2+} and Mg^{2+}) might have an effect on the soil. Additionally, the main ion in the groundwater was bicarbonate, in accordance with the kind of water in the San Joaquin aquifer. Therefore, 87.2% of the samples are inappropriate for irrigation usage, 8.5% are dubious, and only 1.7% are excellent. In this area, RSC has an average value of 6.6 meq/L.

With a pH range of 6.11 to 9.4 and a mean value of 7.4, the water in the San Joaquin aquifer is neutral to alkaline in nature in the 259 examined wells from 2000 to 2019. Sr, Ba, B, U, V, As, and Mo are the order of mean metals, accordingly. However, the water samples are contaminated with V, U, and B when compared to EPA/WHO limits. The mean boron content is 1.16 mg/L, with a range of 0.007 to 1.74 mg/L. Based (B) on EPA, the standard permissible for boron is 0.5 mg/L, accordingly about 6.17% of the studied wells (n=259) have boron contamination with mean of 9.9 mg/L.

In 259 groundwater sample years between 2000 and 2019, the San Joaquin aquifer's HPI

varied from 3.88 to 705.9 with mean values of 80 for 7 heavy metals (Sr, Ba, B, U, V, As, and Mo). It is assumed that 19.7% of the groundwater samples are unsafe for human consumption since they are over the threshold value of 100. HEI, which has also been evaluated for a better understanding of the pollutant loads, has a range of 0.3 to 20.32 and a mean value of 2.59. As a result, according to 85% of studies, wells had HEI values more than 1, making them unsuitable for residential usage.

To determine the degree of metal pollution, the contamination index (Cd) is also used. Cd has a range of -6.5 to 33.3 with a mean value of -2.6. About 12% of the samples have Cd more than 3, and 1.15% (3 samples) range between 1-3. The high correlation between uranium and these indices indicates that among studied heavy metals, U have the most effect on groundwater contamination in San Joaquin aquifer. Furthermore, the relatively high correlation of Sr, Ca, Mg, and Cl with EC shows that they are more solubility in alkaline groundwater.

In 292 groundwater samples, the San Joaquin aquifer's nitrate content varied from 0.03 to 60.2 mg/L as nitrogen, with a mean value of 6.7 mg/L. The Environmental Protection Agency's Maximum Contaminant Level (MCL) for nitrate is exceeded in almost 22% of samples, and 58.9% of the examined wells have nitrate concentrations more than 3 mg/L, demonstrating the impact of human causes on water quality. According to the association between nitrate and the major cations and anions, $\text{NO}_3\text{-Cl}$ and $\text{NO}_3\text{-SO}_4^{2-}$ do not significantly correlate, unlike the Tulare aquifer. On the other hand, the link between nitrate and cations (Ca^{2+} and Mg^{2+}) suggests that they may have the same source of production (s).

The concentration of nitrate in the San Joaquin aquifer ranged from 0.03 to 60.2 mg/L as nitrogen, and mean value of 6.7 mg/L in 292 groundwater samples. About 22% of samples have nitrate concentration more than Maximum Contaminant Level (MCL) set by the Environmental

Protection Agency, and 58.9% of the studied wells have nitrate more than 3 mg/L showing the influence of anthropogenic factors on water quality. The correlation between nitrate and main cations/anions indicated that like Tulare aquifer there is no significant correlation between $\text{NO}_3\text{-Cl}$ and $\text{NO}_3\text{-SO}_4^{2-}$. However, the correlation between nitrate and cations (Ca^{2+} and Mg^{2+}) indicate that they might be generated from the same source(s).

Additionally, between 2003 and 2019, the $\delta^{15}\text{N-NO}_3$ fluctuated from +0.73 to +14.7‰, whereas the $\delta^{18}\text{O-NO}_3$ ranged from -4 to 14.7‰. Organic soil components, chemical fertilizers, and sewage/manure are the primary sources of nitrate in the aquifer. Cl and the molar ratio of NO_3/Cl can be used to reflect biological activities or the mixing of NO_3 sources since Cl^- is a conservative ion. Low Cl concentrations and high NO_3/Cl ratios with low levels of $\delta^{15}\text{N-NO}_3$ suggest that chemical fertilizers are the San Joaquin aquifer's main source of NO_3 . Additionally, the $\delta^{18}\text{O-NO}_3$ values via nitrification vary from -5 to +15‰, showing that nitrification is the primary method of producing NO_3 in the San Joaquin aquifer.

The San Joaquin aquifer's examined wells have an average DO content of more than 5 mg/L, which is not the best environment for denitrification. This suggests that little denitrification took place in the San Joaquin aquifer. Denitrification and simple mixing may also be distinguished using graphs of the $\delta^{15}\text{N-NO}_3$ composition against the natural log and inverse ($1/\text{NO}_3$) concentrations. However, the negative correlation between inverse nitrate concentration and the $\delta^{15}\text{N-NO}_3$ confirmed that mixing may be taking place in the San Joaquin aquifer. The plot of 15N-NO_3 vs. natural log of nitrate did not show the decrease in NO_3 concentration as a result of the $\delta^{15}\text{N-NO}_3$ enrichment to suggest fractionation via denitrification.

References

- Adeloju S.B, Khan S, Patti A.F. Arsenic Contamination of Groundwater and Its Implications for Drinking Water Quality and Human Health in Under-Developed Countries and Remote Communities—A Review. *Appl. Sci.* 2021, 11, 1926.
- Al-Ami M.Y, Al-Nakib S.M, Ritha N.M, Nouri A.M, Al-Assina, A. "Water quality index applied to the classification and zoning of Al-Jaysh canal, Bagdad, Iraq" (1987). - *Journal Environmental Science and Health* 22: 305-319.
- Ali, W., Rasool, A Junaid, M., Zhang, H. A comprehensive review on current status, mechanism, and possible sources of arsenic contamination in groundwater: a global perspective with prominence of Pakistan scenario (review). *Environmental Geochemistry and Health*. Volume 41, Issue 2, 1 April 2019, Pages 737-760.
- Anning DW, Paul AP, McKinney TS, Huntington JM, Bexfield LM, Thiros SA. Predicted nitrate and arsenic concentrations in basin-fill aquifers of the southwestern United States. U.S. Geological Survey; 2012. p. 78.
- Appelo C.A.J, Dieke Postma, Appelo C.A.J, Dieke Postma "Geochemistry, groundwater and pollution, 2th edition", 2005, p 17
- Arslan H." Spatial and temporal mapping of groundwater salinity using ordinary kriging and indicator kriging": The case of Bafra Plain, Turkey" *Agricultural Water Management* 113 (2012) 57–63
- Ayotte, J.D., Nolan, B.T., Gronberg, J.M., 2016. Predicting arsenic in drinking water wells of the central valley, California. *Environ. Sci. Technol.* 50 (14), 7555–7563.
- Babiker, I.S., Mohamed A.A., Terao, H., and et al (2004) Assessment of groundwater contamination by nitrate leaching from intensive vegetable cultivation using geographical information system. *Environ Int* 29:1009–1017
- Backman B , Odis D, Lahermo P, Apant S, and Tarvainen T. "Application of a groundwater contamination index in Finland and Slovakia" 1998. *Environmental Geology*, 36(1-2), 55-64.
- Barnes, R.T., Raymond, P.A., 2010. Land-use controls on sources and processing of nitrate in small watersheds: insights from dual isotopic analysis. *Ecol. Appl.* 20 (7), 1961–1978.
- Bedard-Haughn, A.A., van Groenigen, J.W., van Kessel, C., 2003. Tracing 15N through the landscapes: potential uses and precautions. *J. Hydrol.* 272, 175–190
- Bexfield, L. M., & Jurgens, B. C. (2014). Effects of seasonal operation on the quality of water produced by public-supply wells. *Ground Water*, 52(S1), 10–24.

- Bohlke JK (2002) Groundwater recharge and agricultural contamination. *Hydrogeol J* 10:153–179
- Böttcher, J., Strebel, O., Voerkelius, S., Schmidt, H.L., 1990. Using isotope fractionation of nitrate-nitrogen and nitrate-oxygen for evaluation of microbial denitrification in a sandy aquifer. *J. Hydrol.* 114 (3–4), 413–424.
- Brady N "The nature and properties of soil. In: Prentice Hall (10th ed)" (2002). Delhi, New
- Brown E.J, Rodriquez M, Hoppin C, Spivy-Weber F, Doduc T, Moore S, Marcus F, Howard T” Recommendations addressing nitrate in groundwater”. state water resources control board report to the legislature. 20 February 2013, Updated to Meet ADA Accessibility Standards June 2020
- Burow, K.R., Shelton J.L., and Dubrovsky N.M.”Regional nitrate and pesticide trends in ground water in the eastern San Joaquin Valley, California” *Journal of Environmental Quality* 37, no. 5: 249–263.
- Burow, K.R., Shelton, J.L., Hevesi, J.A., Weismann, G.S., 2004. Hydrogeologic characterization of the Modesto Area, San Joaquin Valley, California. U.S. Geological Survey Scientific Investigation Report 2004-5232.
- Burow, K. R., B. C. Jurgens, K. Belitz, and N. M. Durborsky. 2012.“Assessment of Regional Change in Nitrate Concentrations in Groundwater in the Central Valley, California.” *Environmental Earth Science (Environmental Earth Science)* 69 (8): 2609–2621.
- California Department of Water Resources [DWR]. (2020). California's most significant droughts: Comparing historical and recent condition. Retrieved from https://water.ca.gov/-/media/DWR-Website/Web-Pages/What-We-Do/Drought-Mitigation/Files/Publications-And-Reports/CalSigDroughts19_v9_ay11.pdf
- Chapelle, F.H., Bradley, P.M., Thomas, M.A., and McMahon, P.B., 2009, Distinguishing iron-reducing from sulfate-reducing conditions. *Groundwater*. doi: 10.1111/j.1745-6584.2008.00536.x. Epub 2009 Jan 22
- Chen, J., Gao, Y., Qian, H., Ren, W., Qu, W., 2021. Hydrogeochemical evidence for fluoride behavior in groundwater and the associated risk to human health for a large irrigation plain in the Yellow River Basin. *Sci. Total Environ.* 800, 149428. Craig, H., 1961. Isotopic variations in meteoric waters. *Science* 133, 1702–1703.
- Choi, W.J., Lee, S.M., Ro, H.M., 2003. Evaluation of contamination sources of groundwater NO₃– using nitrogen isotope data: a review. *Geosci. J.* 7 (1), 81–87.
- Clark, I., 2015. Contaminant Geochemistry and Isotopes. In *Groundwater Geochemistry and Isotopes*. Taylor & Francis Group, LLC, Boca Raton, FL.

- Claudia C. Faunt, Randall T. Hanson, Belitz "Introduction, Overview of Hydrogeology, and Textural Model of California's Central Valley" U.S. Department of the Interior, USGS (2009).
- Conant J.B, Cherry J.A, Gillham R.W, "A PCE groundwater plume discharging to a river: influence of the streambed and near-river zone on contaminant distributions"(2004). J. Contam. Hydrol. 73, 249–279.
- Danielescu, S., MacQuarrie, K.T., 2013. Nitrogen and oxygen isotopes in nitrate in the groundwater and surface water discharge from two rural catchments: implications for nitrogen loading to coastal waters. *Biogeochemistry* 115 (1–3), 111–127.
- Davraz A, zdemir A, "Groundwater quality assessment and its suitability in Çeltikçi plain (Burdur/Turkey)" *Environ Earth Sci* (2014) 72:1167–1190, DOI 10.1007/s12665-013-3036-1
- Dawson B.J, and Belitz K. "Status of groundwater quality in the California Desert Region", 2006–2008—California GAMA Program Priority Basin Project: U.S (2012). Geological Survey Scientific Investigations Report 2012-5040, 100 p
- Dede O.T." Application of the Heavy Metal Pollution Index for Surface Waters: A Case Study for Çamlıdere" Ö.T. Dede / Hacettepe J. Biol. & Chem., 2016, 44 (4), 499–504
- Delgado C, Pacheco J, Cabrera A, Batllori E, Orellana R, Bautista F." Quality of groundwater for irrigation in tropical karst environment: The case of Yucatán, Mexico" *Agricultural Water Management* 97 (2010) 1423–1433
- Dennehy, K.F, Reilly, T.E, Cunningham, W.L, Groundwater availability in the United States: the value of quantitative regional assessments. *Hydrogeol J* (2015) 23:1629–1632 DOI 10.1007/s10040-015-1307-5.
- Department of Water Resources. 2014. California water plan update 2013. Sacramento, CA: State of California Dept. of Water Resources.
- Dettinger, M.D., 2013. Atmospheric rivers as drought busters on the US West Coast. *J. Hydrometeorol.* 14 (6), 1721–1732.
- Doneen L. D, "Salinization of soils by salt in irrigation water," *Transactions, American Geophysical Union*, vol. 35, no. 6, pp. 943–950, 1964.
- DWR, 2019c. Groundwater. California Department of Water Resources (DWR), Sacramento, CA, USA. <https://water.ca.gov/Water-Basics/Groundwater>.
- Edet A.E and Offiong O.E" Evaluation of water quality pollution indices for heavy metal contamination monitoring. A study case from Akpabuyo-Odukpani area, Lower Cross River Basin (southeastern Nigeria)" *GeoJournal* 57: 295–304, 2002. © 2003 Kluwer Academic Publishers. Printed in the Netherlands.

- Fabro, A.Y.R., Avila, J.G.P., Esteller Alberich, M.V., Sansores, S.A.C., Camargo-Valero, M. A., 2015. Spatial distribution of nitrate health risk associated with groundwater use as drinking water in Merida, Mexico. *Appl. Geogr.* 65, 49–57.
- Famiglietti, J. S. 2014. “The global groundwater crisis.” *Nat. Clim. Change* 4 (11): 945–948.
- FAO (2011) The state of the world’s land and water resources for food and agriculture—managing systems at risk. Food and Agriculture Organization of the United Nations and Earthscan, Rome
- Faunt, C.C., Belitz, K., Hanson, R.T., 2010. Development of a three-dimensional model of sedimentary texture in valley-fill deposits of Central Valley, California, USA. *Hydrogeol. J.* 18, 625–649.
- Faunt, C. C., R. T. Hanson, and K. Belitz. 2009. Groundwater Availability of the Central Valley Aquifer, California. Professional Paper 1766, Reston, Virginia: U.S. Geological Survey.
- Faunt, C.C., ed., 2009. Groundwater availability in the Central Valley aquifer, California. U.S. Geological Survey Professional Paper 1776.
- Fram M.S, Belitz K. " Occurrence and concentrations of pharmaceutical compounds in groundwater used for public drinking-water supply in California" *Science of the Total Environment* 409 (2011) 3409–3417
- Freitas J.G, Rivett M.O, Roche R.S, Durrant M, Walker C, Tellam J.H, " Heterogeneous hyporheic zone dechlorination of a TCE groundwater plume discharging to an urban river reach"(2015). *Sci. Total Environ.* 505, 236–252.
- Ghafoor A, Murtaza G, Maann A, Qadir M, Ahmad B (2011) Treatments and economic aspects of growing rice and wheat crops during reclamation of tile drained saline-sodic soils using brackish waters. *Irrig Drain* 60(3):418–426
- Ghafoor A, Ahmad B, Maan A, Murtaza G (2004) Farmer participation in technology development and transfer for using agricultural drainage water for growing grain crops during reclamation of saline-sodic soils. Final technical report 3 (June 2001–May 2004).
- Giordano, M. (2009), Global groundwater? Issues and solutions, *Ann. Rev. Environ. Resour.*, 34, 153– 178.
- Granger, J., Wankel, S.D., 2016. Isotopic overprinting of nitrification on denitrification as a ubiquitous and unifying feature of environmental nitrogen cycling. *Proc. Natl. Acad. Sci.* 113 (42), E6391–E6400.
- Great Valley Center (2009) The state of the great Central Valley of California, assessing the region via indicators—the economy, 3rd edn. Great Valley Center, Modesto. Accessed 15

Sept 2011

- Great Valley Center “The state of the great Central Valley of California, assessing the region via indicators—the economy” 2009, 3rd edn. Great Valley Center, Modesto
- Groover, K.D, and Izbicki J.A, "Selected trace-elements in alluvium and rocks, western Mojave Desert, southern California"(2019): *Journal of Geochemical Exploration*, v. 200, p. 234–248
- Groundwater ambient monitoring and assessment (GAMA) domestic well project groundwater quality data report Tulare county focus area, California State water resources control board groundwater protection section, Revised July 2016
- Gronberg J.A, Dubrovsky N.M, Kratzer C.R, Domagalski J.L, Brown L.R, Burow K.R. "Environmental setting of the San Joaquin-Tulare basins, California"(1998). USGS Water-Resources Investigations Report 97–4205. Reston, Virginia: USGS.
- Hansen, J. A., Jurgens, B. C., & Fram, M. S. (2018). Quantifying anthropogenic contributions to century-scale groundwater salinity changes, San Joaquin Valley, California, USA. *Science of the Total Environment*, 642, 125–136.
- Handley-Sidhu, S., Renshaw, J.C., Moriyama, S., Stolpe, B., Mennan, C., Bagheriasl, S., Yong, P., Stamboulis, A., Paterson-Beedle, M., Sasaki, K., Patrick, R.A.D., Lead, J.R., Macaskie, L.E., 2011. Uptake of Sr²⁺ and Co²⁺ into biogenic hydroxyapatite: implications for biomineral ion exchange synthesis. *Environ. Sci. Technol.* 45, 6985–6990.
- Harkness, J.S., Darrah, T.H., Moore, M.T., and et al, Naturally occurring versus anthropogenic source of molybdenum in groundwater: evidence for geogenic contamination from southeast Wisconsin, United states
- Harter. 2009. “Agricultural Impacts on Groundwater Nitrate.” *Southwest Hydrology* 8 (4): 22–23. http://www.swhydro.ari.zona.edu/archive/V8_N4
- Harter, T., J. R. Lund, J. Darby, E. F. Graham, R. Howitt, K. K.Jessoe, S. Pettygrove, J. F. Quinn, and J. H. Viers. 2012. Addressing Nitrate in Californias Drinking Water With a Focus on Tulare Lake Basin and Salinas Valley Groundwater. Report for the State Water Resources Control Board Report to the Legislature, Davis, CA: Center for Watershed Sciences, University of California.
- Harter T, Dzurella K, Kourakoa G, Bell A, King A, and Hollander” nitrate fertilizer loading to groundwater in the central valley” FREP Projects 11-0301 and 15-0454, University of California, Davis, August 2017
- Hassanvand M, Hays P. Hydrogeochemical properties of Mojave Basin Shallow Aquifer located on southern California. AWAR 2022 Geospatial water technology conference. Texas, May 9-11

- Haugen E,A, Jurgens B.C, Arroyo-Lopez J.A, Bennett G.L" Groundwater development leads to decreasing arsenic concentrations in the San Joaquin Valley, California" *Science of the Total Environment* 771 (2021) 145223
- Hernández-del Amo, E., Menció, A., Gich, F., Mas-Pla, J., Bañeras, L., 2018. Isotope and microbiome data provide complementary information to identify natural nitrate attenuation processes in groundwater. *Sci. Total Environ.* 613, 579–591.
- Herojeet R, Rishi M.S, Kishore N “ Integrated approach of heavy metal pollution indices and complexity quantification using chemometric models in the Sirsa Basin, Nalagarh valley, Himachal Pradesh, India” 2015. *Chin J Geochem* 34(4):620–633
- Heyden C.J, New M.G, "Groundwater pollution on the Zambian Copperbelt: deciphering the source and the risk" (2004). *Sci. Total Environ.* 327, 17–30.
- Hoefs, J., Hoefs, J., 2015. *Stable Isotope Geochemistry*. Seventh edition. Springer, Switzerland.
- Hopkins B, Horneck D, Stevens R, Ellsworth J, Sullivan D “Managing irrigation water quality for crop production in the Pacific Northwest” (2007). A Pacific Northwest Extension publication, Oregon State University, University of Idaho, Washington State University
- Horton, R. K., (1965), An index number system for rating water quality, *Journal of Water Pollution Control Federation*, 37(3), pp 300–306.
- Hosono, T., Tokunaga, T., Kagabu, M., Nakata, H., Orishikida, T., Lin, I.-T., Shimada, J., 2013. The use of $\delta^{15}\text{N}$ and $\delta^{18}\text{O}$ tracers with an understanding of groundwater flow dynamics for evaluating the origins and attenuation mechanisms of nitrate pollution. *Water Res.* 47, 2661–2675.
- Howard, J., and M. Merrifield. 2010. “Mapping groundwater dependent ecosystems in California.” *PLoS One* 5 (6): e11249.
- Huang, J., Xu, J., Liu, X., Liu, J., Wang, L., 2011. Spatial distribution pattern analysis of groundwater nitrate nitrogen pollution in Shandong intensive farming regions of China using neural network method. *Math. Comput. Model.* 54, 995–1004.
- Isidoro D, and Grattan S.R. Predicting soil salinity in response to different irrigation practices, soil types and rainfall scenarios. *Irrig Sci* (2011) 29:197–211 DOI 10.1007/s00271-010-0223-7
- Izbicki, J. A., Johnson, R. U., Kulongoski, J., & Predmore, S. (2007). Ground-water recharge from small intermittent streams in the western Mojave Desert, California. *U.S. Geological Survey Professional Paper* 1703-G, pp. 157-184.
- Jasechko, S., & Perrone, D. (2020). California's Central Valley groundwater wells run dry during

recent drought. *Earth's Future*, 8, e2019EF001339

- Jin, Z, Qin X, Chen L, Jin M, Li F. "Using dual isotopes to evaluate sources and transformations of nitrate in the West Lake watershed, eastern China" *Contam. Hydrol.* 2015, 177, 64–75.
- John A, Izbicki, Michel R.L" Movement and Age of Ground Water in the Western Part of the Mojave Desert, Southern California, USA" U.S. GEOLOGICAL SURVEY, Water-Resources Investigations Report 03-4314. Sacramento, California, 2004
- Jurgens BC, Fram MS, Belitz K, Burow KR, Landon MK. Effects of groundwater development on uranium: Central Valley, California, USA. *Ground Water* 2009;49:913–28.
- Jutglar K, Hellwig J, Stoelzle M, Lange J. Post-drought increase in regional-scale groundwater nitrate in southwest Germany. *Hydrological processes*. Volume 35, Issue 8. August 2021
- Jurgens, B. C., Fram, M. S., Rutledge, J., & Bennett, G. L. (2020). Identifying areas of degrading and improving groundwater-quality conditions in the State of California, USA, 1974–2014. *Environmental Monitoring and Assessment*, 192(250). <https://doi.org/10.1007/s10661-020-8180-y>
- Jurgens, B. C.; Fram, M. S.; Belitz, K.; Burow, K. R.; Landon, M. K. Effects of Groundwater Development on Uranium: Central Valley, 913 California, USA. *Ground Water* 2010, 48, 913–928.
- Kabir M.H, Islam M.S, Tusher T.R, Hoq M.E, Al Mamun S." Changes of heavy metal concentrations in Shitalakhya river water of Bangladesh with seasons" *Indonesian Journal of Science & Technology* 5 (3) (2020) 395-409
- Kaushal, S.S., Groffman, P.M., Band, L.E., Elliott, E.M., Shields, C.A., Kendall, C., 2011. Tracking nonpoint source nitrogen pollution in human-impacted watersheds. *Environ. Sci. Technol.* 45 (19), 8225–8232.
- Kendall, C., Macdonnell, J, 1998, *Isotope tracers in catchment hydrology*. ISBN: 978-0-444-81546-0
- Kendall, C., Aravena, R., 2000. Nitrate isotopes in groundwater systems. *Environmental Tracers in Subsurface Hydrology*. Springer, US, pp. 261–297.
- Khanoranga and Khalid S. An assessment of groundwater quality for irrigation and drinking purposes around brick kilns in three districts of Balochistan province, Pakistan, through water quality index and multivariate statistical. *Journal of geochemical exploration*, volume 197, February 2019, Pages 14-26
- Kim S, Chae Y, Moon J, Kim D, Cui R, An G, Jeong S.W, JooAn Y. In situ evaluation of crop productivity and bioaccumulation of heavy metals in Paddy soils after remediation of metal-contaminated soils. *J. Agric. Food Chem.*, 65 (6) (2017), pp. 1239-1246

- Kool, D.M., Wrage, N., Oenema, O., Van Kessel, C., Van Groenigen, J.W., 2011. Oxygen exchange with water alters the oxygen isotopic signature of nitrate in soil ecosystems. *Soil Biol. Biochem.* 43 (6), 1180–1185.
- Kumar P.J.S, Jegathambal P, James E.J.” Chemometric evaluation of nitrate contamination in the groundwater of a hard rock area in Dharapuram, south India” *Appl Water Sci* (2014) 4:397–405 DOI 10.1007/s13201-014-0155-0
- Kumar, M, Kumari, K, Ramanathan, A, Saxena, R. “A comparative evaluation of groundwater suitability for irrigation and drinking purposes in two intensively cultivated districts of Punjab, India”. *Environ. Geol.* 2007, 53, 553–574.
- Kurwadkar s”Emerging trends in groundwater pollution and quality” *Water Environment Research*, Volume 86, Number 10—Copyright © 2014 Water Environment Federation.
- Kwaya M.Y, Hamidu H, Mohammed A.I, Abdulmumini Y.N, Adamu I.A, Grema H.M, Dauda M, Halilu B, Kana A.M." Heavy Metals Pollution Indices and Multivariate Statistical Evaluation of Groundwater Quality of Maru town and environs" *J. Mater. Environ. Sci.*, 2019, Volume 10, Issue 1, Page 32-44
- Lassiter, A., ed. 2015. *Sustainable water: Challenges and solutions from California*. Oakland, CA: University of California Press.
- Li, X.D., Masuda, H., Koba, K., Zeng, H.A., 2007. Nitrogen isotope study on nitratecontaminated groundwater in the Sichuan Basin, China. *Water Air Soil Pollut.* 178, 145–156.
- Li C, Gao X, Li S, Bundschuh J. A review of the distribution, sources, genesis, and environmental concerns of salinity in groundwater. *Environmental Science and Pollution Research* volume 27, pages41157–41174 (2020)
- Liu, C.Q., Li, S.L., Lang, Y.C., Xiao, H.Y., 2006. Using $\delta^{15}\text{N}$ and $\delta^{18}\text{O}$ values to identify nitrate sources in karst ground water, Guiyang, Southwest China. *Environ. Sci. Technol.* 40, 6928–6933.
- Lockhart, K. M., A. M. King, and T. Harter. 2013. “Identifying Sources of Groundwater Nitrate Contamination in a Large Alluvial Groundwater Basin with Highly Diversified Intensive Agricultural Production.” *Journal of Contaminant Hydrology* 151: 140–154. doi:10.1016/j.jconhyd.2013.05.008.
- Lopez A.M, Wells A, Fendorf S. Soil and Aquifer Properties Combine as Predictors of Groundwater Uranium Concentrations within the Central Valley, California. *Environ. Sci. Technol.* 2021, 55, 352–361
- Luthy R.G, Wolfand J.M, Bradshaw J.L" Urban water revolution: sustainable water futures for

- Lund, J., Medellin-Azuara, J., Durand, J., Stone, K., 2018. Lessons from California's 2012–2016 drought. *J. Water Resour. Plann. Manag.* 144, 04018067.
- Majumder RK, Hasnat MA, Hossain S (2008) An exploration of nitrate concentrations in groundwater aquifers of central-west region of Bangladesh. *J Hazard Mater* 159(2–3):536–543
- McMahon, P.B., and Chapelle, F.H., 2008, Redox processes and water quality of selected principal aquifer systems: *Ground Water*, v. 46, p. 259–271.
- Megdal, S.B, Invisible water: the importance of good groundwater governance and management, *Clean Water* (2018) 1:15; doi:10.1038/s41545-018-0015-9
- Mehta, V.K., Young, C., Bresney, S.R., Spivak, D.S., Winter, J.M., 2018. How can we support the development of robust groundwater sustainability plans? *Calif. Agric.* 72, 54–64.
- Merchant, J.M, GIS-based groundwater pollution hazard assessment: a critical review of the DRASTIC model *Photogramm Eng Remote Sens*, 60 (9) (1994), pp. 1117-1127
- Merchan D, Auque LF, Acero P, Gimeno MJ, Causape J (2015) Geochemical processes controlling water salinization in an irrigated basin in Spain: identification of natural and anthropogenic influence. *Sci Total Environ* 502:330–343
- Medellín-Azuara, J., D. MacEwan, R. E. Howitt, G. Koruakos, E. C. Dogrul, C. F. Brush, T. N. Kadir, T. Harter, F. Melton, and J. R. Lund. 2015. "Hydro-economic analysis of groundwater pumping for irrigated agriculture in California's Central Valley, USA." *Hydrogeol. J.* 23 (6):1205–1216
- Mendez G.O, and Christensen A.H. "Regional water table (1996) and water level changes in the Mojave River, the Morongo, and the Fort Irwin ground-water basins, San Bernardino County, California"(1997), U.S. Geological Survey Water-Resources Investigations Report 97-4160, 43 p.
- Mike Nugent, Micheal A. Kamrin, Lois Wolfson and Frank M. D'Itri. (1993). Michigan State University Extension 1993; Nitrate a drinking water concern Michigan's drinking water ext. Bul WQ-19 Revised Dec.1993
- Milnes E, Renard P (2004) The problem of salt recycling and seawater intrusion in coastal irrigated plains: an example from the Kiti aquifer (Southern Cyprus). *J Hydrol* 288:327–343
- Mishra, A.K., Singh, V.P., 2010. A review of drought concepts. *J. Hydrol.* 391 (1), 202–216.
- Moore, S.B., Winckel, J., Detwiler, S.J., Klasing, S.A., Gaul, P.A., 1990. Fish and wildlife

resources and agricultural drainage in the San Joaquin Valley, California: Sacramento, California, San Joaquin Valley Drainage Program, California Department of Water Resources, 974 p.

Moore, K.B., Ekwurzel, B., Esser, B.K., Hudson, G.B., Moran, J.E., 2006. Sources of groundwater nitrate revealed using residence time and isotope methods. *Appl. Geochem.* 21 (6), 1016–1029.

Murtaza G, Rehman M. Z, Qadir M, Shehzad M. T, and et al. High residual sodium carbonate water in the Indian subcontinent: concerns, challenges and remediation. *International Journal of Environmental Science and Technology* (2021) 18:3257–3272

Musgrove M. The occurrence and distribution of strontium in U.S. groundwater. *Applied Geochemistry* 126 (2021) 104867.

Neal C, Williams R.J, Bowes M.J, Harrass M.C, Neal M, Rowland P, et al. Decreasing boron concentration in UK rivers: insights into reductions in detergent formulations since 1990s and within-catchment storage issues. *Sci Total Environ*, 408 (2010), pp.1374-1385

Nikolenko O, urado A, Borges A.V, Knöller K, Brouyère S. Isotopic composition of nitrogen species in groundwater under agricultural areas. *Science of the Total Environment* 621 (2018) 1415–1432.

Nolan, J.; Weber, K. A. Natural Uranium Contamination in Major U.S. Aquifers Linked to Nitrate. *Environ. Sci. Technol. Lett.* 2015, 2, 215–220.

Norouzi H, Asghari Moghadam A. Groundwater quality assessment using random forest method based on groundwater quality indices (case study: Miandoab plain aquifer, NW of Iran) *Arabian Journal of Geosciences* (2020) 13: 912.

Northey JE, Christen EW, Ayars JE, Jankowski J (2006) Occurrence and measurement of salinity stratification in shallow groundwater in the Murrumbidgee Irrigation Area, south-eastern Australia. *Agric Water Manag* 81:23–40

Ojha, C., Shirzaei, M., Werth, S., Argus, D.F., Farr, T.G., 2018. Sustained groundwater loss in California's Central Valley exacerbated by intense drought periods. *Water Resour. Res.* 54, 4449–4460.

Parsad, B. Bose, J.M. "Evaluation of heavy metal pollution index for surface and spring water near a limestone mining area of the lower Himalyas"(2001). - *Environmental Geology* 41: 183-188

Peña, A., Delgado-Moreno, L., & Rodríguez-Liébana, J. A. (2020). A review of the impact of wastewater on the fate of pesticides in soils: Effect of some soil and solution properties. *Science of the Total Environment*, 718, 134468–<https://doi.org/10.1016/j.scitotenv.2019.134468>

- Piper AM (1944) A graphic procedure in the geochemical interpretation of water-analyses. *Trans Am Geophys Union* 25:914–923
- Planert, M., and Williams, J.S., 1995. Ground water atlas of the United States, Segment 1, California, Nevada. U.S. Geological Survey Hydrologic Atlas 730-B.
- Prasanna M. V, Praveena S. M, Chidambaram S, Nagarajan R. and Elayaraja A. “Evaluation of water quality pollution indices for heavy metal contamination monitoring: a case study from Curtin Lake, Miri City, East Malaysia” 2012. *Environmental Earth Sciences*, 67(7)
- Rao N.S, Rao P.S, Reddy G.V, Nagamani M, Vidyasagar G, Satyanarayana N. L. V. V.” Chemical characteristics of groundwater and assessment of groundwater quality in Varaha River Basin, Visakhapatnam District, Andhra Pradesh, India” *Environ Monit Assess* (2012) 184:5189–5214 DOI 10.1007/s10661-011-2333-y.
- Ravikumar P, Somashekar RK, Angami M “Hydrochemistry and evaluation of groundwater suitability for irrigation and drinking purposes in the Markandeya River basin, Belgaum District, Karnataka State, India” 2011, *Environ Monit Assess* 173(1):459–487
- Rosen M.R, Burow K.R, Fram M.S. Anthropogenic and geologic causes of anomalously high uranium concentrations in groundwater used for drinking water supply in the southeastern San Joaquin Valley, CA. *Journal of Hydrology* 577 (2019) 124009.
- Saeedi M, Abessi O, Sharifi F, Meraji H (2010) Development of groundwater quality index. *Environ Monit Assess* 163:327–335
- Sahoo S, Khaoash S.” Impact assessment of coal mining on groundwater chemistry and its quality from Brajrajnagar coal mining area using indexing models”. *Journal of Geochemical Exploration*. Volume 215, August 2020, 106559
- Salman, S.A., Arauzo, M., Elnazer, A.A., 2019. Groundwater quality and vulnerability assessment in west Luxor Governorate, Egypt. *Groundw. Sustain. Dev.* 8, 271–280.
- Samuding K, Abustan I, Rahman MTA, Isa MH "Distribution of heavy metals profile in groundwater system at solid waste disposal site"(2009). *Eur J Sci Res* 37(1):58–66
- Scanlon BR, Gates JB, Reedy RC, Jackson WA, Bordovsky JP (2010) Effects of irrigated agroecosystems: 2. Quality of soil water and groundwater in the southern High Plains, Texas. *Water Resour Res* 46:W09538
- Scanlon, B. R., C. C. Faunt, L. Longuevergne, R. C. Reedy, W. M. Alley, V. L. McGuire, and P. B. McMahon. 2012. “Groundwater depletion and sustainability of irrigation in the US High Plains and Central Valley.” *Proc. Nat. Acad. Sci.* 109 (24): 9320–9325.

- Schoups G, Hopmans G.W, Young C.A, Vrugt J.A, Wallender W.W, Tanji K.K, and Panday S.” Sustainability of irrigated agriculture in the San Joaquin, California PNAS October 25, 2005 102 (43) 15352-15356; first published October 17, 2005
- Seifi, A. and Riahi, M.H., 2017. Qualitative zoning of Shahr-e-Babak aquifer based on its corrosiveness, sedimentation, and applicability for agricultural, drinking, and pressure irrigation uses. *Water and Wastewater*. 28, 92-105. (In Persian).
- Shand P, Edmunds W.M, Lawrence A.R, Smedley P.L, Burke S. “The natural (baseline) quality of groundwater in England and Wales”2007. British Geological Survey Research Report N° RR/07/06 and Environment Agency Technical Report NC/99/74/24, p. 11.
- Sharp, Z., 2007. *Principles of Stable Isotope Geochemistry: Nitrogen*. Pearson Prentice Hal, Upper Saddle River, NJ, pp. 206–219.
- Shrestha A, Luo W. “Analysis of Groundwater Nitrate Contamination in the Central Valley: Comparison of the Geodetector Method, Principal Component Analysis and Geographically Weighted Regression” *ISPRS Int. J. Geo-Inf.* 2017, 6, 297; doi:10.3390/ijgi6100297
- Simsek C, Gunduz O. IWQ index: "A GIS-integrated technique to assess irrigation water quality. *Environ". Monit. Assess.* 2007, 128, 277–300.
- Singh R, Venkatesh A.S, Syed T.H, Reddy A.G.S, “Kumar M, Kurakalva R.M Assessment of potentially toxic trace elements contamination in groundwater resources of the coal mining area of the Korba Coalfield, Central India”. (2017) *Environ Earth Sci* 76(16):566
- Singh K.C, Rina K, Singh R.P, Mukherjee S “Geochemical characterization and heavy metal contamination of groundwater in Satluj River Basin” *Environ Earth Sci* (2014) 71:201–216 DOI 10.1007/s12665-013-2424-x
- Snow, D “Nitrate-N Isotope Results and Interpretation” 2018. Prepared for Eastern Research Group Prime Contract #EP-W-15-006 Daniel Snow, University of Nebraska Water Sciences Laboratory Lincoln, NE 68583-0844
- Spalding R. F, Exner M. E. “Occurrence of nitrate in groundwater – A Review”. *J. Environ. Qual.* 1993, 22 (3), 392–402.
- Stamos, C.L., Martin, P., Nishikawa, T., and Cox, B.F. (2001) *Simulation of Ground-Water Flow in the Mojave River Basin, California*. Water-Resources Investigations Report 01-4002. Version 3, U.S. Geological Survey, Sacramento, CA.
- Stumm W, Morgan JJ (1996) *Aquatic chemistry*. Wiley, New York
- Sutradhar S, Mondal P. Groundwater suitability assessment based on water quality index and hydrochemical characterization of Suri Sadar Sub-division, West Bengal. Volume

64, September 2021, 101335.

- Suresh K.R, Nagesh M.A. "Experimental studies on effect of water and soil quality on crop yield"(2015). International conference on water resources, coastal and ocean engineering (ICWRCOE 2015). Aquat. Procedia 4, 1235–1242.
- Syed A, Sarwar G, Shah S.H, Muhammad S. Soil salinity research in 21st century in Pakistan. Its impact on availability of plant nutrients, grow, and yield of crops. OMMUNICATIONS IN SOIL SCIENCE AND PLANT ANALYSIS2021, VOL. 52, NO. 3, 183-200
- Szaboles I, and Darab C. The influence of irrigation water of high sodium carbonate content of soils.1964. In Proceedings of 8th international congress of ISSS, Trans, II (pp. 803–812).
- Thomas, B.F., Famiglietti, J.S., 2015. Sustainable groundwater management in the arid Southwestern US: Coachella Valley, California. *Water Resour. Manag.* 29 (12), 4411–4426.
- Thomas B.F, Famiglietti J.S, Landerer F.W, Wiese D.N, Molotch N.P, Argus D.F." GRACE Groundwater Drought Index: Evaluation of California Central Valley groundwater drought” *Remote Sensing of Environment* 198 (2017) 384–392
- Thorpe, C.L., Morris, K., Boothman, C., Lloyd, J.R., 2012c. Alkaline Fe(III) reduction by a novel alkali-tolerant *Serratia* sp. isolated from surface sediments close to Sellafield nuclear facility, UK. *FEMS Microbiol. Lett.* 327, 87–92.
- Tomaszewski, M., Cema, G., Ziemińska-Buczyńska, A., 2017. Influence of temperature and pH on the anammox process: a review and meta-analysis. *Chemosphere* 182, 203–214.
- Torres-Martínez, J.A., Mora, A., Mahlknecht, J., Daessl'e, L.W., Cervantes-Avil'es, P.A., Ledesma-Ruiz, R., 2020. Estimation of nitrate pollution sources and transformations in groundwater of an intensive livestock-agricultural area (Comarca Lagunera), combining major ions, stable isotopes and MixSIAR. *Environ. Pollut.* 269, 115445.
- Tóth G., Hermann T., Da Silva M.R., Montanarella L. Heavy metals in agricultural soils of the European Union with implications for food safety. *Environ. Int.* 2016;88:299–309. doi: 10.1016/j.envint.2015.12.017
- Twarakavi N.K.C, Kaluarachchi N.K.C, “Sustainability of ground water quality considering land use changes and public health risks” *J Environ Manage*, 81 (2006), pp. 405-419
- USGS: Groundwater-Quality Data in the Mojave Basin Shallow Aquifer Study Unit, 2018: Results from the California GAMA Priority Basin Project.
- USGS: Groundwater-Quality Data in the Tulare Shallow Aquifer Study Unit, 2014-2015: Results from the California GAMA Priority Basin Project.
- U.S. Environmental Protection Agency. Drinking water contaminants 2012

- USGS, California water science center 2018, https://www.usgs.gov/centers/california-water-science-center/science/californias-central-valley?qt-science_center_objects=0
- U.S. Geological Survey, Principal aquifers of the 48 conterminous United States, Hawaii, Puerto Rico, and the U.S. Virgin Islands, 2003.
- Van Weert F, Van der Gun J, Reckman J (2009) Global overview of saline groundwater occurrence and genesis. Groundwater Resources Assessment Centre, Report GP-2009–1, Utrecht
- Voss, S. A., Jurgens, B. C., Fram, M. S., & Bennett, G. L. (2019). Delineation of spatial extent, depth, thickness, and potential volume of aquifers used for domestic and public water-supply in the Central Valley, California. U.S. Geological Survey. <https://doi.org/10.3133/sir20195076>
- Wallace S.H, Shaw S, Morris K, Small J.S, Fuller A.J, Burke I.T . Effect of groundwater pH and ionic strength on strontium sorption in aquifer sediments: Implications for ⁹⁰Sr mobility at contaminated nuclear sites Appl. Geochem., 27 (2012), pp. 1482-1491, [10.1016/j.apgeochem.2012.04.007](https://doi.org/10.1016/j.apgeochem.2012.04.007)
- Walvoord MA, Phillips FM, Stonestrom DA, Evans RD, Hartsough PC, Newman BD, Streigl RG (2003) A reservoir of nitrate beneath desert soils. Science 302:1021–1024
- Ward MH, deKok T, Levallois P, Brender J, Gulis G, Nolan BT, VanDerslice J (2005) Drinking water nitrate and health: recent findings and research needs. Environ Health Perspect 115:1607–1614
- Weissmann G.S, G.L. Bennett, and A.L. Lansdale. "Factors controlling sequence development on Quaternary fluvial fans, San Joaquin Basin, California" (2005). In Alluvial Fans: Geomorphology, Sedimentology, Dynamics, Special Publications, v. 251, ed. A.M. Harvey, A.E. Mather, and M. Stokes 169–186. London, UK: Geological Society.
- WHO (2011) Revision of guidelines for Drinking water quality 4th ed.
- Wichelns D, Qadir M."Achieving sustainable irrigation requires effective management of salts, soil salinity, and shallow groundwater" Agricultural Water Management 157 (2015) 31–38
- Widory, D., Kloppmann, W., Chery, L., Bonnin, J., Rochdi, H., Guinamant, J.-L., 2004. Nitrate in groundwater: an isotopic multi-tracer approach. J. Contam. Hydrol. 72, 165–188.
- Williams, A.E, Lund, L.J, Johnson, J.A, Kabala, Z.J"Natural and anthropogenic nitrate contamination of groundwater in a rural community, California. Environ. Sci. Technol. 1998, 32, 1, 32–39
- Williard, K.W., DeWalle, D.R., Edwards, P.J., Sharpe, W.E., 2001. 18 O isotopic separation of stream nitrate sources in mid-Appalachian forested watersheds. J. Hydrol. 252 (1), 174–188.

- Xue, Y., Song, J., Zhang, Y., Kong, F., Wen, M., Zhang, G., 2016. Nitrate pollution and preliminary source identification of surface water in a semi-arid river basin, using isotopic and hydrochemical approaches. *Water* 8 (8), 328.
- Xu P, Zhang Q, Qian H, Irrigation Water Quality Evaluation Based on Multivariate Statistical Analysis: A Case Study of Jiaokou Irrigation District, *International Journal of Environmental and Ecological Engineering* Vol:14, No:12, 2020
- Yin, X.J., Lu, J., Wang Y.C., and et al. The abundance of nirS -type denitrifiers and anammox bacteria in rhizospheres was affected by the organic acids secreted from roots of submerged macrophytes *Chemosphere*, 240 (2020), Article 124903
- Yue, X., Yu, G., Lu, Y., Liu, Z., Li, Q., Tang, J., Liu, J. Effect of dissolved oxygen on nitrogen removal and the microbial community of the completely autotrophic nitrogen removal over nitrite process in a submerged aerated biological filter *Bioresour. Technol.*, 254 (2018), pp. 67-74
- Zabala S. Martínez M. Manzano L. Vives “Groundwater chemical baseline values to assess the Recovery Plan in the Matanza-Riachuelo River basin, Argentina” *Science of the Total Environment* 541 (2016) 1516–1530
- Zhang Y, Shi P, Song J, and Li Q.(2019) Application of Nitrogen and Oxygen Isotopes for Source and Fate Identification of Nitrate Pollution in Surface Water: A Review. *Appl. Sci.* 2019, 9, 18; doi:10.3390/app9010018.

Links:

[USGS Water Quality Samples for USA: Sample Data](#)

https://ca.water.usgs.gov/mojave/gen_location.html

<https://ca.water.usgs.gov/projects/central-valley/about-central-valley.html>

<https://ca.water.usgs.gov/projects/central-valley/about-central-valley.html>

<https://geologycafe.com/california/maps/provinces1.htm>